



Universidade de Aveiro
2016/2017

Departamento de Química

**Joana Raquel
Amaral Antunes
68169** **Produção e purificação do interferão alfa-2b a partir de
culturas de *Escherichia coli* utilizando plataformas
alternativas**

**Production and purification of interferon alpha-2b from
Escherichia coli cultures using alternative platforms**



**Joana Raquel
Amaral Antunes
68169** **Produção e purificação do interferão alfa-2b a partir de
culturas de *Escherichia coli* utilizando plataformas
alternativas**

**Production and purification of interferon alpha-2b from
Escherichia coli cultures using alternative platforms**

Dissertação apresentada à Universidade de Aveiro para cumprimento dos requisitos necessários à obtenção do grau de Mestre em Biotecnologia, ramo Industrial e Ambiental, realizada sob a orientação científica da Doutora Mara Guadalupe Freire Martins, Investigadora Coordenadora no Departamento de Química, CICECO, da Universidade de Aveiro, e do Doutor Augusto Quaresma Henriques Pedro, bolseiro de Pós-Doutoramento no Departamento de Química, CICECO, da Universidade de Aveiro.

This work was developed in the scope of the project CICECO-Aveiro Institute of Materials (Ref. FCT UID /CTM /50011/2013), financed by national funds through the FCT/MEC and when applicable co-financed by FEDER under the PT2020 Partnership Agreement.

Part of the research presented was financially supported by the European Research Council under the European Union's Seventh Framework Programme (FP7/2007-2013) / ERC grant agreement n° 337753.



o júri

presidente

Prof. Dr. João Manuel da Costa e Araújo Pereira Coutinho

Professor Catedrático do Departamento de Química da Universidade de Aveiro

Prof. Dr.^a Fani Pereira de Sousa

Professora Auxiliar da Faculdade de Ciências da Saúde da Universidade da Beira Interior

Dr.^a Mara Guadalupe Freire Martins

Investigadora coordenadora do Departamento de Química, CICECO, da Universidade de Aveiro

agradecimentos

À minha orientadora, a Doutora Mara Freire, por ter acreditado nas minhas capacidades, pelas mensagens de coragem e incentivo, por me levar mais longe, por me ensinar tanto e por me ter acompanhado durante este trabalho.

Ao meu orientador, o Doutor Augusto Pedro, por me guiar na jornada inicial no CICS na Covilhã, por me ter ajudado a adquirir novas competências, pela paciência e ajuda no esclarecimento das minhas questões.

Aos meus colegas de laboratório, ao grupo do CICS e a todo o grupo Path, pelos sorrisos, ajuda, apoio e paciência e por estarem sempre disponíveis para me ouvir e esclarecer dúvidas.

Aos meus pais, Cristina e João, por me proporcionarem tudo isto, pela força que me deram, pelos dias a arrancar cabelos que tiveram por minha causa. Muito obrigada por todo o vosso apoio.

À minha avó-madrinha, Aida, por ser a minha maior inspiração.

Ao Filipe, por ter sido o meu maior alicerce nesta caminhada.

A todos os meus amigos, sem vós nada disto seria possível.

Por fim, ao departamento de Química da Universidade de Aveiro e ao CICECO pelas condições e equipamento disponibilizado na realização deste trabalho.

Palavras-chave

interferão alfa-2b, produção recombinante, *Escherichia coli*, biofármacos, hepatite C crônica, purificação, cromatografia aniônica, sistemas aquosos bifásicos, líquidos iônicos.

Resumo

A indústria biofarmacêutica tem vindo a desenvolver diferentes tipos de biofármacos para o tratamento de diversas doenças. A maioria das proteínas terapêuticas são produzidas através da tecnologia do DNA recombinante, e purificadas utilizando técnicas convencionais, tais como a precipitação com sais, eletroforese e cromatografia. O interferão alfa-2b (IFN α -2b) é uma proteína terapêutica de ação imunomoduladora com atividade antiviral e antiproliferativa, que é geralmente obtida a partir de culturas de *Escherichia coli*, e utilizada no tratamento de doenças humanas, tais como a hepatite C, melanomas, alguns linfomas e leucemias, entre outras. Embora a fase de produção recombinante do IFN α -2b já tenha sido amplamente estudada e otimizada, a sua recuperação e purificação assumem-se como os passos economicamente limitantes do processo global de produção. Neste estudo, o IFN α -2b foi produzido na forma de corpos de inclusão utilizando culturas de BL21, no meio SOB, após 3 h de indução. A recuperação desta fração englobou vários passos, tendo sido alcançado um protocolo final que inclui: 1) Lavagem com Triton-X a 1%; 2) Lavagem com ureia a 4 M; e 3) Solubilização em meio alcalino, com ureia a 8 M. Alterando as condições de produção conseguiu-se também produzir e recuperar parte da proteína alvo na forma solúvel, embora com menor rendimento. O IFN α -2b previamente solubilizado foi purificado através de cromatografia aniônica, tendo sido obtido na sua forma biologicamente ativa com uma pureza superior a 95%. Como técnica alternativa de purificação utilizaram-se sistemas aquosos bifásicos constituídos por vários líquidos iônicos e tampão fosfato. Apesar de os resultados serem menos promissores, este estudo permitiu estudar plataformas alternativas para a recuperação e purificação do IFN α -2b através da aplicação de sistemas aquosos bifásicos.

Keywords

interferon alpha-2b, recombinant production, *Escherichia coli* biopharmaceuticals, chronic hepatitis C, purification, anion-exchange chromatography, aqueous two-phase systems, ionic liquids.

Abstract

The biopharmaceutical industry has been developing various biopharmaceutical possibilities for the treatment of several diseases. Most therapeutic proteins are produced through the recombinant protein technology and purified using traditional techniques, such as precipitation with salts, electrophoresis and chromatography. Interferon alfa-2b (IFN α -2b) is a therapeutic protein with immunomodulatory action and antiviral and antiproliferative activities, usually produced by *Escherichia coli* cultures, and used in the treatment of several human diseases, such as hepatitis C, melanomas, some lymphomas and leukemias, among others. Although the recombinant production of IFN α -2b has already been extensively studied and optimized, its recovery and purification correspond to the economically limiting steps of the overall production process. In this study, IFN α -2b was produced in the form of inclusion bodies using BL21 cultures, in SOB medium, after 3 h of induction. The recovery of this fraction involved several steps, and a final protocol was developed: 1) Washing with Triton-X at 1%; 2) Washing with urea at 4 M; and 3) Solubilization in alkaline medium with urea at 8 M. By changing the production conditions, it was also possible to produce and recover part of the target protein in the soluble form, yet with a lower yield. The solubilized IFN α -2b was purified using anion-exchange chromatography, and obtained in a biologically active form with a purity higher than 95 %. As an alternative purification technique, aqueous two-phase systems composed of several ionic liquids and a phosphate buffer were investigated. Although the results obtained are less promising, this study allowed the evaluation of alternative platforms for the recovery and purification of IFN α -2b by the application of aqueous two-phase systems.

Contents

1. General Introduction	1
1.1. Scope and objectives.....	1
1.2. Biopharmaceuticals industry and market.....	3
1.2.1. Interferons market trends.....	4
1.3. Interferons.....	4
1.3.1. Classification of human interferons.....	5
1.3.2. Interferons as biopharmaceuticals	6
1.4. Interferon alpha-2b molecular characteristics and physiological role	9
1.5. Recombinant proteins - upstream processing	14
1.5.1. Expression vectors and host expression cells.....	14
1.5.2. Recombinant interferon alpha-2b biosynthesis	17
1.6. Recombinant proteins - downstream processing	19
1.6.1. Primary recovery and isolation.....	19
1.6.2. Chromatographic-based purification processes.....	21
1.6.3. Aqueous two-phase systems.....	22
1.6.4. Purification of the recombinant interferon alpha-2b	29
2. Experimental section.....	34
2.1. Recombinant interferon alpha-2b production and recovery	34
2.1.1. Chemicals	34
2.1.2. Experimental procedure.....	34
2.2. Chromatographic purification of interferon alpha-2b.....	38
2.2.1. Chemicals	38
2.2.2. Experimental procedure.....	38
2.3. Biological activity of interferon alpha-2b.....	38
2.4. Purification of interferon alpha-2b using IL-based ATPS.....	39
2.4.1. Chemicals	39
2.4.2. Experimental procedure.....	40
2.4.2.1. Synthesis and characterization of ionic liquids	40
2.4.2.2. ATPS ternary phase diagrams	42
2.4.2.3. Extraction of interferon alpha-2b using IL-based ATPS	43
3. Results and Discussion.....	44
3.1. Recombinant interferon alpha-2b production	44
3.1.1. Optimization of the experimental conditions for interferon alpha-2b production.....	44

3.2.	Primary recovery of the active form of interferon alpha-2b	47
3.2.1.	Cellular disruption	47
3.2.2.	Inclusion bodies washing, solubilization and interferon alpha-2b extraction 49	
3.3.	Interferon alpha-2b purification	56
3.3.1.	Chromatographic purification of interferon alpha-2b	56
3.3.2.	Non-chromatographic strategies for interferon alpha-2b purification using ionic-liquid-based aqueous two-phase systems.....	69
3.3.2.1.	Synthesis and characterization of ionic liquids	69
3.3.2.2.	Phase diagrams of aqueous two-phase systems	76
3.3.2.3.	Purification of interferon alpha-2b using aqueous-two phase systems 80	
4.	Final remarks.....	85
4.1.	Conclusions and future work	85
5.	References	87
6.	List of communications	104
Appendix A.....	105
Appendix B.....	106
Appendix C.....	121
Appendix D.....	125

List of tables

Table 1: Commercial formulations and therapeutic applications of interferons commonly used in clinical practice, extended from (39).	8
Table 2: Comparison between different expression systems for the production of recombinant proteins (100, 108–110).	16
Table 3: Host systems, expression nature, expression vectors and production yield of recombinant IFN α -2b.	18
Table 4: Comparison between host, extraction yield, specific activity and purity of different purification methods for the recombinant IFN α -2b.	31
Table 5: Inclusion bodies washing buffers composition used for IFN α -2b recovery. ...	50
Table 6: Extraction buffers compositions and respective time used for IFN α -2b solubilization, at 25 °C.	52
Table 7: Appearance, water content, chemical structure, and ^1H , ^{13}C RMN characterization of the synthesized ILs.	70
Table 8: Identification of the systems able (✓) and not able (✗) to form aqueous two-phase systems with aqueous solutions of $\text{K}_2\text{HPO}_4/\text{KH}_2\text{PO}_4$ at pH 8.2.	76
Table 9: Correlation parameters used to describe the experimental binodal data fitted by Equation 2 and respective standard deviations (σ) and correlation coefficients.	79
Table 10: Tie-lines (TLs) and tie-line lengths (TLLs). Initial mixture points are represented as IL_M and Salt_M ; IL_T and Salt_T are the composition of IL and $\text{K}_2\text{HPO}_4/\text{KH}_2\text{PO}_4$ at the IL-rich phase (top phase), and IL_B and Salt_B are the composition of IL and salt at the $\text{K}_2\text{HPO}_4/\text{KH}_2\text{PO}_4$ -phase (bottom phase).	80

List of figures

Figure 1: General flowchart of the biopharmaceuticals manufacturing process, adapted from (10).....	4
Figure 2: On the left: tridimensional structure of recombinant IFN α -2b. On the right: disulfide patterns of IFN α -2b and its isoforms. The solid line indicates the disulfide bond formation, whereas the dashed line indicates partial disulfide bond formation. Adapted from (79, 80).....	9
Figure 3: General scheme of the transcriptional activation of JAK-STAT pathways by IFN α , adapted from (96).....	12
Figure 4: Schematic summary of the IFN antiviral action. Open hexagons represent virion particles and open circles, IFN proteins. Adapted from (98).....	13
Figure 5: Schematic representation of a phase diagram, adapted from (140).....	23
Figure 6: Chemical structures of the ionic liquids commonly used for aqueous two-phase systems, extended from (165).....	27
Figure 7: General scheme of the pET-3a plasmid; it includes the T7 promoter and terminator, the ribosomal binding site (RBS), the target IFN α -2b gene, the ampicillin selection marker (amp ^R) and the pBR322 origin of replication.	35
Figure 8: Chemical structure and abbreviation of the synthesized ILs.	41
Figure 9: Growth profile of E. coli BL21 harboring the plasmid pET-3a_IFN α -2b at different incubation periods (ranging from 0 to 9 hours) on LB, SOC and SOB media. Fermentation was initiated at an OD ₆₀₀ of 0.2 and the cultures were induced with 0.5 mM IPTG at an OD ₆₀₀ of approximately 0.6, as indicated by the arrow.	44
Figure 10: SDS-PAGE (left) and Western-Blot (right) analysis of the different samples obtained after the subcellular fractionation of E. coli BL21 cultures (37 °C and 250 rpm) in distinct culture media: A – SOB, B – LB, C – SOC, after 0-7 h of induction. Fermentation was initiated at an OD ₆₀₀ of 0.2 and the cultures were induced with 0.5 mM IPTG at an OD ₆₀₀ of approximately 0.6. Samples were lysed using glass beads and the inclusion bodies solubilized in extraction buffer containing 8 M urea, pH 12.5.	45
Figure 11: SDS-PAGE (left) and Western-Blot (right) of the soluble fraction (S) and inclusion body fraction (IB) obtained after the subcellular fractionation of E. coli BL21 cultures, induced with different concentrations of IPTG. Samples were lysed using glass beads and the inclusion bodies solubilized in extraction buffer containing 8 M urea, pH 12.5. Induction temperature was set at 16 °C.	47

Figure 12: Western-Blot analysis of the cellular extract of <i>E. coli</i> BL21 cultures (37 °C and 250 rpm) obtained either using 7 cycles of mechanical lysis (M), with glass beads, and using the enzymatic lysis (E), with lysozyme.....	47
Figure 13: Evaluation of the secondary structure of IFN α -2b using Circular Dichroism (CD). The IFN α -2b was obtained from <i>E. coli</i> BL21 cells using the enzymatic lysis...	48
Figure 14: Evaluation of IFN α -2b anti-proliferative activity against MCF-7 cells.	49
Figure 15: SDS-PAGE analysis of the different washing buffers used for the IFN α -2b recovery. Each condition is highlighted at a different color. Each lane is identified with the numbers 1, 2 and/or 3 corresponding to the 1 st , 2 nd and 3 rd wash, respectively, and with the SIB abbreviation corresponding to the solubilized inclusion body fraction. ...	51
Figure 16: SDS-PAGE analysis of the inclusion bodies' washes using first Triton X-100 1 % (lane 1), and then 4 M urea (lane 2), both in 50 mM Tris, at pH 8.	51
Figure 17: SDS-PAGE analysis of the conditions 1-4 applied to extract IFN α -2b from the insoluble fraction. Both soluble and insoluble fractions were analyzed and are represented as SIB and P, respectively.	53
Figure 18: SDS-PAGE analysis of the conditions 1 and 4-7 applied to extract IFN α -2b from the insoluble fraction. Both soluble and insoluble fractions were analyzed and are represented as SIB and P, respectively.	54
Figure 19: SDS-PAGE analysis of the conditions 5 and 7-9 applied to extract IFN α -2b from the insoluble fraction. Both soluble and insoluble fractions were analyzed and are represented as SIB and P, respectively.	55
Figure 20: SDS-PAGE analysis of the soluble (SIB) and insoluble (P) fractions of the IFN α -2b extracted with a 50 mM Tris buffer containing 8 M urea, pH 12.5 and 1 mM DTT, at 25, 37 and 50 °C.....	55
Figure 21: Optimized protocol for IFN α -2b recovery from <i>E. coli</i> BL21.	56
Figure 22: Chromatographic profile of the SIB fraction by arginine-Sepharose chromatography 1. 0.5 mL of the crude SIB fraction was injected and the elution was performed at 1 mL/min by increasing NaCl concentration from 0 M to 0.5 M, and then to 2 M in 50 mM Tris buffer (pH 8), as represented by the arrows. The collected fractions of each step are represented as I, II and III (A). The SDS-PAGE and Western-Blot results of the collected fractions are represented in B.	57
Figure 23: Chromatographic profile of the SIB fraction by arginine-Sepharose chromatography 2. 0.1 mL of the crude SIB fraction was injected and the elution was performed at 1 mL/min by increasing NaCl concentration from 0 M to 0.5 M, and then to	

2 M in 50 mM Tris buffer (pH 8), as represented by the arrows. The collected fractions of each step are represented as I, II and III (A). The SDS-PAGE results of the collected fractions are represented in B. 59

Figure 24: Chromatographic profile of SIB fraction by arginine-Sepharose chromatography 3. 0.1 mL of the crude SIB fraction was injected and the elution was performed at 1 mL/min by increasing NaCl concentration from 0 M to 0.5 M, and then to 2 M in 50 mM Tris buffer (pH 8), as represented by the arrows. The collected fractions of each step are represented as I, II and III (A). The SDS-PAGE results of the collected fractions are represented in B. 60

Figure 25: Chromatographic profile of the SIB fraction obtained with the HiTrap Desalting column. 1 mL of the crude SIB fraction was injected and the elution was performed with 50 mM Tris, at pH 8. The two maximums of absorbance are highlighted as peak 1 and peak 2. 61

Figure 26: SDS-PAGE analysis of different eluted fractions with 50 mM Tris pH 8, resulting from the HiTrap Desalting chromatography. The lanes correspond to: 1) initial sample, 2) peak 1, 3) peak 2. 62

Figure 27: Chromatographic profile of the SIB fraction obtained from the CIM DEAE monolith chromatography 1. 0.5 mL of the crude SIB fraction was injected and the elution was performed at 1 mL/min by increasing NaCl concentration from 20 mM to 1 M, and then to 2 M in 50 mM Tris buffer (pH 8), as represented by the arrows. The collected fraction is represented as II (A). The SDS-PAGE results of the II fraction are represented in B. 63

Figure 28: Chromatographic profile of the SIB fraction obtained from the CIM DEAE monolith chromatography 2. 0.5 mL of the crude SIB fraction was injected and the elution was performed at 1 mL/min by increasing NaCl concentration from 200 mM to 1 M, and then to 2 M in 50 mM Tris buffer (pH 8), as represented by the arrows. The collected fractions are represented as I, II and III (A). The SDS-PAGE results of the collected fractions are represented in B. 64

Figure 29: Chromatographic profile of the SIB fraction obtained from the CIM DEAE monolith chromatography 3. 0.5 mL of the crude SIB fraction was injected and the elution was performed at 1 mL/min by increasing NaCl concentration from 100 mM to 1 M, and then to 2 M in 50 mM Tris buffer (pH 8), as represented by the arrows. The collected fractions are represented as I and II (A). The SDS-PAGE results of the collected fractions are represented in B. 65

Figure 30: Chromatographic profile of the SIB fraction obtained from the CIM DEAE monolith chromatography 4. 0.5 mL of the crude SIB fraction was injected and the elution was performed at 1 mL/min by increasing NaCl concentration from 60 mM to 1 M, and then to 2 M in 50 mM Tris buffer (pH 8), as represented by the arrows. The collected fractions are represented as I and II (A). The SDS-PAGE results of the collected fractions are represented in B. 66

Figure 31: Chromatographic profile of the SIB fraction obtained from the CIM DEAE monolith chromatography 5. 0.5 mL of the crude SIB fraction was injected and the elution was performed at 1 mL/min by increasing NaCl concentration from 50 mM to 150 mM, and then to 2 M in 50 mM Tris buffer (pH 8), as represented by the arrows. The collected fractions are represented as I, II, III and IV (A). The SDS-PAGE results of the collected fractions are represented in B. 67

Figure 32: Chromatographic profile of the SIB fraction obtained from CIM DEAE monolith chromatography 6. 0.5 mL of the crude SIB fraction was injected and the elution was performed at 1 mL/min by increasing NaCl concentration in a stepwise gradient from 50 mM to 200 mM, during 10 min. Subsequently, the concentration was increased to 1 M in 50 mM Tris buffer (pH 8), as represented by the arrows. The collected fractions are represented as II, III, IV and V (A). The SDS-PAGE results of the collected fractions are represented in B. 68

Figure 33: Ternary phase diagrams for systems composed of IL + K₂HPO₄/KH₂PO₄ + H₂O, in wt%. [N₄₄₄₄][Ac] (●), [P₄₄₄₄][Ac] (●), [N₁₁₁₁][Ac] (●), [N₄₄₄₄][MES] (●), [P₄₄₄₄][MES] (●), [C_{4mim}][MES] (●), and [P₄₄₄₄][Arg] (●), with the corresponding binodal fitting of data using Equation 2. 77

Figure 34: Ternary phase diagrams for ATPS composed of distinct ILs + K₂HPO₄/KH₂PO₄ + H₂O, in mol.kg⁻¹. [N₄₄₄₄][Ac] (●), [P₄₄₄₄][Ac] (●), [N₁₁₁₁][Ac] (●), [N₄₄₄₄][MES] (●), [P₄₄₄₄][MES] (●), [C_{4mim}][MES] (●) and [P₄₄₄₄][Arg] (●). 78

Figure 35: SDS-PAGE results of the IL-based ATPS purification assay 1, where the ATPS constituted by the ILs [N₄₄₄₄][Ac], [P₄₄₄₄][Ac], [N₁₁₁₁][Ac] (left), [N₄₄₄₄][MES], [P₄₄₄₄][MES], [C_{4mim}][MES] (right) and + K₂HPO₄/KH₂PO₄ + H₂O with a total mass of 0.6 g were tested for the partition of the IFN α -2b. The initial sample, the top phase, the bottom phase and the precipitate phase are represented as I, T, D and P, respectively. 40 wt% of IL + 9 wt% of K₂HPO₄/KH₂PO₄. 82

Figure 36: SDS-PAGE results of the IL-based ATPS purification assay 2, where the ATPS constituted by the ILs [P₄₄₄₄][MES], [N₄₄₄₄][MES], [C_{4mim}][MES] (left)

[P₄₄₄₄][Ac], [N₄₄₄₄][Ac] and [N₁₁₁₁][Ac] (right) + K₂HPO₄/KH₂PO₄ + H₂O with a total mass of 0.8 g were tested for the partition of the IFN α -2b. The initial sample, the top phase, the bottom phase and the precipitate phase are represented as I, T, D and P, respectively. The mixture point used in this assay was 40 wt% of IL + 9 wt% of K₂HPO₄/KH₂PO₄..... 83

Figure 37: SDS-PAGE results of the IL-based ATPS purification assay 3, where the ATPS constituted by the ILs [N₄₄₄₄][Ac] and [N₁₁₁₁][Ac] + K₂HPO₄/KH₂PO₄ + H₂O with a total mass of 0.8 and 0.6 g, respectively, were tested for the partition of the IFN α -2b. The initial sample, the top phase, the bottom phase and the precipitate phase are represented as I, T, D and P, respectively. The mixture point used for [N₄₄₄₄][Ac] ATPS was 40 wt% of IL + 9 wt% of K₂HPO₄/KH₂PO₄, while in [N₁₁₁₁][Ac] ATPS the weight fraction of K₂HPO₄/KH₂PO₄ was reduced to 8 wt%..... 84

Abbreviations and acronyms

2-ME: 2-Mercaptoethanol

5'UTR: 5' Untranslated Region

ADAR: RNA-Specific Adenosine Deaminase

APS: Ammonium Persulfate

ATPS: Aqueous Two-Phase Systems

BHK: Baby Hamster Kidney

BSA: Bovine Serum Albumin

CD: Circular Dichroism

CHO: Chinese Hamster Ovary

CPC: Centrifugal Partition Chromatography

DAMPs: Damage-Associated Molecular Patterns

DMEM: Dulbecco's Modified Eagle's medium

DTE: Dithioerythritol

DTT: Dithiothreitol

E. coli: *Escherichia coli*

FBS: Fetal Bovine Serum

FDA: Food and Drug Administration

GB-ILs: Good's Buffer Ionic Liquids

GdnHCl: Guanidine Hydrochloride

GRAS: Generally Recognized as Safe

GST: Glutathione S-Transferase

GSH - L-Glutathione reduce

GSSH - L-Glutathione oxidized

HCV: Hepatitis C Virus

HEK: Human Embryonic Kidney

IFNAR: IFN α/β Receptor

IFNs: Interferons

IFN α -2b: Interferon alpha-2b

IFN α : Interferon alpha

IFN β : Interferon beta

IFN γ : Interferon gamma

IFN λ : Interferon lambda

IFN ω : Interferon omega
ILs: Ionic Liquids
ILTPP: Ionic Liquid-Based Three Phase Partitioning
IPTG: Isopropyl β -D-1-Thiogalactopyranoside
IRF-3: IFN-Regulatory Factor 3
IRF-7: IFN-Regulatory Factor 7
IRF-9: IFN-Regulatory Factor 9
ISGF-3: IFN-Stimulated Gene Factor 3
ISGs: IFN-Stimulated Genes
ISRE: Interferon Stimulating Response Element
IgG: Immunoglobulin G
IgY: Immunoglobulin Y
K₂HPO₄: Di-potassium Hydrogen Phosphate
KH₂PO₄: Potassium Dihydrogen Phosphate
LB: Luria Broth
MBP: Maltose-Binding Protein
MS: Mass Spectrometry
Mw: Molecular Weight
NLRs: NOD-Like Receptors
NS0: Murine Myeloma
OAS: 2',5'-Oligoadenylate Synthetase
OD₆₀₀: optical density at 600 nm
PAMPs: Pathogen-Associated Molecular Patterns
PBS: Phosphate-Buffered Saline
PDIb'a': b'a' Domain of Human Protein Disulfide Isomerase
PEG-IFN α -2a: Pegylated Interferon alpha-2a
PEG-IFN α -2b: Pegylated Interferon alpha-2b
PEG: Polyethylene Glycol
P_F: Purification Factor
PKR: Protein Kinase
PMSF: Phenylmethylsulfonyl Fluoride
PPG: Polypropylene Glycol
PRRs: Pattern Recognition Receptors

PVDF: Polyvinylidene Difluoride
RBS: ribosomal binding site
RLRs: RIG-Like Receptors
RP-HPLC: Reverse-Phase High-Performance Liquid Chromatography
SD: Shine-Dalgarno
SDS-PAGE: Sodium Dodecyl Sulfate-Polyacrylamide Gel Electrophoresis
SIB: Solubilized Inclusion Bodies
TIR: Toll/Interleukin-1 Receptor
TLRs: Toll-like Receptors
TEMED: Tetramethylethylenediamine
TYK-2: Tyrosine Kinase-2
WHO: World Health Organization
mAbs: Monoclonal Antibodies
pI: Isoelectric Point
[C₄mim][Ac]: 1-butyl-3-methylimidazolium acetate
[C₄mim][Arg]: 1-butyl-3-methylimidazolium arginine
[C₄mim][MES]: 1-butyl-3-methylimidazolium 2-(N-morpholino)ethanesulfonate
[Ch][Ac]: choline acetate
[Ch][Arg]: choline arginine
[Ch][MES]: choline 2-(N-morpholino)ethanesulfonate
[N₁₁₁₁][Ac]: tetramethylammonium acetate
[N₁₁₁₁][Arg]: tetramethylammonium arginine
[N₁₁₁₁][MES]: tetramethylammonium 2-(N-morpholino)ethanesulfonate
[N₄₄₄₄][Ac]: tetrabutylammonium acetate
[N₄₄₄₄][Arg]: tetrabutylammonium arginine
[N₄₄₄₄][MES]: tetrabutylammonium 2-(N-morpholino)ethanesulfonate
[P₄₄₄₄][Ac]: tetrabutylphosphonium acetate
[P₄₄₄₄][MES]: tetrabutylphosphonium 2-(N-morpholino)ethanesulfonate
[P₄₄₄₄][Arg]: tetrabutylphosphonium arginine

1. General Introduction

1.1. Scope and objectives

Human ageing is continuously advancing and will become one of the key driving forces of medical and societal changes in the decades ahead (1). Therefore, specific needs of new and effective biopharmaceuticals to treat age- and prosperity-related diseases will considerably increase (2). Biopharmaceuticals have largely improved the treatment of many diseases and, in some cases, are the only approved therapies available for specific human disorders. These biologic-based products are used in several areas, such as vaccination, immunization, oncology, autoimmune, cardiovascular, inflammatory and neurological diseases (3).

Biopharmaceuticals are products of biological origin, with high molecular weight (Mw), and with a molecular composition difficult to define, as they are derived from heterogeneous mixtures of living organisms, cells, animals or plants (4). These include cytokines, enzymes, hormones, clotting factors, monoclonal antibodies, cells, recombinant proteins, nucleic-acid-derived products, among others (3). Protein therapeutics already reached a significant role in several medicine fields, accounting with more than 200 therapeutic proteins approved for clinical use, including interferons (IFNs) (5). Interferons are immunomodulatory molecules that have been used to treat several malignancies; in particular, interferon alpha-2b (IFN α -2b) has been used to treat not only viral infections, such as chronic hepatitis C, but is also considered in the therapy regimens of some cancers, and thus was considered in 2015 an essential therapeutic option by the World Health Organization (WHO) (6). Commercial preparations of IFN α -2b for clinical use were initially obtained from mixtures of many subtypes isolated from human lymphoblastoid cells or primary human blood leucocytes stimulated with Sendai virus (7). However, the major improvements achieved in the last decades in the recombinant bioprocessing of biomolecules shifted the paradigm and allowed to use *Escherichia coli* (*E. coli*) as the main source of IFN α -2b for clinical applications. Currently, there are different recombinant unpegylated IFN α -2b (e.g. Intron-A®, Locteron®) and pegylated (e.g. PEG-Intron™) preparations marketed for clinical use (8, 9).

The general strategy employed in a bioprocess to obtain a recombinant biopharmaceutical includes two major stages: (i) the upstream steps associated to cell culture and maintenance, followed by the scale up enhancements; and (ii) the downstream steps associated with the recovery and purification of the target biomolecule from an

heterogeneous and highly complex biological matrix (10). Although the production of IFN α -2b has been extensively studied and optimized (11, 12), this biopharmaceutical is still quite expensive due to difficulties on its recovery and purification. Currently, it is purified using packed-bed chromatographic techniques (13). However, these chromatographic-based downstream processes are responsible for 50–80% of the final cost of production of biopharmaceuticals (4, 10). Thus, it is of crucial relevance to develop cost-effective purification strategies feasible of application by the biotechnology and pharmaceutical industries.

Recently, conventional aqueous two-phase systems (ATPS) were described as an efficient alternative technique for IFN α -2b purification (14, 15). Compared with conventional purification procedures, the advantages of ATPS include short processing times, high capacity loading, high yields, low environmental toxicity, high biocompatibility, and possibility of scale-up (14). In addition to the typical polymer-polymer and polymer-salt ATPS largely investigated in the past decades, the introduction of ionic liquids (ILs) as phase-forming components in ATPS amplified their range of applications. Indeed, IL-based ATPS show an enhanced capacity to tailor the polarities of the coexisting phases, and thus to obtain high extraction efficiencies and purification factors (16).

Based on the exposed, the main objective of this dissertation consists on the production and development of an alternative and cost-effective strategy for human recombinant IFN α -2b purification from *E. coli* cultures using IL-based ATPS, while envisaging their widespread use at a lower cost. For comparison purposes, chromatographic-based purification techniques were also investigated. Although IL-based ATPS have been described as a promising alternative for the purification of therapeutic proteins (16), to the best of our knowledge there are no studies in the literature describing their use for the purification of IFN α -2b.

1.2. Biopharmaceuticals industry and market

The biopharmaceutical industry is the most important sector in industrial biotechnology, and is one of the most rapidly growing high-tech industries (3). The first recombinant biopharmaceutical approved by the Food and Drug Administration (FDA) was human insulin for diabetes treatment, in 1982 (17). Between 1980 and 1990, the biopharmaceutical industry experienced a significant growth in the production and approval of recombinant proteins, including IFNs, growth hormones, monoclonal antibodies (mAbs) and related products (5). In 1993, the global sales value of biopharmaceuticals reached \$5 billion, and after ten years, this value increased to \$35 billion, which represented about 15% of the total global pharmaceutical market (18). Currently, the total market sales from microbial recombinant products reaches approximately \$50 billion, representing one-third of the total sales of biopharmaceuticals (10). Although significant progresses have been done in the past years, drug development is an extremely complex and expensive process. Analysis from the Tufts Center for the Study of Drug Development showed that it may take approximately 15 years of intense research and approximately \$2.6 billion to develop and implement a pharmaceutical in the market (19). Biopharmaceuticals manufacturing is even more expensive than common pharmaceuticals, mostly due to the high cost technology involved in their production and further steps of recovery/purification from a biological-derived complex medium (3).

Figure 1 presents a flowchart on the global process of biopharmaceuticals manufacturing, from the production stage to the recovery, and further downstream processing. Essential steps on the upstream stages involve the selection of the cell clone, culture media, growth parameters, and the optimization of the process in large-scale bioreactors (10). Downstream processing usually encompasses three main steps, namely recovery, purification and polishing (20). While the technological efforts in scaling up the production processes can be considered as rather straightforward, downstream processing is still facing some challenges (20). In early steps, rapid volume reduction and product concentration are the major issues. For this purpose, the main techniques used are centrifugation, filtration, precipitation and/or chromatography (10). Chromatography also dominates the later steps, the selective purification steps, accounting for more than 70% of the downstream costs, mainly owing to media cost and relatively long cycle times (20). Several alternatives have generated long-standing interest either to replace chromatography or to eliminate the chromatography dependency by reducing the load of

impurities in the feed stream. Some examples include ATPS, induced precipitation, crystallization, membrane filtration and membrane chromatography (21).

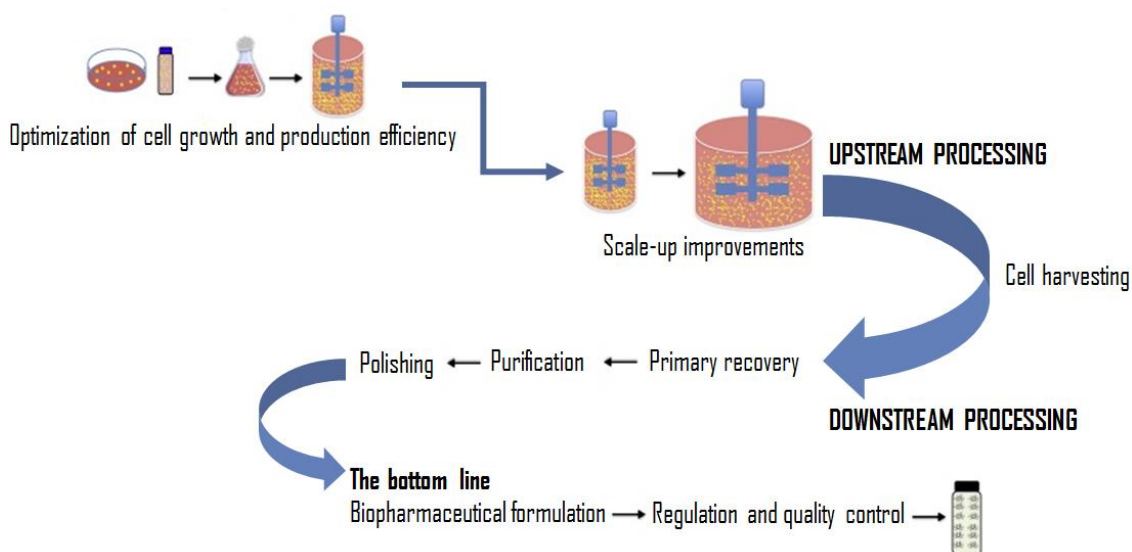


Figure 1: General flowchart of the biopharmaceuticals manufacturing process, adapted from (10).

1.2.1. Interferons market trends

1.3. Interferons

Interferon sales reached a peak between the 1980's and 2000, as it was severely marketed and branded as a “multi-drug” with a growing range of therapeutic effects. The worldwide market for IFNs expanded from \$13.6 million in 1986 to \$751 million in 1992 (18). In 2003, the worldwide sales for therapeutics of interferon alpha (IFN α) (+pegylated) was estimated to be approximately \$2700 million as an antitumor/anti-HIV therapy (22). At the present, the IFN segment covers few diseases due to which they have a limited number of products and modest market shares in the biopharmaceutical industry. Between them, hepatitis and AIDS-related Kaposi's sarcoma disease are the main diseases which generate significant revenues (23). As IFNs can be applied in different diseases, it is expected that they would be able to occupy major market shares across the globe with the developing research. As a result, several interferon therapeutic products are at different stages of clinical trials and will be introduced in the global market in the coming years (23), therefore highlighting the clinical importance of this biomolecule.

1.3.1. Classification of human interferons

Interferons are a multigene family of homologous proteins produced in vertebrates' cells as the body's most rapidly produced defense from the innate non-specific immune system. Most of them have an average Mw in the order of 20 kDa and are involved in cell signaling pathways response, being therefore classified as cytokines (24). In the 80's, Pestka and collaborators (25–27) addressed the molecular characterization and biological activities of IFNs. In humans, although many different types of interferons are produced, the main classes are IFN α , interferon beta (IFN β) and interferon gamma (IFN γ). Based on their structural and functional properties, IFNs have been classified in three main types and several subtypes (28).

Interferons type I [IFN α , IFN β and interferon omega (IFN ω)] are produced in almost all cell types and are considered the primary line of defense against infectious agents and tumour progression (25). IFN ω display a 60–70% amino acid sequence similarity to IFN α sequences, while IFN β only shares 35% (26). The IFN α family is expressed by 18 human genes, 4 of which are pseudogenes, encoding 12 different IFN α proteins subtypes (IFN α 1, IFN α 2... IFN α 21 - gaps in the sequence are due to postulated sequences now known to be erroneous), with one pseudogene and two genes coding for identical IFN α proteins (24, 29). These variants are similar in structure (70-80% homology) with 189 amino acids (188 for IFN α 2) in common. Consequently, they all bind to the IFN α / β receptor (IFNAR), as interferon beta, and exert similar biological activities (30). Some of these subtypes have allelic variants, designated α -2a, α -2b, and α -2c, which differ in only one amino acid at position 23 (arginine in the case of IFN α -2b and lysine in the case of IFN α -2a) (31). There are about 23 different sequences of natural IFN α as well as several recombinant IFN α molecules with novel properties for potential therapeutic applications (8).

Interferons type II only include IFN γ , also known as immune IFN, which binds to the γ receptor (24). It was initially reported by Wheelock (32) in 1965 and shows considerable differences from the remaining ones regarding its biological activity, being induced in response to antigenic or mitogenic stimuli of T cells and natural killer (NK) cells. Finally, interferon lambda (IFN λ) was recently introduced in the interferon family and it was classified as type III. This classification is related with the fact that its structure is more similar to cytokines than other IFNs types, although it shares many functional characteristics with IFN α / β (33).

1.3.2. Interferons as biopharmaceuticals

Interferons were first described in 1957 by Alick Isaacs and Jean Lindenmann as agents that could act against the infection caused by influenza virus (34). The emerging recombinant DNA technology in the 70s and the development of efficient molecular biology tools allowed the production of recombinant IFNs in a larger scale and a broader study of their characteristics, biological activities, and therapeutic potential (35). In 1977, Pestka and collaborators (36) published the first attempts on the purification of IFN α and IFN β from *Xenopus laevis* oocytes. In 1980, Nagata (29) described the successful cloning of at least two distinct sequences corresponding to α -IFNs in *E. coli*. Further studies revealed that these molecules have not only antiviral properties but also potent immunomodulatory and antitumoral activities, allowing broader clinical applications (37).

The production process of the recombinant form of human IFN α -2b was developed by Merck (previously Schering–Plough, Kenilworth, NJ, USA) during the middle 80s, and the genetically engineered protein was first approved by the FDA in 1986 and named as “Intron A” for the treatment of hairy cell leukemia (38). Currently, all 3 types of IFNs are considered as biopharmaceuticals and are applied in monotherapy or in combination with other medicines (39). From the type I IFN, IFN β is extensively used; yet, from the IFN α family, only IFN α 2 is in therapeutic use (39). The formulations of IFN β , such as Betaseron® and Reabif®, are used in the treatment of multiple sclerosis (40), while the formulations of IFN α -2b have been used to treat viral hepatitis infections (41, 42), condylomata acuminata (43), Kaposi's sarcoma (44) and a range of neoplasms, such as melanoma (45), non-Hodgkin's lymphoma (46), chronic myeloid and hairy cell leukaemia (47, 48), and renal cell carcinoma (49) (Table 1).

IFN α 2 is poorly absorbed in the gastrointestinal tract, and its formulations are mainly based on solutions that are administrated parenterally by subcutaneous injection (39). In addition, the conjugation of IFN α with polyethylene glycol (PEG) increases the therapy efficacy. PEG increases the solubility and stability of IFN α by decreasing the proteolysis degradation and renal clearance (50). Moreover, it increases the circulation time from 5 to 90 h, thereby decreasing the amount of protein required for therapeutic efficacy or dosing frequency (42). The pegylated forms of IFN α , with ribavirin as adjuvant, are the currently cornerstone for the treatment of chronic hepatitis C infection, while peginterferon monotherapy is important for the treatment of chronic hepatitis B (51). However, because pegylated forms of IFNs have consequences on

pharmacokinetics, drug dose and patient management, it is important to recognize their differences to ensure an effective treatment (50). Pegylated interferon alpha-2b (PEG-IFN α -2b) is constituted by IFN α -2b and a linear 12 kDa monomethoxylated PEG conjugate (52). It is quickly absorbed, circulates widely, and declines to undetectable serum levels within few days. On the other hand, the PEG conjugate of pegylated interferon alpha-2a (PEG-IFN α -2a) is a larger branched 40 kDa monomethoxylated PEG (53). Therefore, as PEG-IFN α -2a is absorbed slowly, it is largely restricted to the vasculature and well-perfused organs, such as the liver, and is still detectable in serum after a week (50). Compared with peginterferon, hepatitis C treatment with Locteron®, a slow-release microsphere preparation of plant-derived recombinant human IFN α -2b, appears to have comparable efficacy, fewer side effects and reduced dose frequency (51). An estimate of 123 to 170 million people have been infected with hepatitis C virus (HCV) worldwide, and the average cost worldwide for a single treatment using the pegylated interferon and ribavirin can reach \$29,000 (54).

Type II IFN plays a significant role in cellular immune modulation through its effects on T cells and on macrophages. However, its therapeutic potential is currently restricted to use in chronic granulomatous disease (55) and osteopetrosis (56). Ongoing studies have revealed that IFN λ can be important in the treatment of some infections caused by viruses, particularly against chronic hepatitis C. Peginterferon λ 1 is currently at phase III clinical trials (57).

Table 1 shows a summary of commercial formulations and therapeutic applications of IFNs currently used in clinical practice. Most of the formulations are derived from bacterial sources, like *E. coli*, except Locteron®. The patents of first-generation formulations, as Intron-A® and Ropheron-A®, have expired in the United States and Europe countries since 2007, but they are still produced and sold in “off-patent countries”. However, the longer acting pegylated forms of IFNs are the standard therapy in the market (39).

Table 1: Commercial formulations and therapeutic applications of interferons commonly used in clinical practice, extended from (39).

	IFNα	IFNβ	IFNγ	IFNλ
Commercial formulations	Peginterferon α -2a (Pegasys® (58)) Peginterferon α -2b (PEG-Intron™ (59)) Interferon α -2a (Ropheron-A® (60)) Interferon α -2b (Intron-A® (61), Locteron® (62))	Interferon β -1a (Avonex® (63), Rebif® (64)) Interferon β -1b (Betaseron® (65), Extavia® (66))	Interferon γ -1b (Actimmune® (67))	Peginterferon λ 1 (in clinical trials)
Uses	Chronic hepatitis Hairy cell leukemia Chronic myeloid leukemia Renal cell carcinoma	Multiple sclerosis	Chronic granulomatous disease Osteopetrosis	Novel therapy for chronic hepatitis C

The therapeutic potential of IFNs is widely recognized; yet, as they are immunomodulatory molecules involved in several cell signaling pathways, their side effects have limited the effectiveness of treatment leading to decreased adherence and dose-reductions (39). Common side effects are flu-like symptoms (malaise, weakness, fevers, fatigue and headache), neuropsychiatric and dermatological consequences, myelosuppression and the development or exacerbation of autoimmune diseases, specially thyroiditis (39, 68). Furthermore, harmful pulmonary effects are becoming more familiar. Dyspnea is frequently reported (69) and cough in patients infected with HCV is common (70, 71). Other rare but significant side effect is pulmonary arterial hypertension that has been reported to be irreversible in some patients, despite the discontinuation on the IFN therapy (72, 73).

1.4. Interferon alpha-2b molecular characteristics and physiological role

IFN α -2b is a glycoprotein with 165 amino acids, an isoelectric point (pI) of 5.9 (74), and a Mw ranging between 19 and 26 kDa, mainly due to variations in the C-terminal amino acids processing and post-translational modifications (75). The molecule is O-glycosylated at Thr106 (76). According to the tridimensional structure of IFN α -2b depicted in Figure 2, two intramolecular disulfide bonds are formed between four conserved cysteines: Cys1-Cys98 and Cys29-Cys138 (77). The bond formed at the positions 1 and 98 is not essential, while the bond formed at the positions 29 and 138 is essential for biological activity. Other amino acid residues that are important in the biological activity of IFN α -2b are Leu30, Lys31, Arg33, His34, Phe36, Arg120, Lys121, Gln124, Tyr122, Tyr129, Lys131, Glu132, Arg144, and Glu146 (78).

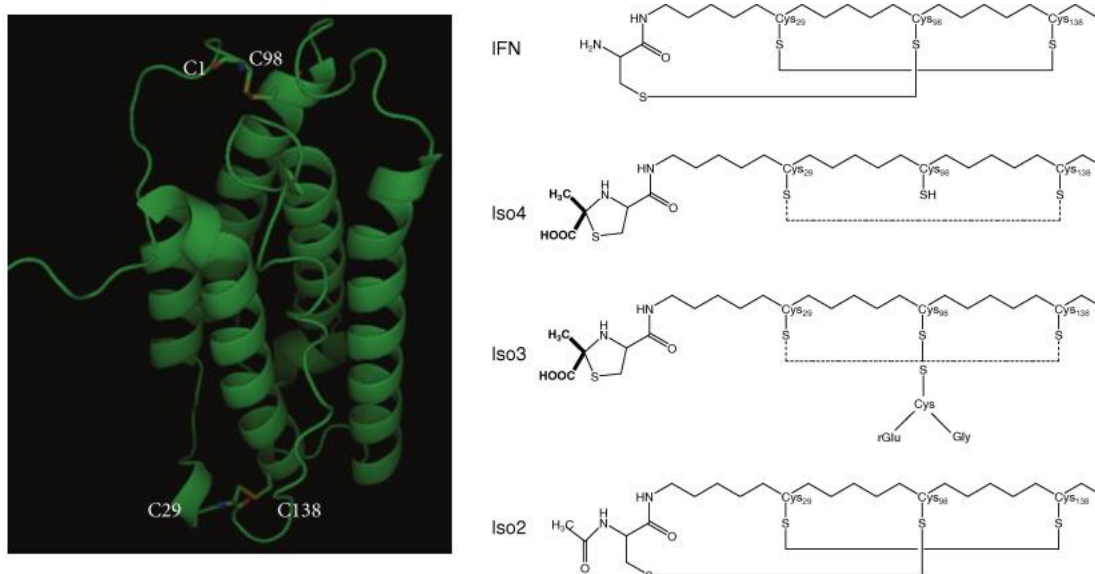


Figure 2: On the left: tridimensional structure of recombinant IFN α -2b. On the right: disulfide patterns of IFN α -2b and its isoforms. The solid line indicates the disulfide bond formation, whereas the dashed line indicates partial disulfide bond formation. Adapted from (79, 80).

Based on the crystal secondary structure mediated by zinc dimer, IFN α -2b can be presented as a monomer or as a non-covalent dimer, being the monomer the active form (78). IFN α -2b monomer consists of five α helices (called helix A to E) that are connected by loops AB, BC, CD, and DE (78). The Cys29-Cys138 disulfide bond connect helix E to the AB loop and helix C to the N-terminal end. Phe36, Tyr122, and Tyr129 are residues important in the structural integrity. Residues that are important in receptor binding are

the AB loop (Arg22, Leu26, Phe27, Leu30, Lys31, Arg33, and His34), helix B (Ser68), helix C (Thr79, Lys83, Tyr85, and Tyr89), D helix (Arg120, Lys121, Gln124, Lys131, and Glu132), and helix E (Arg144 and Glu 146) (78, 79).

Since IFN α -2b can be produced by genetically modified cells, it exists as different isomers. The monomethioninesulfoxide IFN α -2b variant was identified in 1996, and the Met111 residue of the protein did not seem to have a detectable effect on the biological activity of the molecule (81). Other variants of IFN α -2b were identified through reverse-phase high-performance liquid chromatography (RP-HPLC) – Iso-2, Iso-3, and Iso-4 – and further characterized through mass spectrometry (MS) (80).

Human IFN α -2b is encoded by the intronless IFNA2 gene. This gene is located on the short arm of *Homo sapiens* chromosome 9 (9p22) and belongs to the 400 kb alpha interferon gene cluster (82, 83). Its transcription is regulated by several transcription factors including IRF-3 and IRF-7 (IFN-regulatory factor 3 and 7, respectively) (84). The open reading frame of IFNA2 codes for a pre-protein of 188 amino acids, containing a 23 amino acid signal peptide that allows the secretion of the mature protein to the cytosol afterwards (75).

Pathogens induce the production of proinflammatory cytokines and IFNs in host cells, envisaging to protect them from infection. In particular, IFN α is physiologically produced by plasmacytoid dendritic cells (85). Pathogen-associated molecular patterns (PAMPs) and damage-associated molecular patterns (DAMPs) influence the host cell response, thereby leading to alterations in gene expression, causing the start of infectious or non-infectious immune effector mechanisms (86). PAMPs are molecules associated to a group of pathogens that include nucleic acids (RNA and DNA), bacterial lipopolysaccharides, endotoxins, lipoteichoic acid, peptidoglycans and glycoproteins (87) that are recognized by several classes of host pattern recognition receptors (PRRs), including Toll-like receptors (TLRs), RIG-like receptors (RLRs), NOD-like receptors (NLRs) and C-type lectin receptors (86).

TLRs are the best characterized family of receptors. They have differing amino-terminal leucine-rich repeat domains and a carboxyl-terminal intracellular tail with a conserved region, named the Toll/interleukin-1 receptor (TIR) domain. From the 13 TLRs described, only 10 can be found in humans. TLRs 3, 7, 8 and 9 are intracellular and recognize viral PAMPs, whereas the remaining TLRs are involved in bacterial recognition. The recognition by a specific TLR, intra or extracellularly, leads to the activation of MyD88- or TRIF-mediated signaling pathways (88). TRIF-mediated

signaling pathways lead to the translation of inflammatory cytokines such as TNF- α , IL-6, IFN γ and to the activation of transcription factors, like NF- κ B and IRF-3, that lead to the expression of several other genes (89). After activation, these transcription factors translocate to the nucleus and bind to the IFN β promoter leading to the expression of the IFN β and IFN α 4 genes. These are considered the 'primary' IFN genes since their expression is necessary for the subsequent production of other IFNs (84, 90). Moreover, the induction of all other IFN α subtypes, including IFN α -2b, requires the production of other proteins and transcription factors. IFN β and IFN α 4 bind to IFNAR in an autocrine loop and induce IRF-7 expression, which in turn leads to the expression of other IFN α genes, including IFN α 2, and the expression of various IFN-stimulated genes (ISGs) (84). This initiates a positive feedback loop that amplifies the type I IFN response, and rapidly releases a large number of immune effectors (91, 92).

After biosynthesis, the started cascades result in alterations of gene expression by new factors that influence their regulation. This sets up a defensive state both in the cell and in the neighboring cells, through numerous autocrine and paracrine processes ongoing. IFNs exert their actions in the surrounding cells through binding to the cell surface receptors that are specific for each type (30). The alpha, beta, and omega IFNs have a common receptor that is ubiquitously expressed - IFNR. The IFNR have two subunits, IFN-AR1 that is important in signal transduction, and IFN-AR2 which is important in IFN-receptor complex binding (30). A study on the different receptor subunit affinities from various human type I IFNs subtypes led to the conclusion that the binding affinities to the IFN-AR2 domain are higher than that to IFN-AR1 (93). Therefore, as different IFNs will compete for binding to the same receptor, the relative binding affinities and interaction kinetics of each IFN will determine which one will bind to the receptor and, consequently, which signal activation will be developed, thereby explaining the different biological activities (93). Although the affinities were later associated to the anti-proliferative potency of the different IFN α subtypes, no correlation with the anti-viral activities of the subtypes was found (94). The stability of the ternary IFN-receptor complex was later recognized to dictate the biological activity, particularly the anti-proliferative capacity, rather than the affinity to each receptor subdomain (95).

After IFN-receptor binding, signals are sent from the cell surface to the nucleus through different signaling transduction pathways and transcriptional activations. The JAK-STAT pathways, which mechanism is described in Figure 3, is the most common. JAKs are a family of four tyrosine kinases, namely JAK-1, JAK-2, JAK-3 and tyrosine

kinase-2 (TYK-2), each one associated to a corresponding receptor, that are activated through the IFN-receptor binding. Their activation leads to the phosphorylation of STATs, a family of seven cytoplasmic transcription factors: STAT-1, STAT-2, STAT-3, STAT-4, STAT-5a, STAT-5b, and STAT-6. IFN α activates Jak-1 and Tyk-2 kinases that phosphorylate STAT-1 and STAT-2, along with interferon-regulatory factor 9 (IRF-9 or p48), and are translocated to the nucleus while constituting a trimeric complex known as IFN-stimulated gene factor 3 (ISGF-3). The ISGF-3 binds to a cis-acting DNA element, found in the promoter of some IFN α / β -regulated genes, designated interferon stimulating response element (ISRE) and induce the transcription of hundreds of IFN α inducible genes (30, 96, 97).

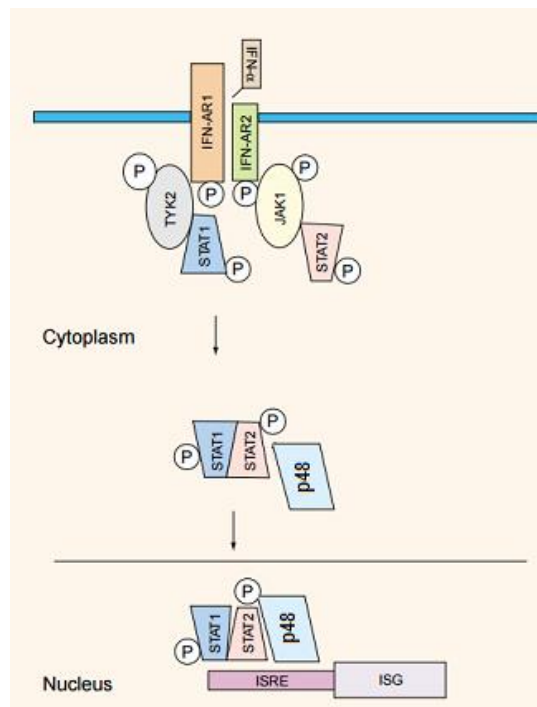


Figure 3: General scheme of the transcriptional activation of JAK-STAT pathways by IFN α , adapted from (96).

IFN α regulates more than 300 genes of signal transduction pathways in cells (79). Individual IFN α subtypes lead to different pathways, different expression of a certain ISG group and different activities, also depending on the cell type (92). The actions of all the IFN α subtypes are pleiotropic and redundant, they are involved in various biological functions (e.g. antiviral, antiproliferative, antitumor and immunomodulatory) and have synergistic or additive effects between them and with other biological response modifiers. Therefore, their individual specific physiological roles are not fully defined. Despite of

IFN α -2b being used mainly in viral and cancer therapy, its major activity is in the modulation of the immune system (30, 92).

Regarding the anti-proliferative capacity, IFN α -2b can either directly inhibit the cancer cell growth through apoptosis or differentiation, or act indirectly on the cancer cells through the activation of immune cells such as T cells, natural killer cells, inhibition of vascularization (anti-angiogenesis) and cytokines induction (79). The molecular mechanisms involved in this process were well described earlier (79), being related with the regulation of proteins translation involved in the MAPK pathway, which control a variety of processes inside the cell, such as proliferation, differentiation, survival and apoptosis.

On the other hand, the IFNs antiviral response strongly depends on the virus, the host cell and the IFN type. For instance, RNA viruses have been reported to induce higher levels of IFN type I transcription than DNA viruses (86). Figure 4 summarizes the mechanisms involved in an antiviral action provided by IFN α , β and γ .

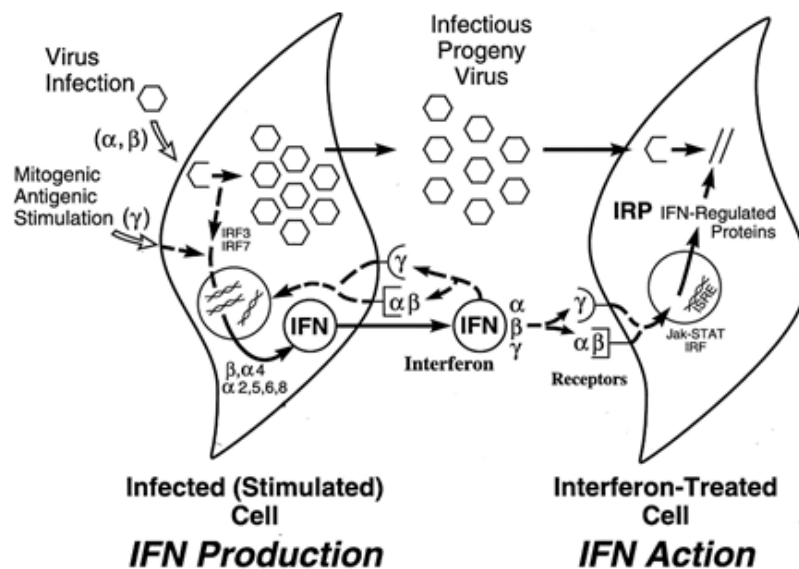


Figure 4: Schematic summary of the IFN antiviral action. Open hexagons represent virion particles and open circles, IFN proteins. Adapted from (98).

The virus induces the cell to synthesize IFN α which exerts a paracrine action on the surrounding cells, further leading to the expression of IFN-regulated proteins which collectively constitute the antiviral response that is responsible for the inhibition of virus multiplication. IFNs may also act in an autocrine manner on the IFN-producer cell. The best-characterized ISG-encoding proteins implicated in the antiviral actions of IFNs in

virus-infected cells are protein kinase (PKR), the 2',5'-oligoadenylate synthetase (OAS) and RNase L, the RNA-specific adenosine deaminase (ADAR), and the Mx protein GTPases, which directly inhibit viral replication. Their functions and mechanisms of action are revised in the literature (98).

1.5. Recombinant proteins - upstream processing

Considering recombinant proteins as a class of biopharmaceuticals, the upstream processing aims to provide large quantities of the target protein, through genetic or chemical engineering, while keeping and/or enhancing their biological characteristics (99). In general, the upstream steps within the recombinant protein manufacturing encompass the isolation of the target gene, cloning this gene into an expression vector, the transformation of the expression host with the recombinant vector, and the biosynthesis of the desired protein in the chosen system (100).

1.5.1. Expression vectors and host expression cells

Any expression vector includes a transcriptional promoter, an origin of replication, the target gene, a selection marker, a 5' untranslated region (5'UTR) and translation initiation site (101). It usually includes fusion tag(s) that can improve protein expression and folding, increase protein solubility or facilitate downstream processes, such as purification and recovery (99). Among these, the promoters, 5'UTR, N-terminal codons and fusion tags, strongly affect protein transcription and translation, protein yields, protein solubility and purification (101).

An effective promoter for heterologous protein expression should be sufficiently strong to allow the accumulation of the target protein to more than (or equal to) 10–30% of the total cellular proteins. It should be tunable, enable simple and inexpensive induction and exhibit minimal basal transcriptional activity in order to avoid transcription before induction (102). Examples of strong promoters used for protein expression in *E. coli* are T7 promoter, the Arabinose promoter, hybrid promoters (*trc* and *tac* promoters) and the *cspA* promoter (102). The pET expression vector featuring the T7 promoter is by far the most widely used system for heterologous protein expression in *E. coli* (103).

The 5'UTR is an untranslated sequence involved in translation initiation and protein expression (104). 5'UTR includes the Shine-Dalgarno (SD) sequence which is responsible for the connection to the ribosome. Therefore, nucleotides and spacing

differences in this region will form different mRNAs, thus affecting the initiation step of protein translation as well as its efficiency, and consequently, production levels (105).

The expression vector can be constructed through the insertion of the target gene into a vector, which can be done by high-throughput cloning-systems: restriction enzyme (RE)-based cloning, recombination-based cloning, annealing-based or ligation-independent cloning. The advantages and disadvantages of each system were revised in the literature (106, 107).

Recombinant proteins can be expressed in prokaryotic, eukaryotic or cell-free systems depending on a variety of biological and technical reasons. The choice of the right host as well as the host strain takes into account: i) security factors, such as pathogenicity and the generally recognized as safe (GRAS) status; ii) protein stability and susceptibility, final quality and functionality; iii) production yield and speed; iv) physicochemical and biological properties of the target protein and host cells; v) expression and regulation of the vector; vi) cell maintenance factors; vii) recovery of the protein; and viii) the desired application (108).

Eukaryotic systems include yeasts (e.g. *Saccharomyces cerevisiae* and *Pichia pastoris*), mammalian cell cultures [e.g. chinese hamster ovary (CHO) cells, murine myeloma (NS0) cells, baby hamster kidney (BHK) cells and human embryonic kidney (HEK) cells], insect cells and plant cells (100). These are usually used to express large proteins, while prokaryotic systems are used to express the smaller ones. Large proteins usually require post-translational modifications, such as disulfide bond formation, phosphorylation or/and glycosylation, that dictate the correct fold of the protein, thus affecting protein stability and biological function (108). Yeasts are the simplest eukaryotic systems. *Saccharomyces cerevisiae* has been used for decades, and its main advantages include: the ability to grow rapidly in cheap media, to perform proteolytic processing, protein folding, disulfide bond formation, and simple post-translational modifications (100). Moreover, it has been accepted as a GRAS organism, which is beneficial in the production of recombinant therapeutic proteins from the regulatory point of view. On the other hand, it is unable to reach high cell densities, and exhibits limited secretion and excessive/irregular glycosylation (109). In contrast with *Saccharomyces cerevisiae*, *Pichia pastoris* can grow up to very high cell densities, performs a less extensive/erroneous glycosylation pattern, and offers higher yields and secretion capacity (Table 2) (110). It should be remarked that the ability of the expression system to produce and secrete soluble folded proteins avoids costly downstream processes of cell rupture,

denaturation and refolding. Mammalian cells are the best option for the production of biologically active proteins since they have a superior ability to perform post-translational modifications. Indeed, most of the therapeutic proteins are produced in mammalian systems (109). While protein quality is an advantage of mammalian cells, protein productivity is not. Moreover, the manipulation of these cells is difficult and expensive since they are suitable to viruses and DNA contamination and require relatively complex culture media (100).

Table 2: Comparison between different expression systems for the production of recombinant proteins (100, 108–110).

	<i>Escherichia coli</i>	<i>Pichia pastoris</i>	<i>Saccharomyces cerevisiae</i>	Mammalian cells	Plant cells
Growth rate	++	+	+	-	-
Protein productivity	+	++	+	-	--
Glycosylation	--	+	++	+	+
Disulfide bonds	--	+	+	+	+
Secretion	-	++	+	+ / ++	+ / ++
Cost	--	--	-	++	++
Examples of produced proteins	Hirudin Insulin Interferons Calcitonin Growth factors	Human serum albumin Collagen Trypsin	Insulin Hepatitis B surface antigen Urate oxidase Eutropin	Blood coagulation factors Erythropoietin Gonadotropin mABs	β -D-glucuronidase Avidin Laccase Trypsin

Legend: ++ high; + / ++ medium to high; + medium; - low; -- very low/absent.

The production of recombinant proteins in plants has also been go through considerable progress. Plant cells have simple growth requirements, an unlimited scalability, and they are versatile production systems able to provide full post-translational modifications (111). The major limiting issues in its commercial application within the biopharmaceuticals industry are the potential immunogenicity of plant-specific glycosylation, the intense surveillance of the transgenic plants varieties by regulatory agencies, and the high costs associated to their regulatory approval (112). The least

expensive, easiest and quickest expression system for recombinant proteins is the bacterium *E. coli*, being the second most popular host for the production of biopharmaceuticals (109). *E. coli* presents the ability to grow on inexpensive carbon sources in short periods of time, it can accumulate recombinant proteins up to 80% of its dry weight, survives in a wide variety of conditions, and its fermentation processes are easily scaled-up (100, 113).

Even though the use of *E. coli* as an expression system has some advantages, there are also some limitations on its use, mainly connected to the protein folding, lack of post-translational modifications, endotoxins contamination and poor secretion (109). Some strains were genetically modified to enhance protein production, as well as the *E. coli* expression strain and culture conditions (e.g. medium density, nutrients, diffused oxygen, pH, temperature, culture by-products, salinity, etc.) (101). In addition, different strains can reduce the potential toxicity exerted by some heterologous proteins on the cell culture itself, increase the stability of mRNA, facilitate cytoplasmic disulfide bond formation, improve the expression of post-translationally modified proteins or facilitate the expression of genes that contain rare codons (114). BL21 strains, which are the most routinely used *E. coli* strains for protein production, contain a chromosomal copy of the T7 RNA polymerase gene and lack the genes for the expression of proteases Lon and OmpT. As a result, they guarantee a simple and efficient expression of the genes under the control of isopropyl β -D-1-thiogalactopyranoside (IPTG) inducible promoters, thus increasing the protein stability (101).

1.5.2. Recombinant interferon alpha-2b biosynthesis

There are several expression vectors described in the literature (Table 3) for recombinant IFN α -2b biosynthesis (13, 74, 113, 115–123). There are also commercially available vectors, such as pGL2BIFN, pALCA1SIFN, PP324, PP326 and pENTR223.1, that already include the IFNA gene and can be found in plasmid repositories (124, 125) or in sellers of biological materials (126).

Table 3: Host systems, expression nature, expression vectors and production yield of recombinant IFN α -2b.

Host	Expression nature	Expression vector	Yield	Ref.
<i>Escherichia coli</i>	Intracellular, insoluble	pAE	0.2 g/L	(116)
<i>Escherichia coli</i>	Intracellular, insoluble	T7 RNA polymerase-based vector pRSET	3 g/L	(74)
<i>Saccharomyces cerevisiae</i>	Extracellular, soluble	YRp7 variants	Not reported	(115)
<i>Streptomyces lividans</i>	Extracellular, soluble	pADXS, pUCIAS, pOVsiIFN and pOW15	Max 0.58 μ g/L	(113)
<i>Pichia pastoris</i>	Extracellular, soluble	pPICZ α -hIFN α 2b	0.6 g/L	(117)
<i>Pichia pastoris</i>	Extracellular, soluble	pPICZaA	0.298 g/L	(13)
<i>Lactococcus lactis</i>	Intra- or extracellular, soluble	pNZ-ifnm and variants	0.024 g/L	(118)
<i>Yarrowia lipolytica</i>	Extracellular, soluble	PICZ α and JME variants	0.43 g/L	(122)
Mouse cells	Extracellular, soluble	pEE12	0.12 g/L	(123)
<i>Trichoderma reesei</i>	Extracellular, soluble	pTTv254 variants	2.4 g/L	(119)
<i>Trichoderma reesei</i>	Extracellular, soluble	pTTv254 variants	>4.5 g/L	(119)
Plant chloroplasts	Intracellular, soluble	pLD-CtV	0.003 g/g of plant leaf	(120)
Transgenic plants cells	Intracellular, soluble	pCB124 and pCB161	Not reported	(121)

IFN α -2b was produced and isolated for the first time in 1980 using *E. coli* (127), and since then, although several host systems have been employed for their biosynthesis (Table 3), *E. coli* is still the current choice for the recombinant production of IFN α -2b.

Recently, *Trichoderma reesei* appeared as a potential competitor host of *E. coli* in the production of IFN α -2b (119). Considering that therapeutic proteins, including the IFN α -2b, are naturally unstable and very susceptible to endogenous proteases, these strains can contribute to overcome a relevant drawback in protein production that is the proteolytic degradation. The strains generated have a producing potential upward, from 2.5 g/L to 4.5 g/L, with the addition of proteases inhibitors (119).

1.6. Recombinant proteins - downstream processing

After recombinant proteins production, the downstream stages foresee the extraction of the target protein from the harvested cells, followed by its purification in a cost-effective way. The final purification level and yield depend not only on the purification strategy, but also on the upstream stage that consequently influences the initial concentration of the protein and its purity. A discussion on the critical factors that influence the early steps of downstream processing and a comparison between traditional purification techniques and ATPS, including IL-based ATPS, will be presented below, focusing on IFN α -2b purification.

1.6.1. Primary recovery and isolation

The recovery of recombinant proteins depends on the physicochemical properties of the protein, expression host and protein location (128). IFN α -2b can be secreted or recovered from the cell, in a soluble or insoluble form, according to the host characteristics, as summarized in Table 3.

From the downstream point of view, secreted proteins are preferred over cytoplasmic ones because of the additional steps involved in their purification. On the other hand, cytoplasmic proteins allow higher production yields (114). In *E. coli*, heterologous proteins like IFN α -2b are often produced intracellularly in the form of inclusion bodies, which are amorphous insoluble aggregates of proteins (74, 116). As an alternative, they can also be expressed intracellularly in a soluble state or be exported to the periplasm (12). Since the cytoplasm is a reducing environment, the inclusion bodies formed are usually inactive and possess non-native intra- and inter-molecular disulfide

bonds and unusual free cysteines (129). The mechanisms of their formation are related with protein properties such as charge, hydrophilicity, cysteine and proline fractions, total number of residues, and culture and folding conditions (temperature, pH, and nutrients) (11). The inclusion bodies formation may also present some advantages: their composition is usually highly enriched in the target heterologous protein, the proteins are less susceptible to the activity of proteases, and can be readily separated from bacterial cytoplasmic proteins through centrifugation (101). The strategies for protein extraction from inclusion bodies are quite common, but to obtain the active protein the aggregates must be removed from the cells, solubilized and refolded. This not only extends the downstream stage, but also affects the integrity and yield of the refolded protein (130).

It has been reported that insoluble recombinant proteins can be overexpressed in *E. coli*, in the soluble form, by adding compatible solutes, such as sorbitol, arginine, and trehalose, to the culture medium (131). Moreover, several approaches have been undertaken to avoid inclusion bodies formation in *E. coli*, including periplasmic secretion, lower culture temperatures, lower inducer concentrations, and lower induction periods, and the use of fusion tags such as glutathione S-transferase (GST) and maltose-binding protein (MBP) (130). High-throughput methods for inclusion bodies purification can also be performed using a robotic microfuge. This automated approach excludes the need of using tags and allows the protein expression, recovery and purification alongside, because inclusion bodies can be readily separated from soluble proteins through centrifugation (101).

In a typical procedure of inclusion bodies recovery, the harvested *E. coli* cells are firstly separated from the culture medium through centrifugation. Further, the cells are disrupted either by mechanical forces (e.g. high-pressure homogenization, sonication, glass beads, liquid homogenization, freeze-thaw cycles), chemical methods (e.g. osmotic lysis, organic solvents, surfactants) and enzymatic methods (e.g. lysozyme) (100). Regarding this step, the optimized conditions should maximize cell lysis, the extraction yield and stability of the recombinant protein, while minimizing protein oxidation, unwanted proteolysis and sample contamination with genomic DNA through the addition of reducing agents, proteases inhibitors and DNases/Benzonase, respectively (103). Then, the inclusion bodies are removed from the cell lysate by centrifugation and the pellet is washed from adhering impurities and solubilized in a high concentration of denaturant, such as urea and guanidine hydrochloride (GdnHCl), or ionic detergents, such as N-lauroylsarcosine, Triton X-100 and sodium deoxycholate, or with phosphate-buffered

saline (PBS). In addition, dithiothreitol (DTT), 2-mercaptoethanol (2-ME), or dithioerythritol (DTE) are commonly added to reduce the non-native disulfide bonds (11, 132). Finally, after solubilization, the inclusion bodies are refolded using refolding techniques that take into account several factors, such as protein concentration, co-aggregation of protein contaminants, temperature, pH, and ionic strength. The yield of the refolded protein decreases with the increasing concentration of the solubilized proteins undergoing renaturation and with the aggregation of contaminant proteins (11). Therefore, some purification protocols of inclusion bodies include a purification step *prior* to refolding (11, 132, 133). Conventional refolding techniques are based on the gradual decrease of the denaturant concentration through dilution on a refolding buffer or dialysis. Other alternatives, such as the co-expression of chaperones and foldases, the addition of small chemical molecules and the refolding on a laminar flow in microfluidic chips, have been also attempted aiming to decrease the degree of aggregated and/or misfolded proteins (132). Dashbolaghi and co-workers (134) described an improved refolding method of IFN α -2b via pH modulation. In this study (134), although an increase in the pH of the refolding buffer from 7 to 8.5 led to an improvement in the refolding efficacies from 42.28 % to 71.22 %, the highest biological activity of IFN α -2b was achieved at pH 8.

Valente and colleagues (11) described an optimized protocol for the primary recovery of IFN α -2b from *E. coli* inclusion bodies. Based on the sequential evaluation of the parameters involved in the aforementioned recovery steps – cell lysis, inclusion body isolation, washing and solubilization – the authors were able to maximize both the IFN α -2b recovery yield and purity (11).

1.6.2. Chromatographic-based purification processes

Conventional chromatography is a well-established technique that is widely applied in biomolecules separation/purification, and is based on differences in the movement rate of the species carried by a fluid mobile phase toward a solid stationary phase. In a packed bed chromatography, the sample is introduced and transported by the eluent along the column. The sample components will percolate the chromatographic column at different speeds, according to the degree/strength of interaction, and will eventually allow the separation and collection of products of interest in a high purity degree (135). Based on the type of interactions established between the solid stationary phase and biomolecules, chromatographic techniques can be summarized into five

classes: i) affinity; ii) ion-exchange; iii) hydrophobic interactions; iv) size exclusion; and v) mixed-mode chromatography (135).

Chromatography presents high resolution, being often applied in therapeutic proteins purification. However, despite chromatography has been the workhorse of protein separation, it is the main responsible for the major drawback in biopharmaceuticals production, i.e. the high cost (20). Upstream developments that end with processes capable of delivering higher-titers have been pushing chromatography beyond their physical and economical limitations and, consequently, the current platforms have reached their limits of throughput and scalability (20, 136). Scaling up problems are related with the optimization of column size and operation conditions, as well as column stability during the processing. Large columns can be as robust and reliable as small ones, but require larger media and longer cycle times. The high costs of the resins, buffers, and other consumables may also exceed the upstream gains (136). Furthermore, there are some mass transfer limitations involving key parameters as flow-rate, average pore size and solute diffusion coefficient in solid chromatographic columns (137), which may result in unpredictable fluid distribution and pressure drops. Moreover, due to the batch mode, separation usually requires long times of operation because successive steps of extraction, purification and polishing are required (21).

1.6.3. Aqueous two-phase systems

ATPS were found by Beijerinck in 1869 (138), by mixing agar and gelatin at certain concentrations in aqueous media, from which two fully separated aqueous phases were formed. The extractive potential of ATPS was only explored almost a century later, when Albertsson (139) studied the possibility of using these systems for the fractionation of cell walls materials from microorganisms. Since then, ATPS have been largely investigated (140).

ATPS are established above certain concentrations of two solutes dissolved in aqueous media, resulting in the formation of two phases, each one enriched in one of the solutes. Since two aqueous phases exist, these systems are promising strategies within liquid-liquid extraction approaches. ATPS have been already applied in the separation and purification of different biological materials, such as cells, virus, organelles, nucleic acids, lipids, amino acids, proteins, antibodies and enzymes from complex mixtures (16). Nevertheless, to apply ATPS in the extraction and purification of distinct compounds, their phase diagrams and respective tie-lines should be determined and known in advance.

Phase diagrams are specific for each ATPS, under certain conditions of temperature and pH (140). They provide information about the concentration of components to form a two-phase system, the concentration of the phase components in the top and bottom phases, and the ratio of phases volume or weight. In Figure 5 it is presented the schematic representation of an ATPS phase diagram, in an orthogonal representation for which the amount/content of water is omitted. The binodal curve TCB separates the concentrations that form immiscible phases (above the curve – biphasic region) from the concentrations that are miscible and form only one phase (below the curve – monophasic region) (16). The larger the biphasic region, the higher the ability of the phase-forming components to undergo liquid-liquid demixing. The TB line is the tie-line (TL) that connects two nodes of the binodal curve, and gives the composition of each phase for mixtures prepared along the given TL. The tie-line length (TLL) is a numerical indicator of the composition difference between the two phases and is generally used to correlate trends in the partitioning of solutes between both phases (16). S1, S2 and S3 represent three mixture compositions; because they are on the same tie-line, they have the same top phase and bottom phase equilibrium compositions, although differing in their volume ratio. The point C on the binodal curve is the critical point (140).

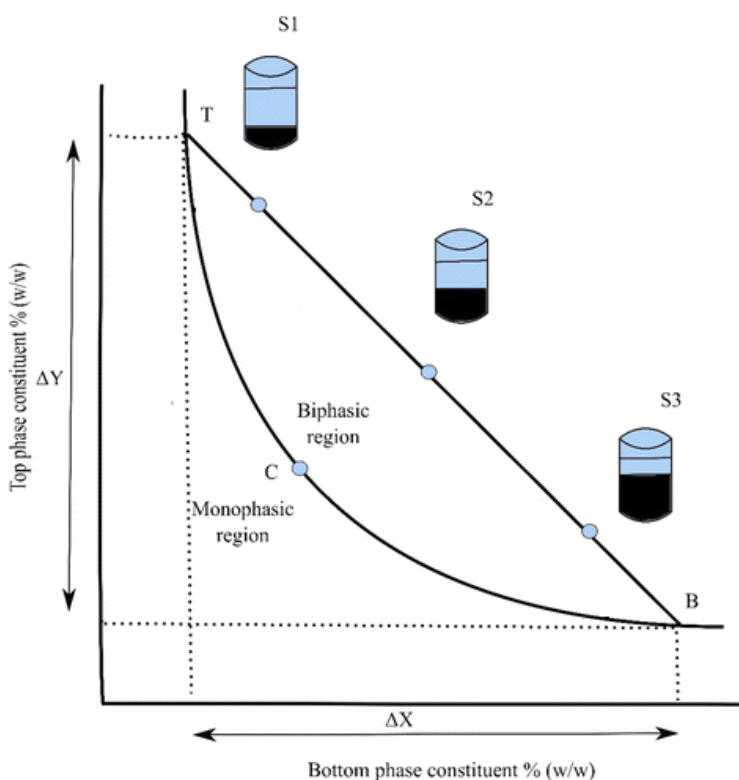


Figure 5: Schematic representation of a phase diagram, adapted from (140).

ATPS are mainly composed of water and overcome several limitations of other separation techniques, namely the conventional liquid-liquid systems which use volatile organic solvents that easily promote proteins denaturation, in addition to the low protein solubility in these organic media and environmental and human safety concerns (16). ATPS display a higher biocompatibility due to their predominantly water-based nature, that provides a good environment for biomolecules, allowing them to maintain their characteristics (141). Moreover, organic solvents are volatile, toxic and inflammable, making them difficult to handle considering the security measures that have to be adopted (142). In addition to liquid-liquid extraction strategies, ATPS also present some advantages over chromatographic-based techniques, since the scale-up of ATPS is simple and can be done in a single-step (143). In fact, their technical feasibility has been reported up to a 100000 L scale for the purification of proteins (136).

A study comparing the performance of ion-exchange chromatography with an ATPS composed of PEG1450/phosphate for the partial purification of penicillin acylase, confirms that ATPS is a more cost-effective technique and can significantly reduce the unit operation steps (144). Other comparative studies between ATPS and other techniques revealed a higher capacity, higher biomolecules recovery (145), higher purities (146), and a reduction in investment and operational costs. The integration of ATPS with other processes and tools can be the breakthrough in the downstream processing of biopharmaceuticals (140). ATPS are already used in extractive fermentation, integrated with other separation techniques or integrated with other analytical techniques to reduce the number of individual processing steps and to improve the overall performance of manufacturing (21). Besides penicillin purification with ATPS, alcohol dehydrogenase was also efficiently purified using an integrated process of PEG precipitation and ATPS (147). Furthermore, centrifugal partition chromatography (CPC) in combination with ATPS was demonstrated to be a promising separation technique for biomolecules (148).

The general characteristics of phase formation in ATPS have been largely explored (149); however, the physicochemical interactions involved are very complex, making the partition behavior of biomolecules poorly understood. In fact, the partitioning of a target biomolecule into one specific phase is a complex process that depends on the surface properties of all molecules involved in the system and their interactions. These properties include size [Mw, surface area], charge, hydrophobicity, and structural conformation of the target molecule, as well as the type, size, concentration and characteristics of the phase-forming components (140). The interactions that influence

the partitioning in ATPS are usually short-range (van der Waals) and long-range electrostatic interactions between the biomolecule and the surrounding phases (150), as well as excluded volume effects (16). Ideally, at the end, the target biomolecule should be concentrated in one phase and the contaminants in the other, in one-step extraction (141).

Regarding proteins partitioning in ATPS, most of the proteins tend to concentrate in the most hydrophobic and less polar phase (151). Hydrophobic interactions are considered the most important effects in protein separation in ATPS, particularly in polymer/salt systems (152). However, the partitioning trend of proteins depends on the ATPS constituents, and electrostatic interactions were also considered by other authors as the driving forces for separation (153). Although ATPS is a promising technique, the main limitations in downstream processing at an industrial scale is the poor understanding of the partition mechanism and the handling, storage and disposal of residues (136). Modern high throughput screening platforms can be a viable option to reduce the laborious and time consuming screening of the various variables involved in the partitioning (143).

The most common ATPS investigated are constituted by polymer/polymer (usually PEG and dextran), polymer/salt or salt/salt (e.g. potassium phosphate, potassium sulfate or sodium citrate) combinations in aqueous media. Other types of ATPS include ILs, short-chain alcohols (e.g., propanol and ethanol), surfactants, thermo- or pH-sensitive polymers, modified affinity polymers, among others. All of these systems were developed to upgrade their performance in what concerns the recovery of the target biomolecule with a high purification level and yield (21, 140).

Polymer-based ATPS composed of PEG are largely studied, not only because PEG is commercially available at low prices in a large range of Mw, but also because it is biodegradable, presents low toxicity, as well as low volatility (141). Polypropylene glycol (PPG) has an additional methyl group than PEG, and is thus more hydrophobic and tend to form ATPS with a wider range of other phase-forming components. PPG is also biodegradable and can be easily recovered by heating (thermoseparating polymer) at low working temperatures (154). It has been demonstrated that PEG stabilizes the protein three-dimensional structure through the formation of a non-associating PEG-intermediate complex and therefore contributes to proteins refolding and reestablishment of their biological activities (155). However, most of these polymer-based ATPS have a restricted polarity difference between the coexisting phases and thus lead to low extraction

efficiencies and low selectivity values. To overcome this drawback, IL-based ATPS were proposed in the last decade as a more efficient alternative for the extraction and purification of a wide plethora of compounds (16).

ILs are molten salts with a melting temperature below 100 °C, usually formed by an asymmetric organic cation and an organic or inorganic anion (156). Figure 6 depicts the chemical structures of some ILs extensively investigated. Although they were reported for the first time in the beginning of the 20th century by Paul Walden (157), few interest was devoted at that time on these new solvents. Some years later, new families of ILs were developed through the combination of the 1-ethyl-3-methylimidazolium cation and a large range of anions (e.g. ethanoate, sulfate, nitrate, biscyanamide, etc), and further combination of these anions with new classes of cations (e.g. phosphonium and pyrrolidinium) (158). Currently, there are more than two thousand reported ILs (156). The ILs properties are mainly related with their ionic character: negligible vapor pressure, high thermal and chemical stabilities, and an enhanced solvation ability for organic, inorganic and organometallic compounds. Their negligible volatility and non-flammability have contributed to their common designation of “green solvents” (16). “Designer solvents” is also a common designation of ILs since their physical and chemical properties can be adjusted by appropriate anion/cation pairs for a specific application (156). Although ILs have been considered as non-toxic solvents due to their negligible vapor pressure, studies demonstrated that many ILs display some toxicity (159). Their toxicity is already known to be associated to the hydrophobic character of the IL. The ILs toxicity is primordially determined by the cation nature and it is directly correlated with the length of the alkyl side chain as well as with the number of alkyl groups at the cation (160). For instance, imidazolium-based ILs are more toxic than cholinium-based, which are usually derived from choline chloride, a vitamin/nutrient that can be found in different food sources, either vegetables or animals, and supports several essential biological functions (161).

In 2003, the Rogers research group (162) reported for the first time that it was possible to create an ATPS by the addition of an inorganic salt (K_3PO_4) to an aqueous solution of ionic liquid (1-butyl-3-methylimidazolium chloride). Figure 6 shows the chemical structures of the ILs commonly used for ATPS formation. It has been latter found that the formation of an IL-based ATPS follows the decrease in the hydrogen-bond-accepting strength or the decrease in the hydrogen-bond basicity of ILs anions (163). The

increase of the number of alkyl groups present in the cation also enhances the formation of IL-based ATPS, whereas the insertion of a double bond has the opposite effect (164).

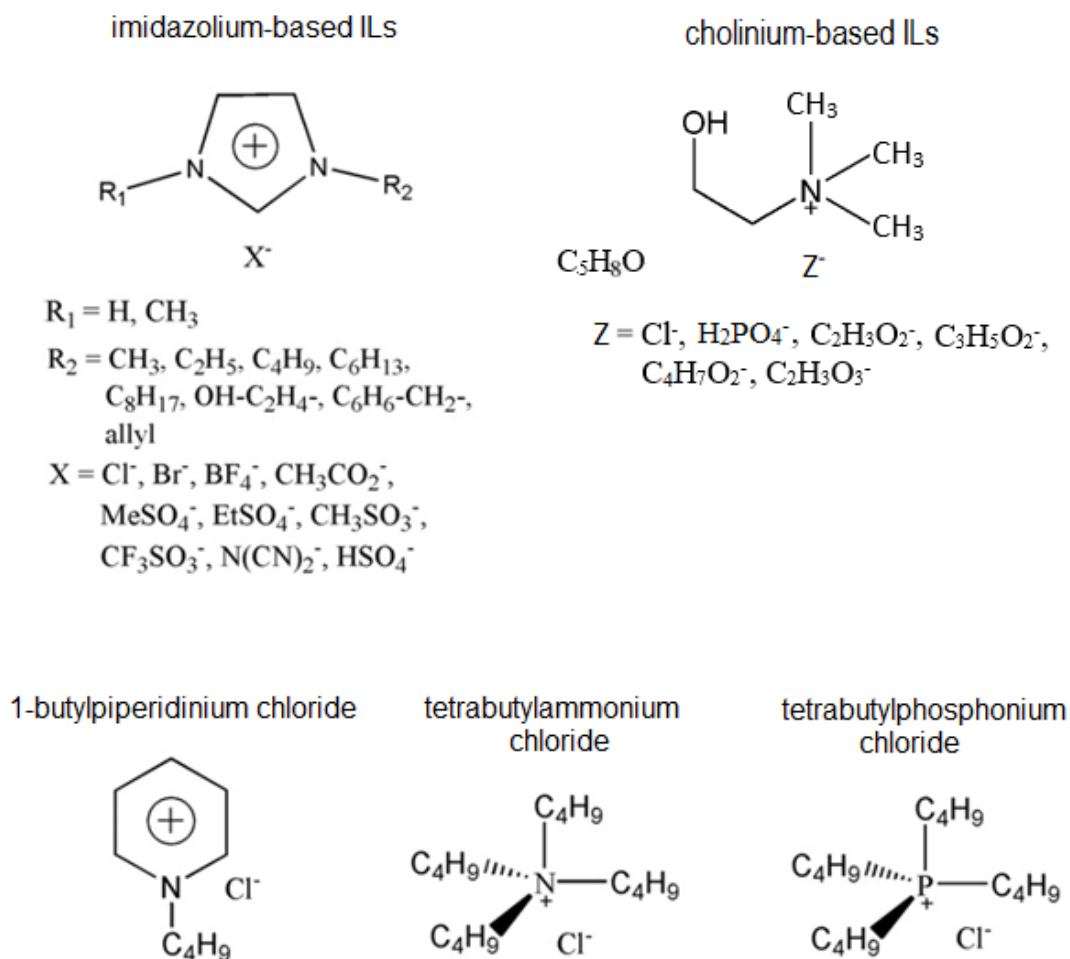


Figure 6: Chemical structures of the ionic liquids commonly used for aqueous two-phase systems, extended from (165).

Compared with polymer-based ATPS, IL-based ATPS have a relatively lower viscosity due to the IL nature (165). The decrease of viscosity allows overcoming mass transfer limitations for extraction purposes, allowing a rapid phases separation (16). Furthermore, polymer/polymer and polymer/salt ATPS have a restricted polarity range that can be only manipulated by the polymer and salt type, and their composition, or through the addition of adjuvants or polymer chemical modifications (166). IL-based ATPS overcome this issue since ILs can be tuned by the manipulation of the anion/cation, allowing to enhance the differences in polarities between the two phases and to enhance

the selectivity for the extraction of a target compound (167). Accordingly, the partition coefficients of L-tryptophan in IL-based APTS are higher than those typically obtained with polymer-inorganic salts or polymer-polysaccharides aqueous systems (163, 164). The addition of ILs as adjuvants in conventional APTS was also demonstrated, being a determinant factor in the biomolecules partitioning trend during extraction (166, 168–171). Pereira and collaborators (166) demonstrated that the partition behavior of L-tryptophan depends mainly on the IL employed. The addition of imidazolium-based ILs at 5 % wt to a PEG-based APTS increased the extraction performance from 175.6 ± 2.4 to 245.0 ± 9.5 of lyophilic lipase produced from *Bacillus sp.* (168). On the other hand, the addition of polymers to IL-APTS was also recently reported (172), where PEG was investigated as adjuvant, allowing to increase the partition coefficients of α -amylase. In general, larger differences in polarity result in larger partition coefficients of biomolecules in IL-based APTS, as demonstrated by Ruiz-Angel and colleagues (173). Moreover, some studies also demonstrated that ILs used in APTS formation can be recycled and reused after extraction procedures (174).

PEG/IL APTS were reported for the first time by Freire and collaborators (175), who suggested that the occurrence of these biphasic systems is dependent on the interactions between the polymer and the ionic species, and not only on the hydration forces of the individual IL or salt ions as typically observed in IL/salt APTS. Further works on this line have been recently published (176–179).

It is important to guarantee that proteins maintain their native conformation in order to be biologically active, after the purification step using IL-based APTS. In 2007, Du and co-workers (180) tested, for the first time, APTS based on the 1-butyl-3-methylimidazolium chloride IL and K_2HPO_4 for the extraction of proteins, demonstrating that IL-based APTS are enhanced extraction platforms for proteins (165). In the purification of dehydrogenases with IL-based APTS, their specific activity was shown to increase in presence of ILs (181). Several IL-based APTS have been successfully used in the extraction of folded model proteins (182–186), as well as from complex matrices (161, 187), but since ILs inevitably affect the pH of the aqueous solution, phosphate-based buffered solutions were usually used (16). Nevertheless, phosphate ions can bind with metal ions (calcium, zinc or magnesium) and interfere with the integrity of some proteins/enzymes (188). Therefore, a novel class of ILs named Good's buffer ILs (GB-ILs) were recently used to form IL-based APTS with aqueous solutions of inorganic or organic salts (189), with outstanding stabilizing characteristics on the protein secondary

structure. In this work (189), GB-ILs were able to extract folded bovine serum albumin (BSA) with 100% efficiency in a single step. GB-ILs were also demonstrated to be an excellent stabilizing medium for enzymes, independently of temperature, while showing the capacity to form ATPS with a biodegradable citrate salt, with significant selectivity for the extraction of lipase (190).

In addition to the largely investigated imidazolium-based ATPS, the employment of cholinium-based ILs in ATPS not only results in more biocompatible systems, but also have been proved to be efficient in the extraction and purification of proteins/biopharmaceuticals, such as BSA (182), trypsin, papain and lysozyme (183), and immunoglobulin G (IgG) (191). The GB anions tricine, TES, CHES, HEPES, and MES were combined with cholinium cations (184, 192), resulting in self-buffering ILs able to form ATPS with higher biocompatibilities and non-toxic character. The use of cholinium instead of imidazolium cations allowed to form ATPS with biodegradable polymers as substitutes of high-charge density salts. This favored the partition of proteins since it also increased the difference of the ionic strength between the phases (184). The use of self-buffering ILs and PPG 400, as phase constituents in polymer/GB-IL ATPS, allowed to stabilize and extract immunoglobulin Y (IgY) to the GB-IL rich phase from the water soluble fraction of proteins from egg yolk with extraction efficiencies ranging from 79-94% (184), while the extraction of BSA was completely achieved in a single-step (192). Therefore, GB-IL-based ATPS are currently considered one of the most biocompatible systems for the efficient separation and extraction of biologically active biomolecules, including therapeutic proteins (184).

1.6.4. Purification of the recombinant interferon alpha-2b

Since IFN α -2b is obtained from a heterologous matrix of biological compounds, the purification ratio depends not only on the initial concentration of the IFN α -2b in the crude feedstock but also on the concentration of other biological components, which depend on the host expression system and on the existence, or not, of prior recovery and isolation procedures. There are some studies that report the purification of IFN α -2b. Ion-exchange chromatography (13, 74, 116, 117, 193) and affinity chromatography (123, 130, 194) are the most reported methods, as single methods or in combination with other techniques. A summary of the host, extraction yield, specific activity and purity of different purification methods for recombinant IFN α -2b is provided in Table 4.

In general, the purification yield seems to be proportional to the initial concentration of IFN and its purity, with higher purification yields achieved when the initial concentration and purity of IFN α -2b is higher (13, 74). The highest extraction yield (64%) was achieved with two chromatographic steps, the first with a Q-Sepharose ion-exchange column, followed by ultrafiltration, and the second with a SuperdexTM 75 size-exclusion column (13). The IFN α -2b was obtained directly from the fermentation supernatant of *Pichia pastoris*, with a final purity higher than 95 % in RP-HPLC (13). *Pichia pastoris* is capable of secreting IFN, and since it does not secrete a large amount of intrinsic proteins, higher purity levels are expected. However, the recovery yields depend on the applied purification/recovery procedure (13, 117). The second highest extraction yield (58 %) was obtained in a single-chromatographic step with a Q-Sepharose ion-exchange column (74). In this study (74), extra steps of cell lysis, washing/denaturation, solubilization and refolding were used in order to obtain the refolded IFN α -2b from the intracellular inclusion bodies produced by *E. coli*. However, since the inclusion bodies constituted more than 40 % of the total cellular proteins, these could be recovered without significant loss by pelleting them out from the total cell lysate followed by washing with a deoxycholate buffer (74). These steps allowed to obtain initial IFN α -2b purities of 80 % and simultaneously lead to the concentration of the protein prior to the principal purification step. The purity was evaluated through silver-stained sodium dodecyl sulfate-polyacrylamide gel electrophoresis (SDS-PAGE), with a final reported purity of 99 % (74). Although the extraction yield was lower than the one mentioned previously, a single ion-exchange chromatography step was sufficient to eliminate the remaining contaminants. In addition, the specific activity of the IFN α -2b was higher in the single-step chromatographic procedure than in the two-step chromatographic procedure: 3×10^9 IU/mg and 1.9×10^9 IU/mg, respectively (Table 4). Beldarrain and colleagues (194) reported a similar study where the IFN α -2b was obtained from the refolding of inclusion bodies. Although the purities of the IFN α -2b obtained were high, the renaturation procedure led to a 50 % loss of the protein, with a significantly low recovery yield (12 %). Moreover, in this study (194), the effect of the pH and temperature on the conformational stability of the IFN α -2b was evaluated. The thermal unfolding as a function of the pH showed only one endotherm at a temperature higher than 45 °C, an irreversible phenomenon at pH values ranging between 4 and 10. The most suitable condition was obtained at pH 7.0, but the conformational stability depends on the protein concentration and ionic strength (194).

Table 4: Comparison between host, extraction yield, specific activity and purity of different purification methods for the recombinant IFN α -2b.

Purification steps	Host	Extraction/ Recovery yield (%)	Specific Activity (IU/mg)	Purity (%)	Ref.
Single step ATPS (alcohol/salt)	<i>Escherichia coli</i>	74.64	Not reported	Not reported	(15)
Anion-exchange chromatography, ultrafiltration and gel filtration	<i>Pichia pastoris</i>	64	1.9×10^9	>95	(13)
Anion-exchange chromatography	<i>Escherichia coli</i>	58	3×10^9	~99	(74)
Single step ATPS (PEG/salt)	<i>Escherichia coli</i>	40.7	Not reported	Not reported	(14)
Filtration, desalting and ion- exchange chromatography	<i>Pichia pastoris</i>	30	1.5×10^8	100	(117)
Immobilized metal-ion- affinity chromatography, RP-HPLC and ion-exchange chromatography	<i>Escherichia coli</i>	12	$>1 \times 10^8$	100	(194)
Immuno-affinity chromatography	Mouse cells	Not reported	2×10^8	Not reported	(123)
Two immobilized metal- affinity chromatographies, anion-exchange chromatography	<i>Escherichia coli</i>	10.5	Not reported	99.8	(130)
Cation-exchange chromatography	<i>Escherichia coli</i>	92.1	Not reported	91.7	(193)
		72	Not reported	56.8	
Immunomagnetic separation, size-exclusion HPLC	<i>Pseudomonas sp.</i>	89.5	2.7×10^8	92.9	(195)

Xu and collaborators (193) reported both soluble and insoluble production of endogenous recombinant IFN α -2b in *E. coli*. Although the expression level of the soluble protein was lower than the insoluble fraction, their results suggest that the soluble expression have more advantages than the insoluble one. The soluble IFN α -2b could be purified directly by chromatography, while the insoluble fraction had to be dissolved with guanidinium hydrochloride and refolded by dilution. The soluble protein expression could facilitate the downstream process and allow higher recovery yields, higher purities and higher biological activities (Table 4) (193). Is important to notice that the extraction yield in this study (193) was calculated based on the biological activity, and not in mass percentage. Therefore, this yield cannot be compared with the ones discussed before. Moreover, it was found that the use of three protein fusion tags, namely the b'a' domain of human protein disulfide isomerase (PDIB'a'), MBP and NusA, increased the intracellular soluble expression of IFN α -2b from 30 to more than 45 % of total proteins (130). Nevertheless, the fusion tag can facilitate the initial steps of affinity purification but also requires an additional step of cleavage of the tag. It should be remarked that clinical applications of bacterially produced biopharmaceuticals may be affected by the potential presence of endotoxins, sometimes present in *E. coli* expressed protein preparations. These endotoxins are contaminants of expressed protein preparations, and thus should be considered in the determination of the purity level of IFN α -2b, and additional care has to be taken into account (130).

Cao and colleagues (195) reported the purification of IFN α -2b using magnetic microspheres coupled with anti-IFN α -2b mAb for immunomagnetic separation. This technique takes advantage of the selectivity of immunoaffinity chromatography combined with the efficiency of magnetic response. In this study (195), the purity of IFN α -2b obtained was of 92.9 %, and the extraction yield, which was calculated regarding the biological activity, was lower than the one obtained with a cation-exchange chromatography (88.5 % and 92.1 %, respectively).

Chromatographic-based techniques present high resolution, leading to purities near 100% required for the commercial application of IFN α -2b as a biopharmaceutical. However, these techniques are laborious and high-cost procedures. To overcome these drawbacks, ATPS have been also investigated as alternative purification techniques. Lin and collaborators (14, 15) investigated, for the first time, the use of ATPS for the purification of IFN α -2b. In both studies, IFN α -2b was obtained from the periplasm of *E. coli* after osmotic shock, centrifugation, and two sequential cell pellets resuspension in a

cold buffer solution comprising 20 % (w/v) sucrose, 0.03 M Tris-HCl, 5 mM sodium EDTA (pH 8.0) and cold ultra-pure water. Compared to conventional chromatographic purification methods, the IFN α -2b extraction yields obtained with ATPS composed of PEG/potassium phosphate or 2-propanol/ammonium sulfate were outstanding: 40.7 % and 74.64 %, respectively (Table 4). The purity of IFN α -2b was evaluated by SDS-PAGE, and provided as purification factor (P_F). The P_F obtained with polymer/salt ATPS was 26.30, while the P_F obtained with alcohol/salt ATPS was lower (16.24), meaning that the latest system was less efficient for the purification of IFN α -2b. ATPS were also investigated as concentration techniques, as demonstrated by the SDS-PAGE results in which the IFN α -2b band was shown to be significantly more intense in the top phase than in the crude stock sample (14). Although the specific activity of the IFN α -2b was not reported and its conformational stability was not studied, these results suggest that polymer/salt and alcohol/salt ATPS are a valuable alternative for IFN α -2b extraction and purification since they are a simpler, cheaper and fast one-step methods.

To the best of our knowledge, the investigation on the addition of ILs as adjuvants in these ATPS or the use of IL-based ATPS still remain uncovered in the recovery and purification of IFN α -2b. Taking into account the high complexity and disadvantages of conventional chromatographic methods, as well as the limitation of conventional polymer/polymer and polymer/salt ATPS, the introduction of ILs as phase-forming components of ATPS to develop cost-effective platforms for the purification of IFN α -2b seems feasible of further investigation.

2. Experimental section

2.1. Recombinant interferon alpha-2b production and recovery

2.1.1. Chemicals

Tryptone and yeast extract were obtained from Biokar diagnostics (Allonne, France). Sodium chloride (≥ 99.0 % purity), dextrose (D-Glucose), trimethylolaminomethane (Tris base, ≥ 99.8 % purity), hydrochloric acid, Triton™ X-100, urea (99.5 % purity) and tetramethylethylenediamine (TEMED) were obtained from Thermo Fisher Scientific (Waltham, MA, USA). Ampiciline and DNase (DNase I 200U, from bovine pancreas recombinantly produced in *Pichia pastoris*), IPTG (> 99 % purity) and SDS were acquired from Nzytech (Lisbon, Portugal). *E. coli* BL21 cells, magnesium chloride (MgCl₂ anhydrous line, ≥ 98 % purity), magnesium sulfate heptahydrate [MgSO₄·7H₂O BioUltra line, ≥ 99.5 % purity (KT)], phenylmethylsulfonyl fluoride (PMSF) and EDTA-free Protease Inhibitor Cocktail, lysozyme from chicken egg white (protein lyophilized powder ≥ 90 % purity, ≥ 40.000 U/mg protein), L-Glutathione reduced (GSH, > 98.0 % purity), L-Glutathione oxidized (GSSH, > 98 % purity), ammonium persulfate (APS) and rabbit anti-chicken were bought from Sigma-Aldrich (St Louis, MO, USA). The chicken polyclonal to IFN α -2b antibody was obtained from Abcam (London, United Kingdom). DTT was acquired from Himedia (Einhausen, Germany). Penicillin/Streptomycin solution (10000 U/mL Penicillin and 10 mg/mL Streptomycin in 0.9 % NaCl), fetal bovine serum (FBS with origin in South America) and acrylamide were obtained from Grisp (Porto, Portugal). pET-3a containing the codon optimized sequence of IFN α -2b was acquired from Genscript (Piscataway, NJ, USA). Polyvinylidene Difluoride (PVDF) membrane and ECL substrate were brought from GE Healthcare Biosciences (Uppsala, Sweden).

2.1.2. Experimental procedure

The plasmid pET-3a containing the human IFN α -2b gene (Figure 7) was employed for the expression of the target protein in its native form. This plasmid is based on the pBR322 plasmid, and it contains the T7 promoter, which is inducible by IPTG, the target gene and the amp^R gene, which was used as a selectable marker as it confers resistance to ampicillin. *E. coli* BL21 cells were transformed with the target recombinant plasmid by heat-shock. Moreover, to favor the expression of IFN α -2b onto this bacterial host, the human IFNA2 gene, without any glycosylation signal, was codon-optimized to

E. coli codon usage bias (OptimumGene™ algorithm, Genscript). The main constituents of the plasmid are illustrated in Figure 7.

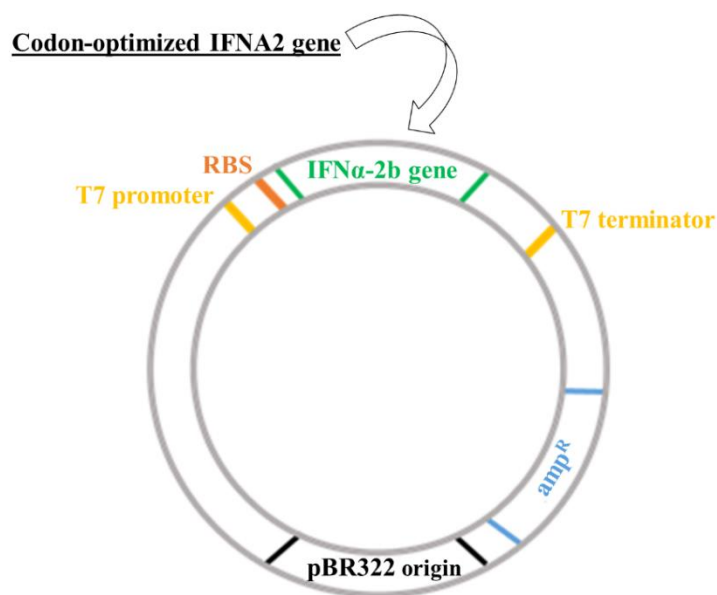


Figure 7: General scheme of the pET-3a plasmid; it includes the T7 promoter and terminator, the ribosomal binding site (RBS), the target IFN α -2b gene, the ampicillin selection marker (amp^R) and the pBR322 origin of replication.

Unless otherwise stated, the recombinant biosynthesis of IFN α -2b was performed according to the following protocol: *E. coli* BL21 cells containing the expression construct were grown overnight at 37 °C in Luria Broth (LB) (1 % w/v tryptone, 0.5 % w/v yeast extract, and 1 % w/v NaCl, supplemented with ampicillin 100 μ g/mL) plates. Then, for the pre-fermentation, colonies were picked and used to inoculate 62.5 mL of SOB medium (2 % w/v tryptone, 0.5 % w/v yeast extract, 0.05 % w/v NaCl, supplemented with ampicillin 100 μ L/mL) in 250 mL shake-flasks at 37 °C and 250 rpm, until the optical density at 600 nm (OD₆₀₀) reached 2.6. Then, and according to Equation 1, a certain volume obtained from the pre-fermentation was added to 125 mL of SOB medium in 500 mL shake-flasks, since the inoculation volume was fixed to achieve an initial OD₆₀₀ of 0.2 units. When the culture reached an OD₆₀₀ of 0.6 units, the induction was initiated through the addition of 0.5 mM IPTG. Finally, after a 3 h growth period at 37 °C and 250 rpm, cells were harvested by centrifugation (3900 g, 20 min, 4 °C) and stored at – 20 °C until use. The LB and SOC (SOB supplemented with 2 % w/v glucose) media were also tested for the expression of the target protein.

$$\begin{aligned}
& OD_{600} \text{ Pre} - \text{Ferm} \times V\text{Pre} - \text{Ferm} \\
& = (V\text{Pre} - \text{Ferm} + V\text{Ferm}) \times \text{Initial}OD_{600}\text{Ferm}
\end{aligned}
\tag{1}$$

where $OD_{600} \text{ Pre} - \text{Ferm}$ corresponds to the OD_{600} values in the pre-fermentation, $V\text{Pre} - \text{Ferm}$ is the volume of the pre-fermentation medium used to initiate the fermentation, $V\text{Ferm}$ is the volume of fermentation medium, and $\text{Initial}OD_{600}\text{Ferm}$ corresponds to the OD_{600} values at the beginning of the fermentation.

All measurements of optical densities were performed at 600 nm, while 0.8 % NaCl was used as the blank since it reflects the sterile media. *E. coli* was produced at 37 °C and 250 rpm, until the cell culture suspension reached an OD_{600} near 2.6. All the employed materials and media were autoclaved at 120 °C during 15 min, while all the manipulations were performed using aseptic techniques in a laminar flow cabinet, or otherwise using flame.

The bacterial cell pellets were resuspended in a lysis buffer composed of 50 mM Tris-HCl pH 7.5, 150 mM NaCl, and 5 mM DTT in a ratio of 20:1. A protease inhibitor cocktail (10 uL/mL) and 1 mM PMSF were also added to inhibit the activity of the host proteases over the IFN. The cellular lysis was accomplished either with a mechanical method using glass beads, or with an enzymatic method using lysozyme. Regarding the mechanical method, a ratio of 1:2:2 was employed, namely to 0.5 g of wet cells, 1 g of glass beads and 1 mL of lysis buffer were added; then, the lysis was accomplished by vortexing the mixture during 7 cycles of 1 min, spaced with 1 min incubations in ice. Regarding the enzymatic method, the cells were incubated with 10 mg/mL lysozyme and stirring at 4 °C during 3 h.

After the lysis process, and envisaging the decrease of the sample contamination with genomic DNA, the mixture was incubated during 20 min with DNase (1 µL) on ice, until it was centrifuged (5000 g, 10 min, 4 °C). Then, a subcellular fractionation was performed and the samples classified as soluble and insoluble – inclusion bodies. As it was verified that the target protein is mainly produced in the form of inclusion bodies, the experimental procedure adopted for the recovery of IFN α -2b was based on that previously reported by the Valente research group (11). Briefly, the cells were centrifuged at 5000 g, 4 °C, during 10 min and further resuspended, washed and solubilized in specific buffer formulations at different conditions. In particular, different solubilization buffers were applied for IFN α -2b extraction, composed of 50 mM Tris-HCl buffers at distinct pH

values – 8.0 and 12.5 -, 10 uL/mL protease inhibitor cocktail, 1 or 20 mM DTT and supplemented with 2, 4, 6 or 8 M urea. It should be remarked that 6 M GdnHCl was also evaluated as an alternative to urea. Several washing buffers were also screened, namely with 50 mM Tris-HCl buffers at pH 8, 10 uL/mL of protease inhibitor cocktail, 1 % deoxycholic acid, H₂O Mili-Q, Triton X-100 0.5 % or 1 %, and 2, 4 and 8 M urea at pH 8. Between and in the end of the extraction/washes, centrifugations of 15000 g, 4 °C, during 10 min were performed. The ability of the washing buffers to remove contaminants, the IFN α -2b yield and the ability of the extraction buffer to promote the fully extraction of the target protein from the insoluble fraction, were evaluated by SDS-PAGE and Western-Blot assays. At the end, the supernatant corresponding to the solubilized inclusion bodies (SIB) was stored at 4 °C for further refolding and purification. The SIB fraction was refolded through successive dialysis against refolding buffers containing 10 mM Tris pH 8, 50 mM NaCl, 1 mM GSH, 0.1 mM GSSH and decreasing concentrations of urea. The first dialysis was performed during 6 h with 4 M urea, the second during 8 h with 2 M urea, the third during 6 h with 1 M urea, the fourth during 6 h with 0.5 M urea, and the fifth overnight using 0 M of urea.

The experimental procedure adopted for the SDS-PAGE and Western-Blot analysis is as follows: the samples were boiled for 5 min in a loading buffer containing 0.5 M Tris-HCl pH 6.8, 10 % SDS (w/v), 0.02 % bromophenol blue (w/v), 0.2 % glycerol (v/v), 31 % DTT (w/v) and then run on SDS gels (4.7 % stacking, 15 % resolving) at 90 V for 15 min and at 110 V for 2 h. The stacking gel was prepared with 1.25 M Tris-HCl pH 6.8, 0.05 % acrylamide (v/v), 0.28 % Mili-Q H₂O (v/v), 0.001 % SDS (v/v) and the resolving gel was prepared with 1.875 M Tris-HCl pH 8.8, 0.15 % acrylamide (v/v), 0.60 % Mili-Q H₂O and 0.01 % SDS (v/v). Both gels were supplemented with 50 μ L TEMED and 200 μ L APS and placed in a Bio-Rad Mini Protean 3 Cell Gel Electrophoresis System. After running, the gels were stained by Coomassie brilliant blue or transferred to a PVDF membrane to perform the Western-Blots. The transference of the proteins was done in a Bio-Rad Criterion™ Blotter during 30 min at 200 mA, at 4 °C, in a buffer containing 0.58 % 50 mM Tris-HCl pH 7.5 (w/v), 0.29 % 380 mM glycine (w/v) and 20 % methanol (v/v). After the blotting, the membranes were blocked with TBS-T (pH 7.4) containing 5 % (w/v) non-fat milk for 1 h at room temperature and exposed overnight at 4 °C to a chicken polyclonal antibody (AB14039), that cross reacts with the IFN α -2b, at 1:2000 dilution in TBS-T 0.5 % of non-fat milk. Then, the membranes were washed three times, during 15 min each, with TBS-T 0.1 % and incubated with rabbit anti-chicken IgY

secondary antibody, during 1 h, at a 1:10000 dilution in TBS-T 5% of non-fat milk. After antibody adherence, the membranes were washed again with TBS-T 0.1 %, as mentioned before, and finally observed by incubation with 300 μ L of ECL substrate and exposure to chemiluminescence's detection.

2.2. Chromatographic purification of interferon alpha-2b

2.2.1. Chemicals

L-Arginine-Sepharose 4B gel and HiTrap Desalting column (5 mL) were obtained from GE Healthcare Biosciences (Uppsala, Sweden). CIM® DEAE-1 monolithic tube column was obtained from BIASeparations (Ajdovščina, Slovenia).

2.2.2. Experimental procedure

All the chromatographic experiments were performed in an ÄKTA Avant system with UNICORN 6 software (GE Healthcare, Uppsala, Sweden). The SIB of IFN α -2b were purified using an arginine column, a HiTrap Desalting containing Sephadex G-25 Superfine column and on a CIM DEAE monolith.

The L-arginine-Sepharose 4B gel was packed within a 10 mm diameter \times 20 mm long (about 4 mL) column. All solutions were filtered through a 0.20 μ m pore size membrane. Chromatographic runs were performed at room temperature. Unless otherwise stated, for the experiments performed with L-arginine-Sepharose and CIM DEAE monolith, the column was initially equilibrated with 50 mM Tris buffer (pH 8.0). The *E. coli* SIBs were applied onto the column using a 1.0 mL loop at a flow rate of 1.0 mL/min. After the elution of unbound species, the ionic strength of the buffer was increased to 0.35 M of NaCl and then to 1 M NaCl in 50 mM Tris buffer (pH 8.0). The absorbance of the eluate was continuously monitored at 280 nm. In what concerns the HiTrap Desalting experiments, the isocratic elution of the different protein species was performed at 0.3 mL/min with 50 mM Tris buffer (pH 8.0).

Fractions were pooled according to the chromatograms obtained, concentrated and desalted with Vivaspin concentrators (10,000 MwCO), and further analyzed by SDS-PAGE and Western-Blot.

2.3. Biological activity of interferon alpha-2b

The biological activity of IFN α -2b was measured through its anti-proliferative capacity against MCF-7 cells, based on the protocol previously reported by the Ningrum

research group (196). MCF-7 adenocarcinoma cells from human mammary glands were brought from ATCC[®] HTB-22[™] (Barcelona, Spain). These were cultured in Dulbecco's Modified Eagle's Medium (DMEM) high glucose, containing 10 % of Fetal Bovine Serum (FBS) and 1 % of streptomycin/penicillin. After 90 % of confluency, the cells were washed with phosphate buffer saline (1.15 g Na₂HPO₄; 0.2 g KH₂PO₄; 8 g NaCl and 0.2 g KCl per liter, pH 7.2), and detached with 500 μL of trypsin at 37 °C for 5 min. Then, the cells were seeded in 96 well plates (2000 cells/well) and further grown until a confluency of 40-60 % was reached. Then, chromatographic-purified IFNα-2b at a concentration of 50 μg/mL was used for transfection that lasted 5 days. The IFNα-2b biological activity was measured by its ability to induce cell death, measured as cytotoxicity in the MTS cell proliferation assay acquired from Promega (Madison, USA). The absorbance was measured at 490 nm. Ethanol was used as the positive control. Circular Dichroism (CD) experiments were performed in a Jasco J-815 spectropolarimeter (Jasco, Easton, MD, USA), using a Peltier-type temperature control system (model CDF-426S/15). CD spectra were acquired at a constant temperature of 25 °C using a scanning speed of 10 nm/min with a response time of 1 s over wavelengths ranging from 190 to 260 nm. The results were expressed as the molar mean residue ellipticity (mdeg) at a given wavelength. The recording bandwidth was 1 nm with a step size of 1 nm using a quartz cell with an optical path length of 1 nm. Three scans were averaged per spectrum to improve the signal to-noise ratio and the spectra were smoothed by using the noise-reducing option in the operating software of the instrument.

2.4. Purification of interferon alpha-2b using IL-based ATPS

2.4.1. Chemicals

The salt di-potassium hydrogen phosphate (K₂HPO₄, 99.0 ≥ wt% purity) was brought from Panreac (Barcelona, Spain) and the salt potassium dihydrogen phosphate (KH₂PO₄, purity ≥ 99.5 wt%) was obtained from Sigma-Aldrich (Sintra, Portugal). The 2-(N-morpholino)ethanesulfonate hydrate (99.5 % purity), tetramethylammonium hydroxide (25 wt% in H₂O), tetrabutylammonium hydroxide (40 wt% in H₂O), tetrabutylphosphonium hydroxide (40 wt% in H₂O), choline hydroxide (45 %wt in methanol) and deuterium oxide (D₂O > 99.9 wt% purity) were also acquired from Sigma. Ethyl acetate (> 99.0 % purity) was obtained from Carlo Herba (Lisbon, Portugal). Methanol (HPLC grade, purity > 99.9 %) was obtained from Chem-Lab. Acetonitrile

(HPLC grade, purity > 99.9 %), acetic acid (> 99.99 %) and the L(+)-arginine amino acid (> 98 %) were obtained from Thermo Fisher Chemical. 1-butyl-3-methylimidazolium methylcarbonate (30 wt% in methanol) was obtained from Proionic (Grambach, Austria). Sodium hydroxide pellets were acquired from Eka Chemicals (Lisbon, Portugal).

2.4.2. Experimental procedure

2.4.2.1. Synthesis and characterization of ionic liquids

In this work, fifteen ILs were investigated, namely tetrabutylammonium acetate ([N₄₄₄₄][Ac]), tetrabutylammonium 2-(N-morpholino)ethanesulfonate ([N₄₄₄₄][MES]), tetrabutylammonium arginine ([N₄₄₄₄][Arg]), tetrabutylphosphonium acetate ([P₄₄₄₄][Ac]), tetrabutylphosphonium 2-(N-morpholino)ethanesulfonate ([P₄₄₄₄][MES]), tetrabutylphosphonium arginine ([P₄₄₄₄][Arg]), 1-butyl-3-methylimidazolium acetate ([C_{4mim}][Ac]), 1-butyl-3-methylimidazolium 2-(N-morpholino)ethanesulfonate ([C_{4mim}][MES]), 1-butyl-3-methylimidazolium arginine ([C_{4mim}][Arg]), tetramethylammonium acetate ([N₁₁₁₁][Ac]), tetramethylammonium 2-(N-morpholino)ethanesulfonate ([N₁₁₁₁][MES]), tetramethylammonium arginine ([N₁₁₁₁][Arg]), choline acetate ([Ch][Ac]), choline 2-(N-morpholino)ethanesulfonate ([Ch][MES]) and choline arginine ([Ch][Arg]), and their chemical structures are shown in Figure 8. These ILs were synthesized *via* neutralization of the base with the corresponding acid, and as described in detail in the literature (184, 197, 198). For instance, to synthesize [N₁₁₁₁][Ac], an aqueous solution of acetic acid was added through repetitive drop-wise into an aqueous solution of tetramethylammonium hydroxide. Then, the mixture was stirred at room temperature during 24h. To guarantee the formation of the IL, a 1:1.1 mole relation between the base and the acid was considered, and the precursors were added by weight. The water or methanol solvents obtained as an excess were evaporated at 50-60 °C under reduced pressure. The amino-acid-based ILs were washed with a mixture of acetonitrile and methanol (1:1, v/v) while vigorously stirred. Since arginine is not soluble in this solvent, the excess buffer was removed through filtration followed by solvent evaporation. The other ILs were washed three times with ethyl acetate, which was also removed by evaporation. After eliminating most of the impurities, the ILs were dried in vacuum (10 Pa) for a maximum of 6 days at 25-50 °C to remove all the remaining volatile solvents. The chemical structures of the ILs were confirmed by ¹H and ¹³C NMR spectroscopy (Bruker AMX 300) operating at 300.13 and 75.47 MHz, respectively. Chemical shifts are expressed in δ (ppm) using

tetramethylsilane (TMS) as internal reference and D₂O as deuterated solvent. The water content of the synthesized ILs was determined by coulometric Karl Fischer titration (Mettler Toledo DL 39) with the Hydranal Coulomat AG reagent (Riedel de Haën), except for [N₄₄₄₄][Arg] and [P₄₄₄₄][Arg] which water content was determined by dry weight.

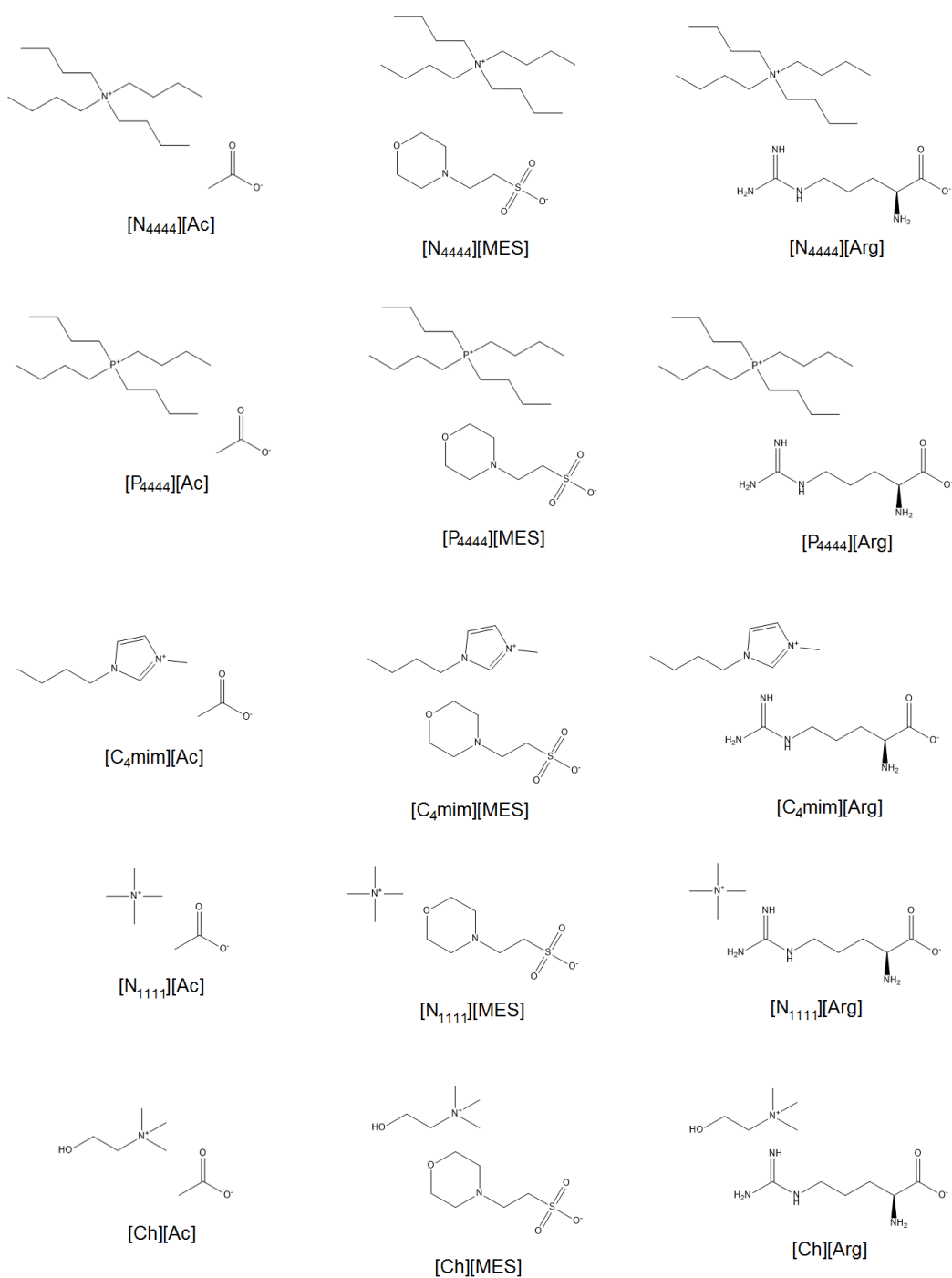


Figure 8: Chemical structure and abbreviation of the synthesized ILs.

2.4.2.2. ATPS ternary phase diagrams

The new ATPS phase diagrams of the ILs + K₂HPO₄/KH₂PO₄ + H₂O were determined at room temperature (≈ 25 °C) and at atmospheric pressure. The ILs used were [N₄₄₄₄][MES], [P₄₄₄₄][MES], [P₄₄₄₄][Ac], [N₄₄₄₄][Ac], [C_{4mim}][MES], [N₁₁₁₁][Ac] and [P₄₄₄₄][Arg]. The potassium buffer used was a mixture of two aqueous solutions of potassium phosphate dibasic and monobasic at a ratio of 20.05, resulting in an aqueous solution with a pH of 8.2. The aqueous inorganic salt solution was added to an IL rich solution using the drop-wise addition method until the detection of a cloudy biphasic solution. Then, the drop-wise addition of water was done until the formation of a clear monophasic region. The opposite addition, *i.e.* a repetitive drop-wise addition of the IL aqueous solution to the potassium phosphate solution until the detection of a cloudy biphasic solution, followed by the drop-wise addition of water until the detection of a monophasic region, was also carried out to obtain more complete phase diagrams. The pH values of both the IL-rich and salt-rich aqueous phases were determined at (25 ± 1) °C using a METTLER TOLEDO SevenMulti pH meter within an uncertainty of ± 0.02 .

The binodal data obtained for the systems composed of H₂O, K₂HPO₄/KH₂PO₄ and the ILs [N₄₄₄₄][MES], [P₄₄₄₄][MES], [C_{4mim}][MES], [N₄₄₄₄][Ac], [N₁₁₁₁][Ac], [P₄₄₄₄][Ac] and [P₄₄₄₄][Arg] were fitted using Equation 2 (199):

$$[IL] = A \exp[(B[Salt]^{0.5}) - (C[Salt]^3)] \quad (2)$$

where [IL] and [Salt] are the IL and salt concentrations, respectively, and *A*, *B* and *C* are fitted constants obtained by least-squares regression. Each individual TL was determined by the application of the lever-arm rule to the relationship between the weight of the top and bottom phases and the overall system composition. For the determination of the TLs, the following system of four equations (Equations 3-6) (199) was solved to estimate the four unknown values (IL_T , IL_B , $Salt_T$, $Salt_B$):

$$[IL_T] = A \exp[(B[Salt_T^{0.5}) - (C[Salt_T^3])] \quad (3)$$

$$[IL_B] = A \exp[(B[Salt_B^{0.5}) - (C[Salt_B^3])] \quad (4)$$

$$[Salt_T] = \frac{[Salt_M]}{\alpha} - \frac{1 - \alpha}{\alpha} [Salt_B] \quad (5)$$

$$[Salt_B] = \frac{[IL_M]}{\alpha} - \frac{1 - \alpha}{\alpha} [IL_B] \quad (6)$$

where the subscripts [IL] and [Salt] designate the salt- and IL-rich phases, respectively, M , T , and B denote respectively the mixture, the top phase and the bottom phase. The parameter α is the ratio between the top weight and the total weight of the mixture. The solution of this system results in the concentration (wt%) of the IL and salt in the top and bottom phases, and thus the, TLs can be easily represented.

For the calculation of the TLL, Equation 7 was applied:

$$[IL] = \sqrt{([Salt_T] - [Salt_B])^2 + ([IL_T] - [IL_B])^2} \quad (7)$$

All the calculations considering the mass fraction or molality of the K_2HPO_4/KH_2PO_4 buffer were carried out discounting the complexed water in the salt. In all systems, the IL-rich phase corresponds to the top phase while the bottom phase corresponds to the K_2HPO_4/KH_2PO_4 phase.

2.4.2.3. Extraction of interferon alpha-2b using IL-based ATPS

The ATPS composed of ILs + K_2HPO_4/KH_2PO_4 + H_2O were used to purify the IFN α -2b SIB; however, before any experiment and to remove any possible interferences, urea was removed using the HiTrap desalting matrix in an Akta system, as mentioned above. The total protein concentration in these samples was determined using Pierce™ BCA Protein Assay Kit (Thermo Scientific, USA), using bovine serum albumin as the standard (0.025–2.0 mg/mL), according to manufacturer's instructions.

In general, ATPS with 0.8 g of total weight were prepared, and the chosen extraction point for the experiments was 40 wt% IL + 9 wt% K_2HPO_4/KH_2PO_4 . At this mixture point all systems form two-phases that could be easily separated. The IL and the phosphate salt aqueous solutions were gravimetrically added and stirred in an orbital rotator overnight. Then, the IFN α -2b SIB was weighted and added to the mixture. After 10 min of contact in an orbital rotator at room temperature, the ATPS were centrifugated at 5000 g, at room temperature during 10 min. The systems were left in equilibrium at the workbench for more 10 min to guarantee the equilibration of the coexisting phases at the target temperature, and to achieve the complete partitioning of IFN α -2b and the remaining

contaminant proteins between the two phases. The phase's separation was then carefully performed, using disposable syringes of 1 mL, and both phases were weighted. In some systems, there was the formation of an interphase precipitate – three-phase partitioning – which was isolated and solubilized with 75 μ L 50 mM Tris-HCl, during 2 h under soft stirring. All the resulting samples (i.e. top phase, bottom phase, and solubilized precipitate) were analyzed by SDS-PAGE.

3. Results and Discussion

3.1. Recombinant interferon alpha-2b production

3.1.1. Optimization of the experimental conditions for interferon alpha-2b production

The cellular growth of *E. coli* BL21 harboring the plasmid pET 3-a_{IFN} α 2b over the fermentation time in three different compositions media (LB, SOB and SOC) is shown in Figure 9. The experimental data are reported in Appendix A. All culture media are suitable for *E. coli* proliferation, once the three microbial cultures are able to achieve the exponential phase, although the growth is less pronounced for LB. Moreover, the highest biomass levels ($OD_{600} = 4.13$) were obtained using the SOC medium after 9 h of fermentation; yet, the production levels were distinct.

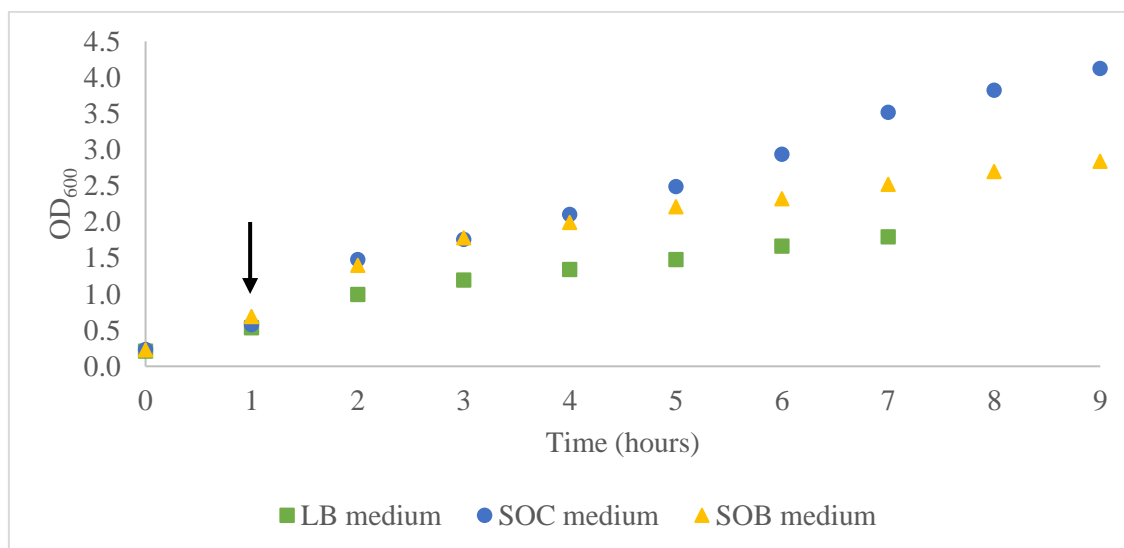


Figure 9: Growth profile of *E. coli* BL21 harboring the plasmid pET-3a_{IFN} α 2b at different incubation periods (ranging from 0 to 9 hours) on LB, SOC and SOB media. Fermentation was initiated at an OD_{600} of 0.2 and the cultures were induced with 0.5 mM IPTG at an OD_{600} of approximately 0.6, as indicated by the arrow.

In the earlier steps, using 0.5 mM IPTG and an induction temperature of 37 °C, assays were carried out with the three-culture media, and a subcellular fractionation into soluble and insoluble samples was performed. These results are depicted in Figure 10, demonstrating that IFN α -2b is not detected in the soluble fraction, which corresponds to the supernatant of the centrifuged extract; indeed, as expected [72], the IFN α -2b appeared with a Mw between 17-20 kDa exclusively in an insoluble form as inclusion bodies.

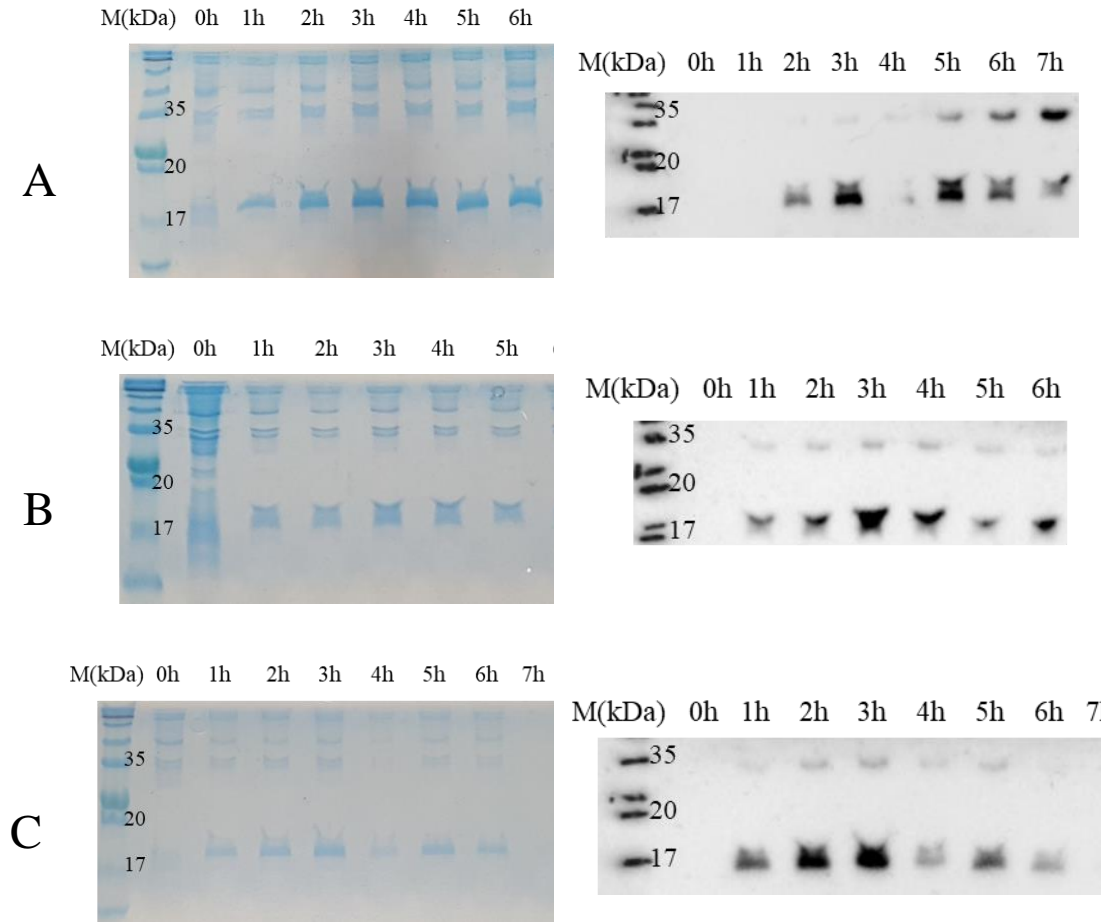


Figure 10: SDS-PAGE (left) and Western-Blot (right) analysis of the different samples obtained after the subcellular fractionation of *E. coli* BL21 cultures (37 °C and 250 rpm) in distinct culture media: A – SOB, B – LB, C – SOC, after 0-7 h of induction. Fermentation was initiated at an OD₆₀₀ of 0.2 and the cultures were induced with 0.5 mM IPTG at an OD₆₀₀ of approximately 0.6. Samples were lysed using glass beads and the inclusion bodies solubilized in extraction buffer containing 8 M urea, pH 12.5.

Following these initial results, where it was verified that IFN α -2b was produced exclusively in an insoluble form as IB, experiments were conducted to find out which

culture medium and which induction period would be more suitable for maximizing the expression of this protein. In these experiments, the typical fermentation features were maintained, and the outlines are described in Figure 10 A, B and C, respectively, for the media SOB, LB and SOC. After analyzing these media and induction periods ranging from 0 to 7 h, the SDS-PAGE and Western Blot analysis of the SIB fraction showed that IFN α -2b is expressed in its monomeric form with a Mw ranging between 17 and 20 kDa (74). However, a higher band of approximately 35 kDa, which may correspond to dimers, was also obtained (Figure 10). The estimation of the quantification of the expression levels of the target protein was based on a densitometric analysis of the IFN α -2b bands obtained in the Western-Blot analysis.

In the LB and SOC media, the highest level of protein production was obtained after 3 h of fermentation. The presence of dimers is always noticed over time in the LB medium, but on the SOC medium, both the monomeric and dimeric forms of IFN α -2b are no longer produced or are at low and non-detectable levels. In the SOB medium (Figure 10), the highest levels of protein production are recorded at 3 h and 5 h of induction, and the dimerization seems to increase over time. However, since the active form of the IFN α -2b is its monomeric form and that the dimerization is undesirable, the SOB medium and 3 h of induction were the experimental conditions adopted in the next steps since they lead to higher protein yields in a monomeric and active form. However, by decreasing both the IPTG concentration and the induction temperature down to 16 °C and increasing the fermentation period to 24 h, a portion of the target protein in the soluble fraction was recovered in the absence of chaotropic agents, which were necessary to recover/solubilize the inclusion bodies. According to Figure 11, using a concentration of 0.1 or 0.5 mM of IPTG, the immunologically active IFN was detected in the soluble fraction. Still, the highest production yield was obtained while producing the IFN α -2b in the form of inclusion bodies, in the SIB fraction.

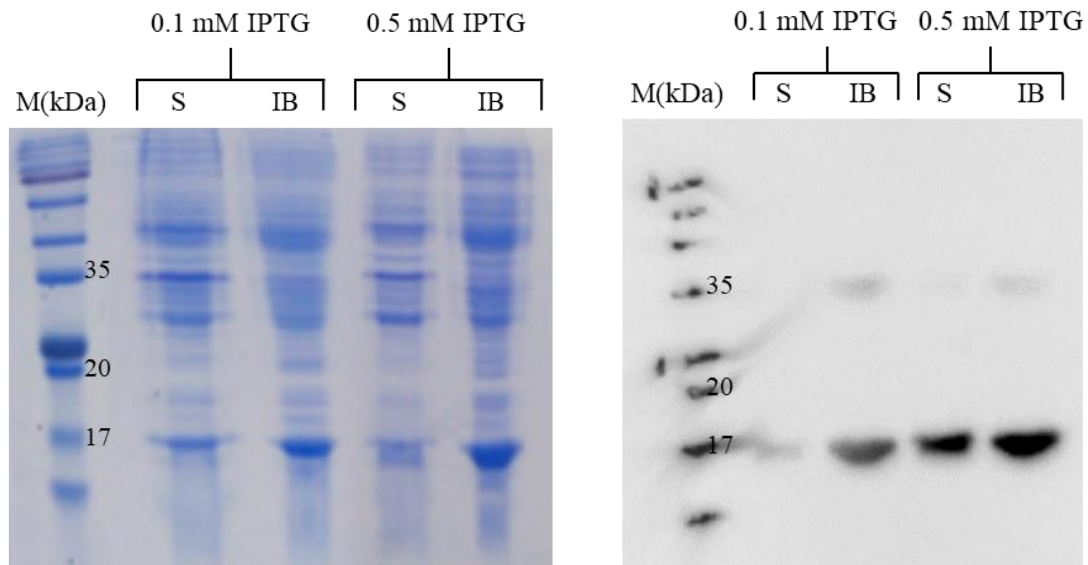


Figure 11: SDS-PAGE (left) and Western-Blot (right) of the soluble fraction (S) and inclusion body fraction (IB) obtained after the subcellular fractionation of *E. coli* BL21 cultures, induced with different concentrations of IPTG. Samples were lysed using glass beads and the inclusion bodies solubilized in extraction buffer containing 8 M urea, pH 12.5. Induction temperature was set at 16 °C.

3.2. Primary recovery of the active form of interferon alpha-2b

3.2.1. Cellular disruption

The disruption of *E. coli* cells was accomplished using two distinct methods, namely by a mechanical procedure using glass beads and by an enzymatic method using lysozyme. In general, the results show that both lysis methods allow to recover the IFN α -2b in an immunologically active form, as shown in Figure 12. However, the presence of dimers is more accentuated in the enzymatic method.

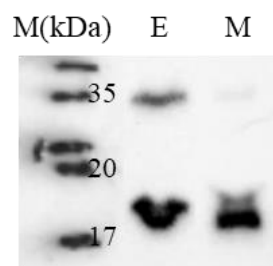


Figure 12: Western-Blot analysis of the cellular extract of *E. coli* BL21 cultures (37 °C and 250 rpm) obtained either using 7 cycles of mechanical lysis (M), with glass beads, and using the enzymatic lysis (E), with lysozyme.

The secondary structure of the recovered/purified IFN α -2b and its antiproliferative activity against MCF-7 cells was then analyzed. The recovery/purification protocol used will be discussed in the next sections of this work. The secondary structure was evaluated through CD. For comparison purposes, a denaturated form of the IFN α -2b, previously submitted to 100 °C (IFN α -2b + 100 °C) was included in the analysis. The resulting CD spectra are illustrated in Figure 13, which are in agreement with the CD results presented in the literature for commercial IFN α -2b (200). Thus, it can be concluded that in the end of the lysis process, IFN α -2b keeps its proper structure.

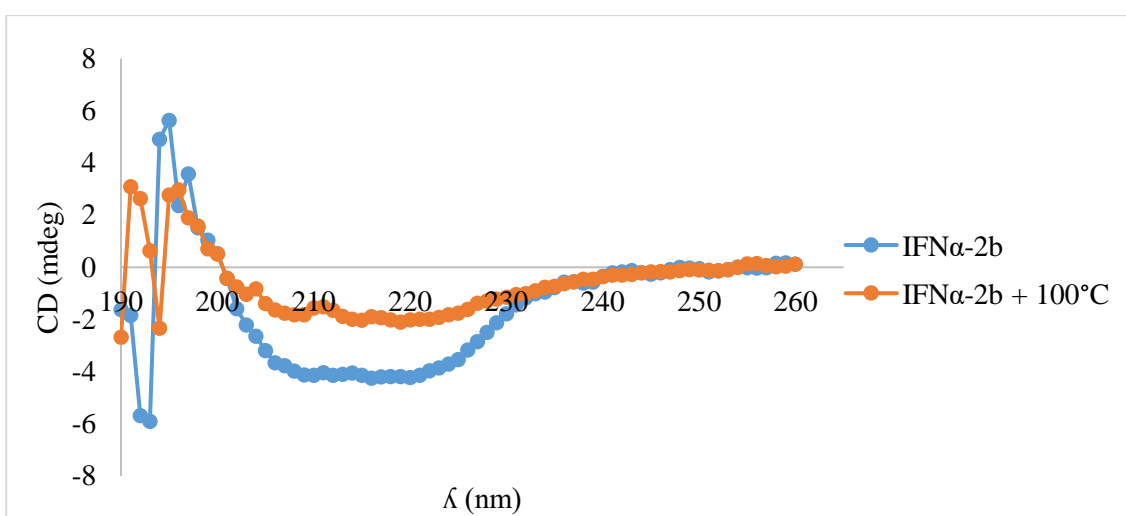


Figure 13: Evaluation of the secondary structure of IFN α -2b using Circular Dichroism (CD). The IFN α -2b was obtained from *E. coli* BL21 cells using the enzymatic lysis.

After cell lysis, the extract was submitted to optimized protocols of recovery and purification. One important aspect to mention is that the recovery procedure includes the dialysis against decreasing concentrations of a chaotropic agent, in the presence of GSH and GSSH, which promote the formation of IFN α -2b disulfide bonds, important for its biological activity. As demonstrated in Figure 14, it was observed that the IFN α -2b derived from an enzymatic lysis was obtained with high biological activity, thus being capable of promoting more than 50 % of cell death of the breast cancer cells, as measured by the MTS assay. On the other hand, when the mechanical lysis procedure was used, no biological activity was registered. Indeed, this method seems to be more aggressive for cells, and as it leads to an efficient lysis by releasing all the intracellular content, it can also cause the destruction of the IFN α -2b structure. The enzymatic lysis is a common

procedure at the laboratory scale but it has to be taken into account that the introduction of an extra contaminant/protein in the lysate can influence further purification assays. Even so, in this work, this method was chosen for further assays due to the advantage of allowing to obtain the target protein with biological activity.

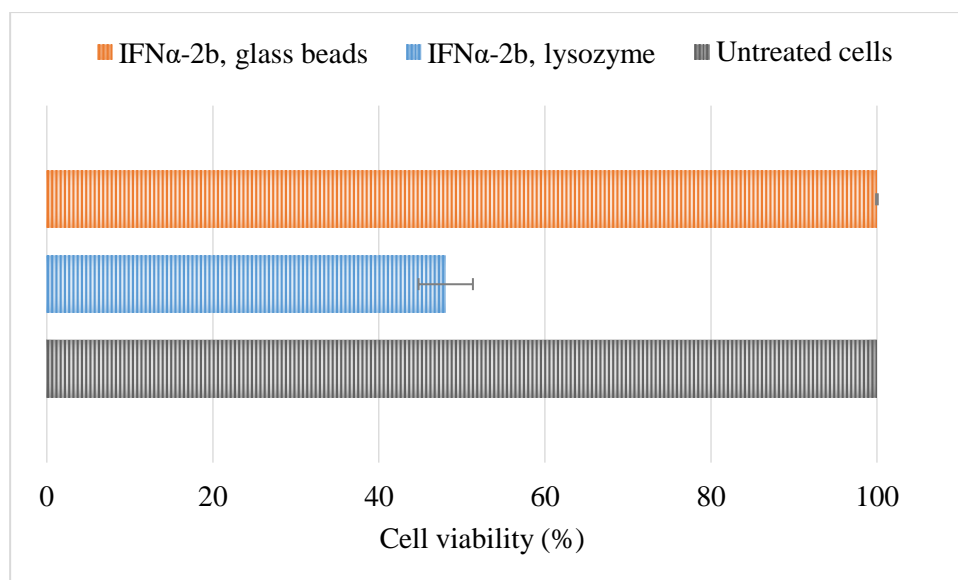


Figure 14: Evaluation of IFN α -2b anti-proliferative activity against MCF-7 cells.

Taking into account that the ultimate goal of this work is to study alternative platforms of purification of IFN α -2b in order to apply them at the industrial level as new methodologies to the downstream production of this biopharmaceutical, the enzymatic lysis using lysozyme was the chosen method adopted for the next experiments.

3.2.2. Inclusion bodies washing, solubilization and interferon alpha-2b extraction

The extract obtained by cellular disruption is a complex matrix that contains several contaminants and various host proteins, apart from the target IFN α -2b. Therefore, envisaging the IFN α -2b recovery from the insoluble fraction with less contaminants, the extract was centrifuged, washed and solubilized at different conditions. In initial steps, the optimization aimed the removal of adherent impurities from the inclusion bodies. To this end, the cellular extract was centrifuged and resuspended in several washing buffers, sometimes two or three consecutive washes were used, according to the description given in Table 5. After washing, all the washed fractions were solubilized in the extraction buffer (50 mM Tris-HCl pH 12.5, 8 M urea, 1 mM DTT, protease inhibitor cocktail)

during 1 h at room temperature, centrifuged, concentrated and analyzed through SDS-PAGE.

Table 5: Inclusion bodies washing buffers composition used for IFN α -2b recovery.

Conditions	1 st Wash	2 nd Wash	3 rd Wash
1	50 mM Tris pH 8; 1% deoxycholic acid	50 mM Tris pH 8; 1% deoxycholic acid	–
2	50 mM Tris pH 8; 1% deoxycholic acid	50 mM Tris pH 8; 1% deoxycholic acid	Mili-Q H ₂ O
3	50 mM Tris pH 8; Triton X-100 0.5 %	–	–
4	50 mM Tris pH 8; Triton X-100 1 %	–	–
5	50 mM Tris pH 8; 2 M urea	–	–
6	50 mM Tris pH 8; 6 M urea	–	–
7	50 mM Tris pH 8; Triton X-100 1 %	50 mM Tris pH 8; 8 M urea	–
8	50 mM Tris pH 8; Triton X-100 1 %	50 mM Tris pH 8; 4 M urea	–

The results obtained from each washing condition are depicted in Figure 15. The 1% deoxycholic acid is able to remove a fraction of the high Mw contaminants in the first washing step (condition 1 and 2, 1st wash), but the second wash does not remove the remaining ones (condition 2), and the Mili-Q H₂O is unable to remove any contaminant. The condition 2 was previously studied by Srivastava and co-workers (74) who described it as an effective washing method, resulting in approximately 80 % of purity prior to chromatographic purification. However, their results were not reproducible in this work. The wash with Triton X-100 0.5 % (condition 3) seems to be more efficient than the 1% deoxycholic acid approach, and an increase to 1 % in Triton X-100 concentration enhanced the recovery (condition 4, 1st wash). Triton X-100 is a non-ionic surfactant that promotes the solubility and the disaggregation of proteins and it has already been applied in the optimization of IFN α -2b recovery (11). Moreover, the use of urea at pH 8.0 has also been reported for the removal of some contaminants (11). However, since part of

the target protein is solubilized either with 6 and 8 M urea, thereby leading to losses in the washing step (condition 6, 1st wash and condition 7, 2nd wash), we chose to reduce the urea concentration to 4 M.

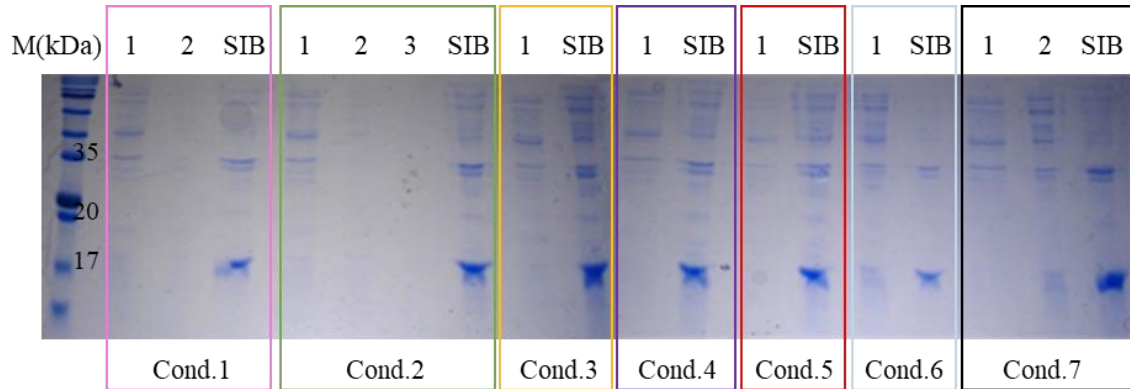


Figure 15: SDS-PAGE analysis of the different washing buffers used for the IFN α -2b recovery. Each condition is highlighted at a different color. Each lane is identified with the numbers 1, 2 and/or 3 corresponding to the 1st, 2nd and 3rd wash, respectively, and with the SIB abbreviation corresponding to the solubilized inclusion body fraction.

The experimental condition that led to the best results in terms of higher IFN α -2b extraction yields was obtained in a less contaminated sample, obtained from two successive washes, first with Triton X-100 1 % and then with 4 M urea, both in Tris 50 mM pH 8 (condition 8). The results obtained are shown in Figure 16.

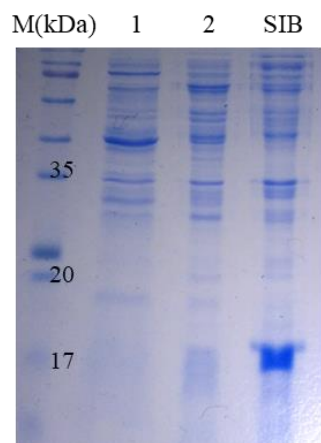


Figure 16: SDS-PAGE analysis of the inclusion bodies' washes using first Triton X-100 1 % (lane 1), and then 4 M urea (lane 2), both in 50 mM Tris, at pH 8.

The next step aimed to evaluate different extraction buffers concerning their ability to extract the target protein, as summarized in Table 6. After solubilization, the samples were centrifuged to separate the SIB fraction from the remaining cell debris and non-solubilized proteins. Both samples were analyzed through SDS-PAGE and Western-Blot.

Table 6: Extraction buffers compositions and respective time used for IFN α -2b solubilization, at 25 °C.

Conditions	Time (h)	Extraction buffer composition
1	1	8 M Urea, pH 7.4, 20 mM DTT
2	1	2 M Urea, pH 12.5, 20 mM DTT
3	16	8 M Urea, pH 7.4, 1 mM DTT
4	1	8 M Urea, pH 7.4, 1 mM DTT
5	1	4 M Urea, pH 12.5, 1 mM DTT
6	1	2 M Urea, pH 12.5, 1 mM DTT
7	1	6 M GdnHCl, pH 7.5, 20 mM DTT
8	1	6 M Urea, pH 12.5, 1 mM DTT
9	1	8 M Urea, pH 12.5, 1 mM DTT

The SDS-PAGE results in Figure 17 show that despite 8 M urea was included in the solubilization buffers of conditions 1, 3 and 4, the IFN α -2b was poorly extracted and detected only in the non-soluble pellet. However, using the 2 M urea buffer at pH 12.5, with 20 mM DTT (condition 2), it was possible to solubilize a part of the target protein from the inclusion body fraction. This led us to infer that a more alkaline pH is important to solubilize IFN α -2b, in addition to the presence of a chaotropic agent. Moreover, the incubation period does not seem to enhance the solubilization (the SIB lanes of condition 3 and 4 are similar); therefore, a solubilization time of 1 h was maintained in the following experiments.

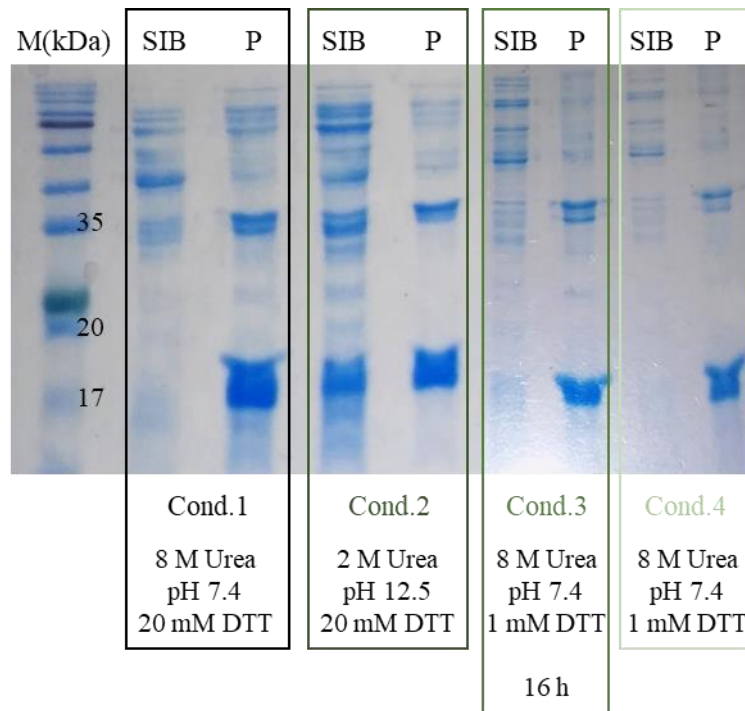


Figure 17: SDS-PAGE analysis of the conditions 1-4 applied to extract IFN α -2b from the IB fraction. Both soluble and insoluble fractions were analyzed and are represented as SIB and P, respectively.

According to the results depicted in Figure 18, the target protein appears in two soluble fractions, conditions 5 and 6, meaning that 2 M of urea buffer at pH 12.5 is capable to solubilize the IFN α -2b independently of the DTT concentration. However, the importance of DTT should not be depreciated. DTT is a reducing agent that in denatured samples helps to avoid the formation of erroneous disulfide bonds, being therefore important to maintain the protein biological activity. Moreover, the buffer containing 4 M urea, pH 12.5 with 1 mM DTT, is also able to solubilize IFN α -2b. In the condition 7, wrapped bands are seen, which are related with the precipitation of GdnHCl in the presence of SDS, hampering electrophoresis. Although GdnHCl has been described as a good solubilizing agent of IFN α -2b' inclusion bodies by Valente and co-workers (11), a poor solubilization was observed in this work.

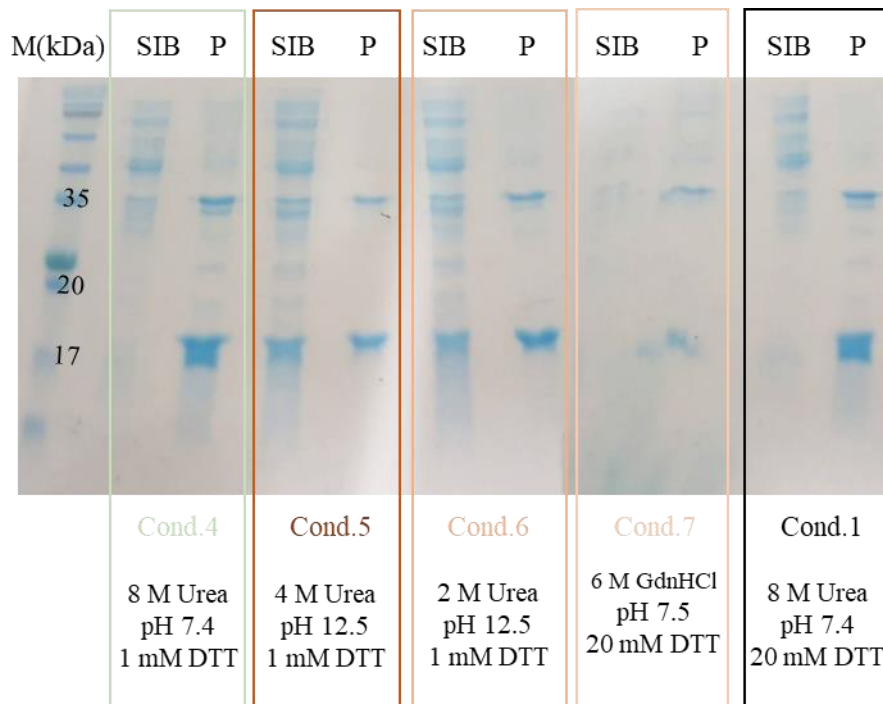


Figure 18: SDS-PAGE analysis of the conditions 1 and 4-7 applied to extract IFN α -2b from the insoluble fraction. Both soluble and insoluble fractions were analyzed and are represented as SIB and P, respectively.

In the following assays, the urea concentration was increased, while the pH 12.5 and 1 mM of DTT were maintained. The results obtained are illustrated in Figure 19, demonstrating that the best result was obtained using 8 M urea, pH 12.5 (SIB, condition 9). However, the IFN α -2b was also successfully solubilized with 4 M and 6 M urea (SIB conditions 5 and 6, respectively). The precipitation of the GdnHCl samples were attempted with ethanol and resuspended in 50 mM Tris, pH 8, before injection in the SDS-PAGE gel, but since no protein was detected in both fractions, we may conclude that the precipitation was not effective. These results were further confirmed through the repetition of these assays.

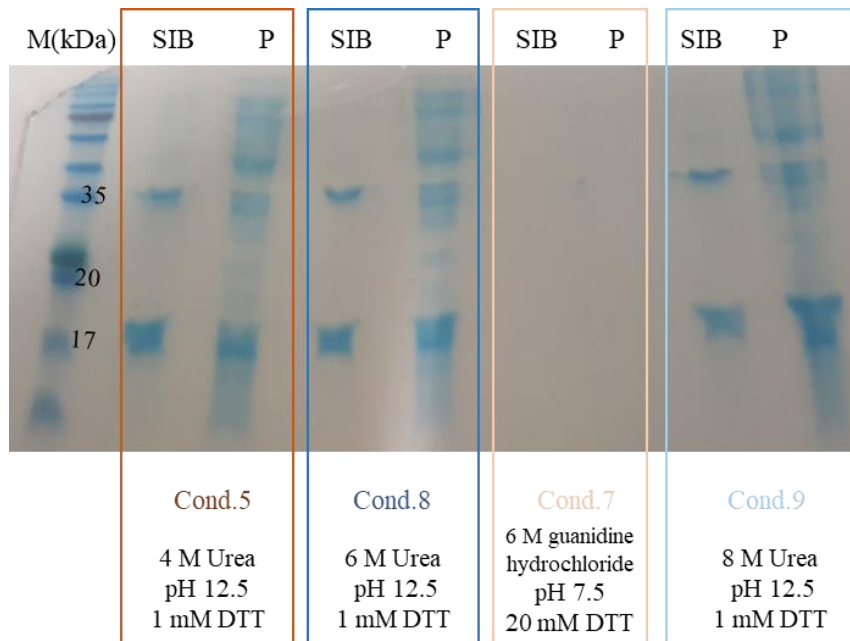


Figure 19: SDS-PAGE analysis of the conditions 5 and 7-9 applied to extract IFN α -2b from the insoluble fraction. Both soluble and insoluble fractions were analyzed and are represented as SIB and P, respectively.

In addition to RT ($\approx 25^\circ\text{C}$), other solubilization temperatures, namely 37 and 50 $^\circ\text{C}$, were also tested. Nevertheless, an increase in the solubilization temperature does not favor the extraction of IFN α -2b, as shown in Figure 20. Therefore, the solubilization temperature adopted was kept at 25 $^\circ\text{C}$ throughout this work.

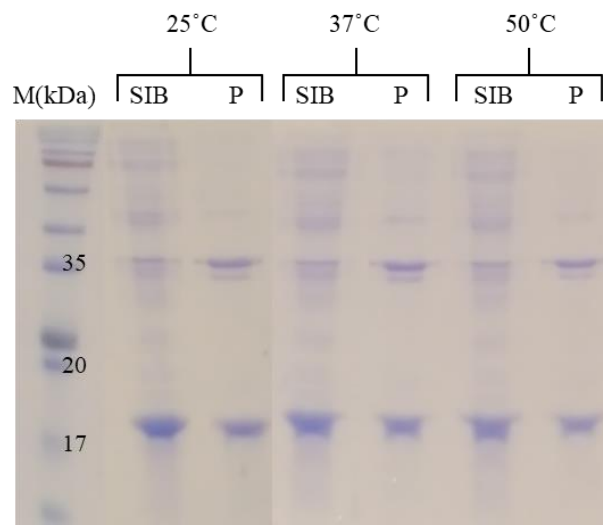


Figure 20: SDS-PAGE analysis of the soluble (SIB) and insoluble (P) fractions of the IFN α -2b extracted with a 50 mM Tris buffer containing 8 M urea, pH 12.5 and 1 mM DTT, at 25, 37 and 50 $^\circ\text{C}$.

After the optimization of the recovery step, the IFN α -2b was refolded using dialysis against decreasing concentrations of urea, and reduced and oxidized glutathiones, a redox system that enhances the catalysis of the IFN α -2b disulfide bond formation. The final optimized protocol adopted for the primary recovery of IFN α -2b is presented in Figure 21.

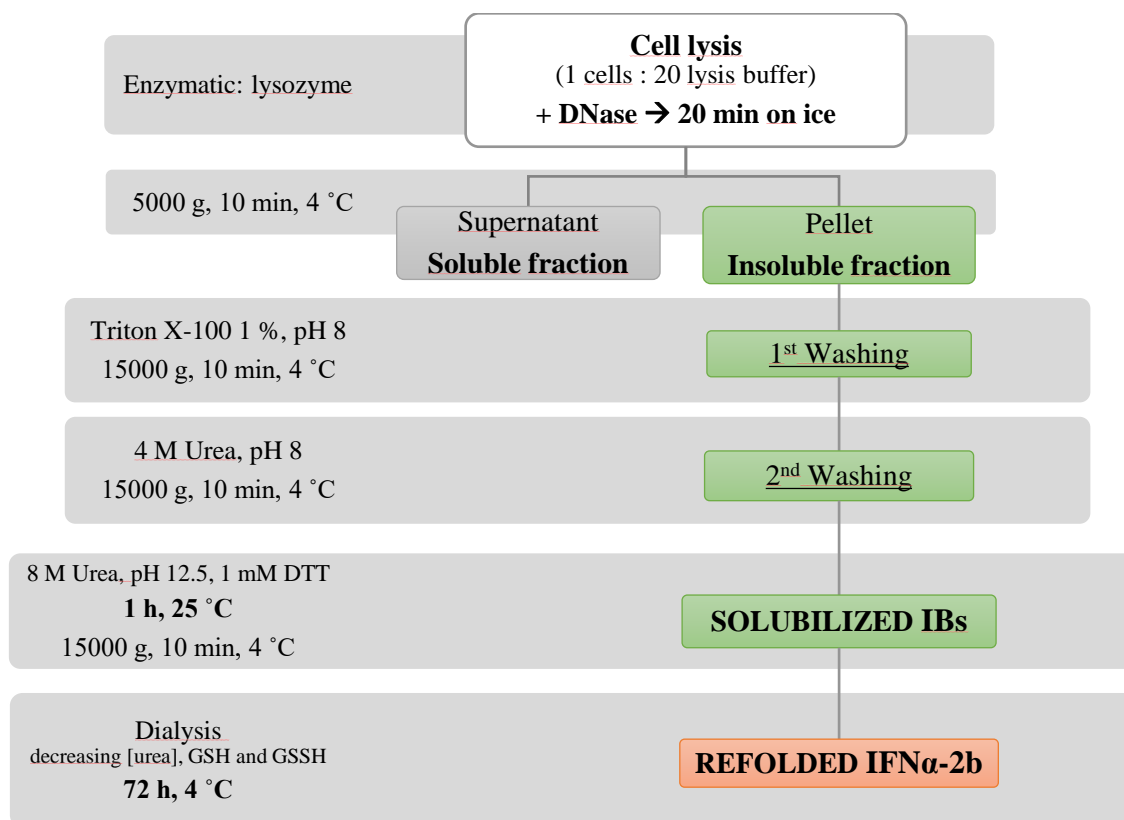


Figure 21: Optimized protocol for IFN α -2b recovery from *E. coli* BL21.

3.3. Interferon alpha-2b purification

3.3.1. Chromatographic purification of interferon alpha-2b

Envisaging the separation of IFN α -2b from the remaining host proteins present in the crude SIB, conventional chromatographic matrices, such as Arginine and a CIM DEAE monolith, were used. A Hi-Trap Desalting matrix was also used as an intermediate step prior to purification. The flow-rates, the protein mass of SIB and the elution methods were optimized to improve capacity, recovery, and resolution of the chromatographic separation.

The first strategy explored for IFN α -2b purification was arginine affinity chromatography; this technique has been extensively used in the purification of

biomolecules from biological matrixes (201), and therefore can be an interesting alternative for IFN α -2b purification. In the SIB fraction (pH 12.5), the IFN α -2b is negatively charged (pI = 5.9 (74)), while arginine has a positive charge. Therefore, non-covalent electrostatic interactions between the chromatographic ligands and the target molecule are expected to exist. As the sample passes through the column, some proteins will be retained depending on their interactions with arginine. There are however several proteins in the medium and their type of interactions are not fully known. Size, charge and hydrophobicity between the column and ligands are some factors that additionally affect affinity (202). Ideally, all the target protein will bind to the matrix in a first step and the elution occurs at a certain ionic strength that disrupts non-covalent interactions (201, 202). The arginine column was initially loaded with 0.5 mL of SIB fraction, at 1 mL/min. After elution of the unretained species using 50 mM Tris buffer, pH 8, the NaCl concentration was increased in a stepwise mode up to 0.5 M, and then to 2 M, according to that described in Figure 22.

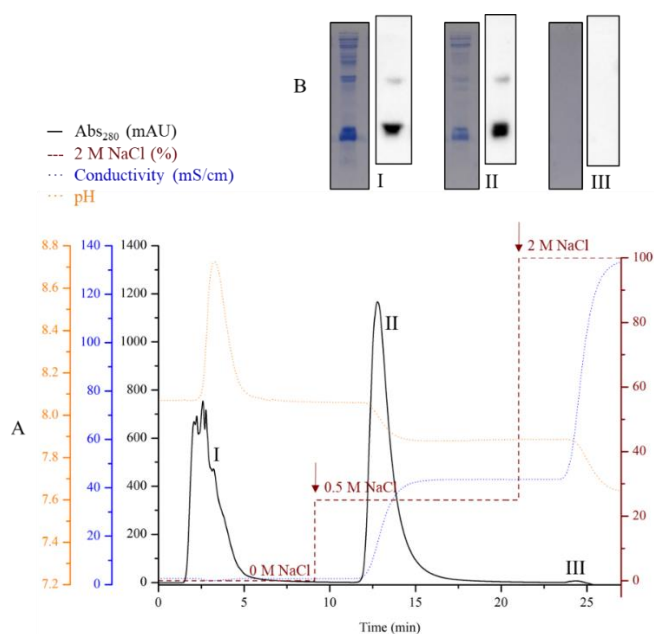


Figure 22: Chromatographic profile of the SIB fraction by arginine-Sepharose chromatography. 0.5 mL of the crude SIB fraction was injected and the elution was performed at 1 mL/min by increasing NaCl concentration from 0 M to 0.5 M, and then to 2 M in 50 mM Tris buffer (pH 8), as represented by the arrows. The collected fractions of each step are represented as I, II and III (A). The SDS-PAGE and Western-Blot results of the collected fractions are represented in B.

According to the chromatogram depicted in Figure 22, there is a considerable amount of proteins eluted within the binding step, while the increase of the ionic strength up to 0.5 M NaCl promotes the elution of the proteins bounded to the matrix; the final elution step with 2 M NaCl ensures that the matrix capacity is not reduced in consecutive chromatographic assays - "regeneration step". Each of these chromatographic peaks were separately collected, concentrated, and analyzed by SDS-PAGE and Western-Blot. Despite some contaminants that are eluted in the binding step, a considerable amount of the target protein was also eluted, leading to significant losses in the target protein recovery yield. In what concerns the fraction eluted with 2 M NaCl, no proteins were visualized in the SDS-PAGE. As the matrix binding capacity may have been exceeded, in an attempt to improve the amount of IFN α -2b that bind to the matrix, a new assay was performed (A2), where a smaller amount of sample (100 μ L) was loaded. The stepwise gradients employed were the same as in assay 1: 50 mM Tris buffer, pH 8, followed by 500 mM and 2 M NaCl, in Tris 50 mM pH 8. As expected, the intensity of the peaks (Abs₂₈₀) decreased, that is related with the smaller volume injected. According to Figure 23 B, less proteins were eluted in the binding step, but the target protein is eluting in equal amounts with 50 mM Tris and 500 mM NaCl (I and II), meaning that the problem is, at least, not exclusively related with the matrix capacity nor with the injected volume.

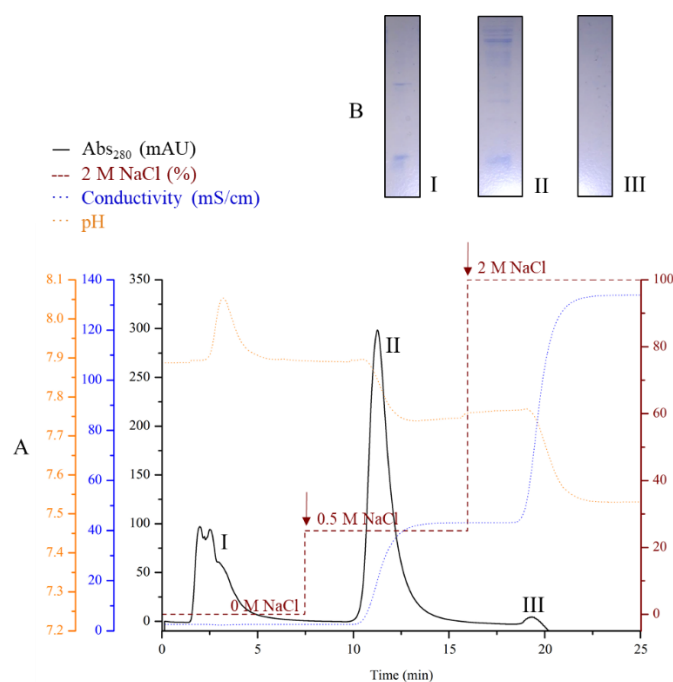


Figure 23: Chromatographic profile of the SIB fraction by arginine-Sepharose chromatography 2. 0.1 mL of the crude SIB fraction was injected and the elution was performed at 1 mL/min by increasing NaCl concentration from 0 M to 0.5 M, and then to 2 M in 50 mM Tris buffer (pH 8), as represented by the arrows. The collected fractions of each step are represented as I, II and III (A). The SDS-PAGE results of the collected fractions are represented in B.

Since the pKa of arginine is 12.48 (203), and due to the high alkaline pH-microenvironment surrounding the arginine ligands, in the previous assay there is the possibility of having the uncharged form of arginine, thereby not establishing electrostatic interactions with IFN. An additional experiment consisting in the injection of a sample for which HCl was added to a pH below 10 was carried out, mainly to ensure that the arginine side chain is positively charged and thereby available for interacting with the negatively charged target protein. At this pH, the target protein (pI = 5.9 (74)) is negatively charged while arginine should be positively charged. In a third assay (A3), 100 μ L were injected using the same chromatographic buffer compositions and stepwise gradients. However, the A3 chromatogram illustrated in Figure 24 is similar to the chromatogram of A2 shown in Figure 23. Again, the IFN α -2b equally eluted with 50 mM Tris and with 500 mM NaCl, meaning that it is not binding to the column, and the problem is not related with the pH of the initial sample. However, it is worthwhile to notice that in step 2 the high Mw contaminant proteins were also eluted in high quantities.

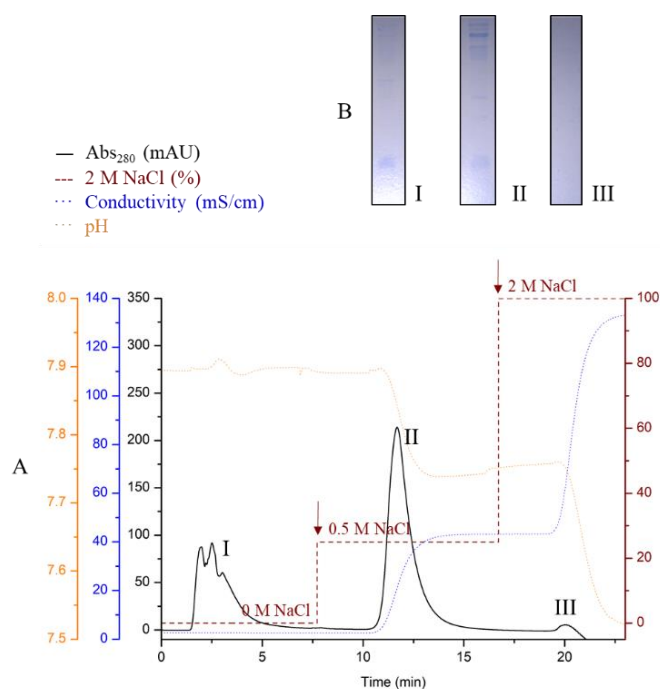


Figure 24: Chromatographic profile of SIB fraction by arginine-Sepharose chromatography 3. 0.1 mL of the crude SIB fraction was injected and the elution was performed at 1 mL/min by increasing NaCl concentration from 0 M to 0.5 M, and then to 2 M in 50 mM Tris buffer (pH 8), as represented by the arrows. The collected fractions of each step are represented as I, II and III (A). The SDS-PAGE results of the collected fractions are represented in B.

Motivated by the idea of improving the recovery yield, additional experiments were performed maintaining the stepwise gradients and buffers compositions. The urea of the extraction buffer may be interfering in binding since it causes a decrease in the conductivity. Thus, two distinct assays were performed with 200 μ L of sample, either solubilized at pH 12.5 with 4 M urea or in the absence of urea at pH 12.5. However, the chromatographic profiles were similar to the ones previously obtained, and lower extraction efficiencies of the target protein were obtained using concentrations of urea lower than 8 M, thereby compromising the initial recovery yield. Moreover, despite the changes in the solubilization buffer compositions, the IFN also eluted almost equally in the binding and in the first elution steps.

Despite the optimization efforts, the arginine Sepharose matrix did not provide the desired selectivity to separate the IFN from the host contaminants. Moreover, the recovery yield was always low. Therefore, alternative strategies based on ion-exchange chromatography were adopted for IFN α -2b purification, namely by the use of a CIM

DEAE monolith. However, prior the application of any of these chromatographic separations, a method based on a HiTrap Desalting column was employed, envisaging the removal of urea from the sample and, simultaneously, to proceed to the buffer exchange to Tris buffer at pH 8. A 1 mL sample was injected at a flow rate of 0.3 mL/min, while an isocratic elution was performed with Tris 50 mM pH 8. According to the chromatograms shown in Figure 25, two major peaks were obtained.

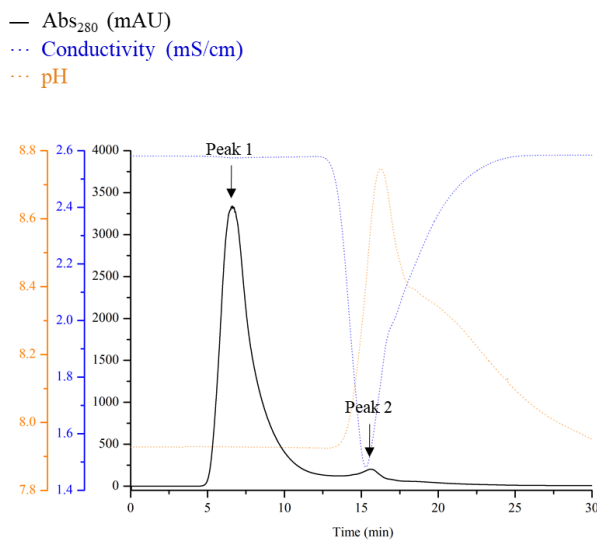


Figure 25: Chromatographic profile of the SIB fraction obtained with the HiTrap Desalting column. 1 mL of the crude SIB fraction was injected and the elution was performed with 50 mM Tris, at pH 8. The two maximums of absorbance are highlighted as peak 1 and peak 2.

The majority of the proteins present in the SIB fraction were desalted and eluted in peak 1, resulting in a small decrease of the contaminant proteins or/and an enhancement of the IFN α -2b concentration (Figure 26). Also, it was possible to observe that the protein target was obtained in a high purity degree in peak 2, although with a low recovery yield. The IFN α -2b present in peak 1 was successfully collected in an urea-free buffer composed of 50 mM Tris pH 8, and therefore was considered for further chromatographic studies.

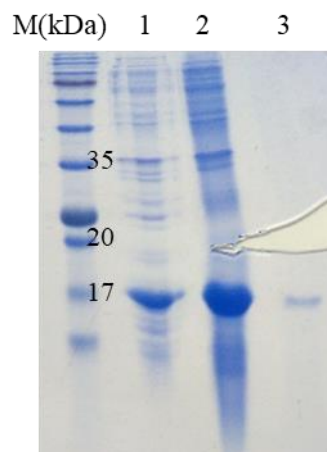


Figure 26: SDS-PAGE analysis of different eluted fractions with 50 mM Tris pH 8, resulting from the HiTrap Desalting chromatography. The lanes correspond to: 1) initial sample, 2) peak 1, 3) peak 2.

In order to evaluate if the size exclusion separation could be more effective with improved IFN- α 2b recovery yield, an assay where the sample was loaded at 0.2 mL/min was carried out. However, this flow-rate was too low and it did not work as expected. Thus, the conditions of the first assay at 0.3 mL/min where the protein is desalted were considered satisfactory and further applied to remove urea in subsequent studies.

The fractions collected from the HiTrap Desalting column were concentrated and 1.0 mL was injected in CIM DEAE monolith. The flow-rate was 1 mL/min and the chromatographic buffers used were 50 mM Tris pH 8, 1 M and 2 M NaCl. The first assay conducted in the CIM monolith consisted in the injection of a 0.5 mL SIB fraction at 1.0 mL/min in 20 mM NaCl, followed by two stepwise gradients at 1 M and 2 M NaCl in Tris 50 mM, pH 8. According to Figure 27, it was found that all the target protein bind to the monolith, being eluted at 1 M NaCl, as well as the majority of the remaining contaminants present in the initial sample.

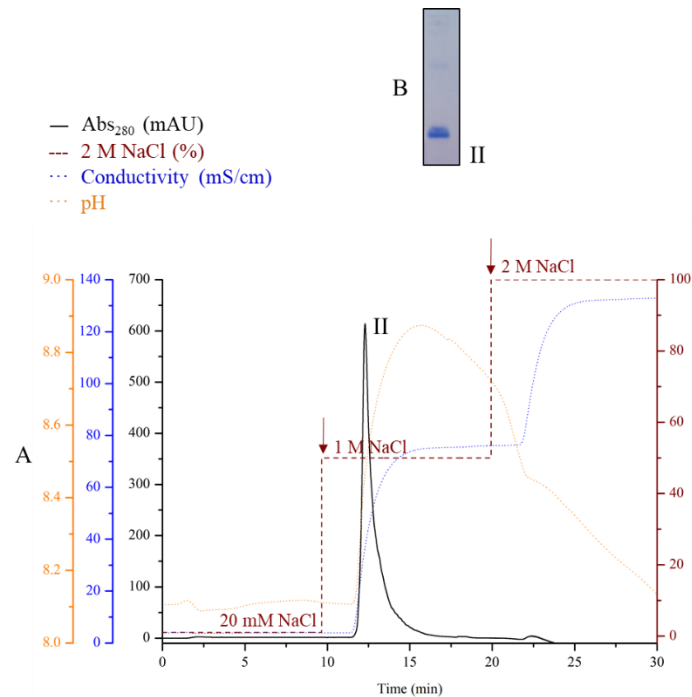


Figure 27: Chromatographic profile of the SIB fraction obtained from the CIM DEAE monolith chromatography 1. 0.5 mL of the crude SIB fraction was injected and the elution was performed at 1 mL/min by increasing NaCl concentration from 20 mM to 1 M, and then to 2 M in 50 mM Tris buffer (pH 8), as represented by the arrows. The collected fraction is represented as II (A). The SDS-PAGE results of the II fraction are represented in B.

After the previous optimization assays, the following set of experiments were designed to evaluate the maximum of the NaCl concentration employed in the binding step where only the protein contaminants could be eluted. In assays 2, 3 and 4 the sample load and flow rate were maintained, while new stepwise gradients were studied: 200 mM, 1 M, and 2 M NaCl; 100 mM, 1 M and 2 M NaCl, and 60 mM, 1 M and 2 M NaCl, respectively. The chromatograms referring to each assay are illustrated in Figures 28-30. Assays 1 and 2 have different chromatographic profiles; in assay 2 three different peaks are seen. Furthermore, with 200 mM NaCl, a considerable amount of the IFN- α 2b does not bind to the matrix, thus leading to low recovery yields (Figure 28).

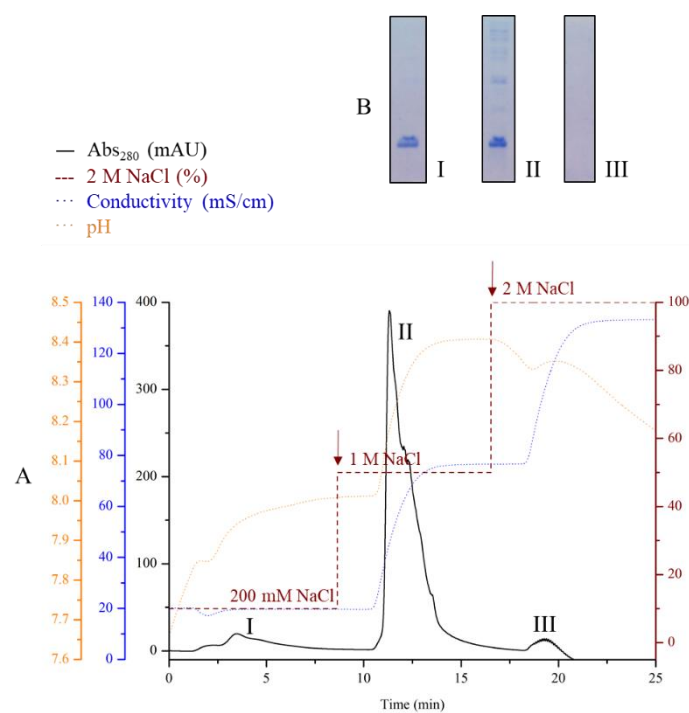


Figure 28: Chromatographic profile of the SIB fraction obtained from the CIM DEAE monolith chromatography 2. 0.5 mL of the crude SIB fraction was injected and the elution was performed at 1 mL/min by increasing NaCl concentration from 200 mM to 1 M, and then to 2 M in 50 mM Tris buffer (pH 8), as represented by the arrows. The collected fractions are represented as I, II and III (A). The SDS-PAGE results of the collected fractions are represented in B.

In assay 3, the employment of 100 mM NaCl allowed to increase the recovery, but a portion of the target was still detected in the SDS-PAGE, as illustrated in Figure 29.

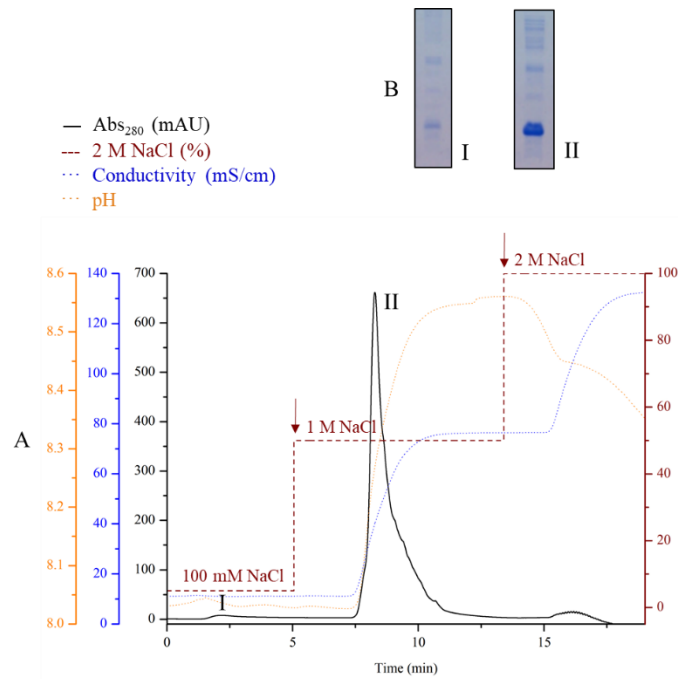


Figure 29: Chromatographic profile of the SIB fraction obtained from the CIM DEAE monolith chromatography. 3.05 mL of the crude SIB fraction was injected and the elution was performed at 1 mL/min by increasing NaCl concentration from 100 mM to 1 M, and then to 2 M in 50 mM Tris buffer (pH 8), as represented by the arrows. The collected fractions are represented as I and II (A). The SDS-PAGE results of the collected fractions are represented in B.

Comparing the SDS-PAGE results of Figures 29 and 30 it is seen that a decrease of the ionic strength in the binding step, from 100 – 60 mM, allows to enhance the recovery of IFN α -2b, since no proteins were detected in the first eluted fraction.

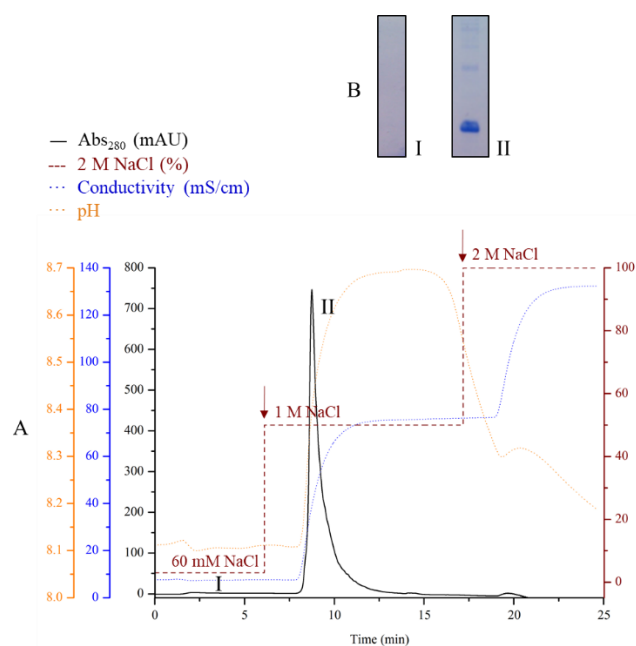


Figure 30: Chromatographic profile of the SIB fraction obtained from the CIM DEAE monolith chromatography 4. 0.5 mL of the crude SIB fraction was injected and the elution was performed at 1 mL/min by increasing NaCl concentration from 60 mM to 1 M, and then to 2 M in 50 mM Tris buffer (pH 8), as represented by the arrows. The collected fractions are represented as I and II (A). The SDS-PAGE results of the collected fractions are represented in B.

To guarantee the complete binding of the target to the column, in a subsequent assay, the NaCl concentration was decreased to 50 mM NaCl in the binding step, followed by two stepwise gradients at 150 mM NaCl and 2 M NaCl, as demonstrated in Figure 31. As expected, no IFN α -2b was eluted in the binding step (I). On the other hand, the fraction obtained with 150 mM NaCl seems to contain more than one protein and was treated as two independent samples - II and III. The majority of IFN- α 2b is present in the first peak obtained with 150 mM NaCl in a more purified degree, although contaminants with high Mw were still in this fraction. Part of the target is still observable in the last step (IV), meaning that it remains attached to the column until a higher ionic strength is applied.

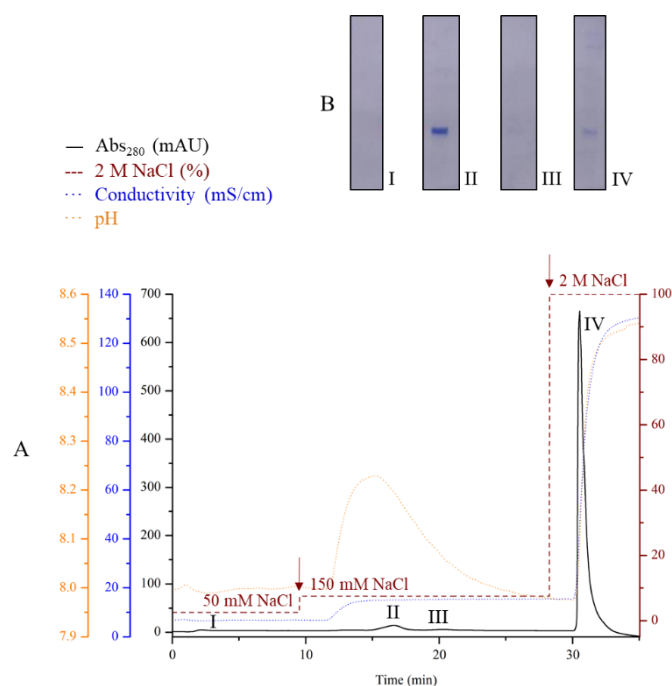


Figure 31: Chromatographic profile of the SIB fraction obtained from the CIM DEAE monolith chromatography. 5.0 mL of the crude SIB fraction was injected and the elution was performed at 1 mL/min by increasing NaCl concentration from 50 mM to 150 mM, and then to 2 M in 50 mM Tris buffer (pH 8), as represented by the arrows. The collected fractions are represented as I, II, III and IV (A). The SDS-PAGE results of the collected fractions are represented in B.

After the optimization of the NaCl concentration in the binding step, the next step aimed the optimization of the elution steps to obtain IFN α -2b in a high-purity degree. Therefore, an additional chromatographic experiment was performed, where the NaCl concentration in the binding buffer was maintained at 50 mM, followed by an increasing linear gradient from 50 to 150 mM NaCl during 10 min, and a final elution step with 1 M NaCl. The results obtained are depicted in Figure 32. Three different samples were defined and collected separately (II, III, IV). Although there is some loss of the target protein in the further steps, it is lower than in previous assays, and the IFN- α 2b was recovered in the linear gradient with high purity, as demonstrated in Figure 32 B (II).

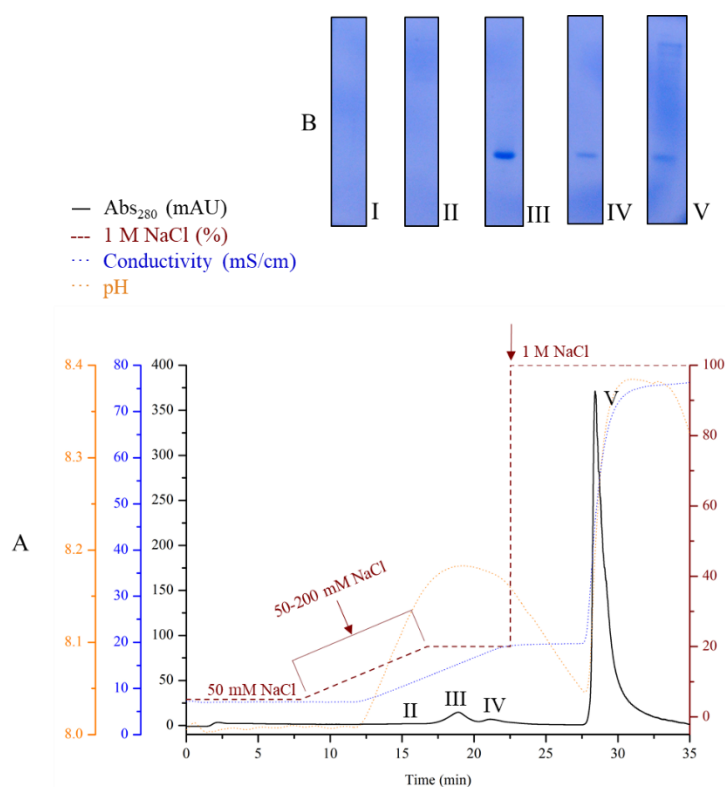


Figure 32: Chromatographic profile of the SIB fraction obtained from CIM DEAE monolith chromatography 6. 0.5 mL of the crude SIB fraction was injected and the elution was performed at 1 mL/min by increasing NaCl concentration in a stepwise gradient from 50 mM to 200 mM, during 10 min. Subsequently, the concentration was increased to 1 M in 50 mM Tris buffer (pH 8), as represented by the arrows. The collected fractions are represented as II, III, IV and V (A). The SDS-PAGE results of the collected fractions are represented in B.

The degree of purity obtained with the CIM monolith seems to be similar to the one reported by other authors (Please see Table 4 for a complete review). Therefore, it can be considered that we have developed an effective chromatographic strategy for the IFN α -2b purification. However, an important drawback still remains - the low recovery yield of IFN α -2b. It is known that in order to make the production of IFN α -2b cost-effective, so that it can be easily applied at the industrial level, the outcome amount should provide higher profits than the expenses related with the process. Indeed, the downstream processing of recombinant proteins is the major bottleneck associated to their high cost (10). The removal of different impurities usually requires different unit operations and although other options are starting to being considered, chromatography is still mastering the downstream stage due to its highly selective character (20). In this work, two

chromatographic steps were used, the HiTrap Desalting column and the CIM monolith. Although these matrixes are well known, and the IFN α -2b was obtained with a high purity degree, the chromatography application at higher scales is expensive, and additionally comprises the need of batch operation and pressure drops (140).

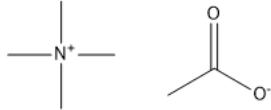
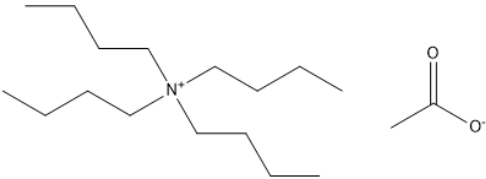
In order to overcome the shortcomings of chromatographic techniques, ATPS systems have been investigated as alternative methods for the purification of a wide variety of biomolecules (141). Comparing with the currently established packed-bed chromatography, ATPS have been shown to display good performance and have important economic and technological advantages, such as simplicity, higher biocompatibility and an easy scale-up (143). Taking this into account, in the next chapter, the use of IL-based ATPS for the purification of IFN α -2b will be presented and discussed.

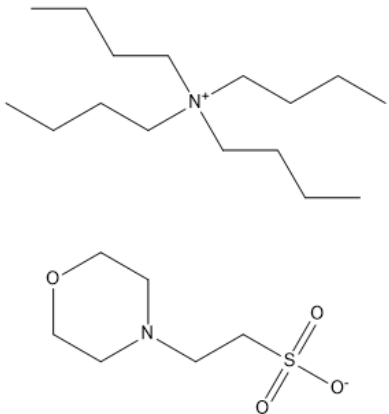
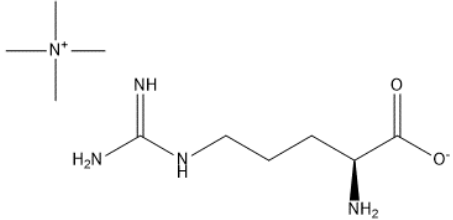
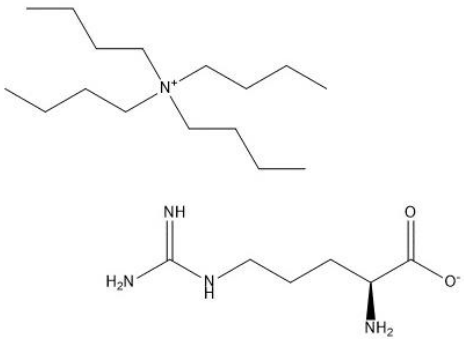
3.3.2. Non-chromatographic strategies for interferon alpha-2b purification using ionic-liquid-based aqueous two-phase systems

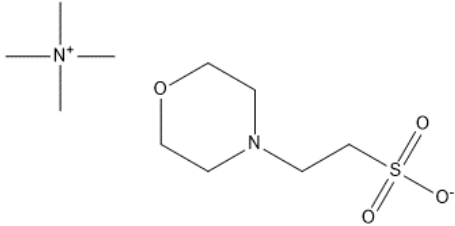
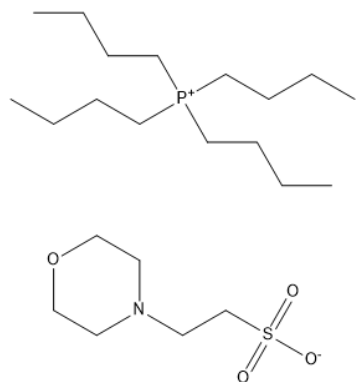
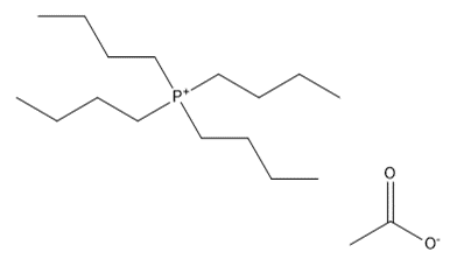
3.3.2.1. Synthesis and characterization of ionic liquids

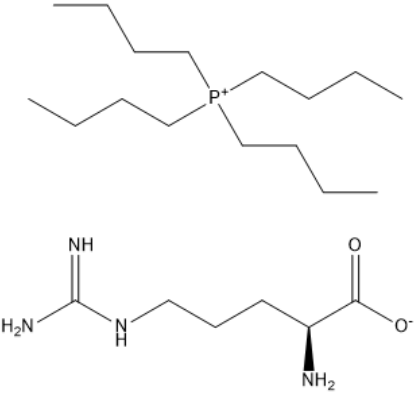
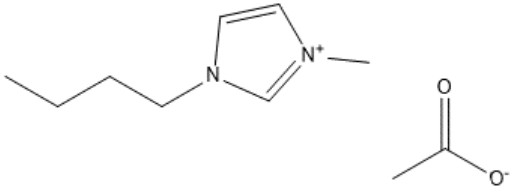
The ILs synthesized in this work were obtained via neutralization of the base with the corresponding acid. The ^1H and ^{13}C NMR spectra were recorded to confirm the formation of the target ILs, and are presented in Appendix B. Their appearance at room temperature was appraised, and their water content determined. The description of the synthesized ILs, chemical structures, ^1H and ^{13}C NMR data, water content, and their appearance at room temperature are given in Table 7.

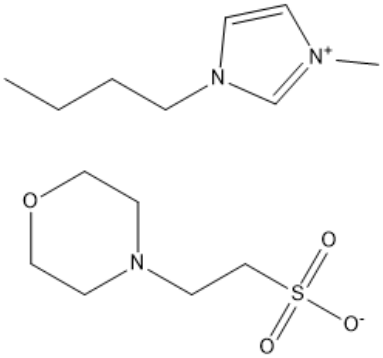
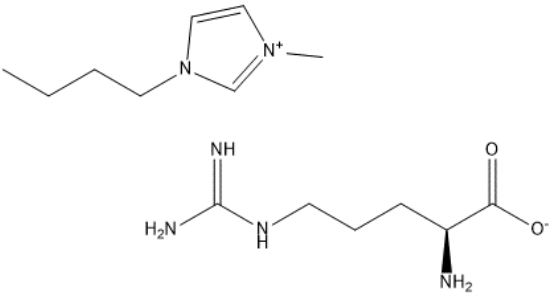
Table 7: Appearance, water content, chemical structure, and ^1H , ^{13}C RMN characterization of the synthesized ILs.

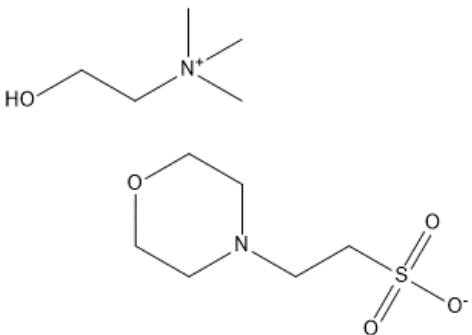
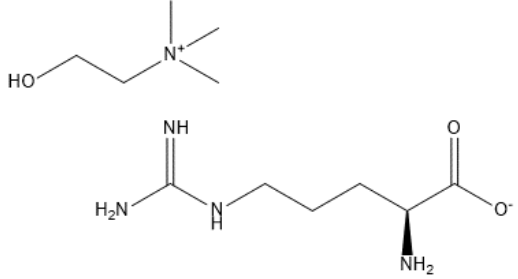
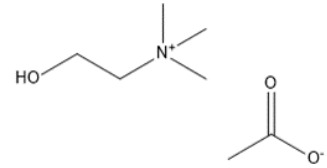
IL	Appearance at room temperature	Water content (wt%)	^1H NMR (D_2O , 300 MHz, [ppm])	^{13}C NMR (D_2O , 75.47 MHz, [ppm])	Chemical structure
[N ₁₁₁₁][Ac]	White liquid	2.02	3.192 (s, 12H, NCH ₃), 1.917 (s, 3H, CH ₃ -CO ₂)	181.38; 55.15; 23.20	
[N ₄₄₄₄][Ac]	Yellow viscous liquid	3.54	3.205 (t, 8H, NCH ₂ CH ₂ CH ₂ CH ₃), 1.917 (s, 3H, CH ₃ -CO ₂), 1.659 (p, 8H, NCH ₂ CH ₂ CH ₂ CH ₃), 1.369 (h, 8H, NCH ₂ CH ₂ CH ₂ CH ₃), 0.952 (t, 12H, NCH ₂ CH ₂ CH ₂ CH ₃)	181.34; 58.12; 23.22; 23.06; 19.09; 12.75	

[N4444][MES]	White solid	4.17	3.763 (t, 4H, O-CH ₂ CH ₂ -N), 3.318-3.040 (m, 10H, NCH ₂ CH ₂ CH ₂ CH ₃ , N-CH ₂ CH ₂ - SO ₃), 2.832 (p, 2H, N-CH ₂ CH ₂ - SO ₃), 2.607 (t, 4H, O-CH ₂ CH ₂ -N), 1.659 (p, 8H, NCH ₂ CH ₂ CH ₂ CH ₃), 1.369 (h, 8H, NCH ₂ CH ₂ CH ₂ CH ₃), 0.954 (t, 12H, NCH ₂ CH ₂ CH ₂ CH ₃)	66.03; 58.09; 52.51; 52.20; 47.25; 23.09; 19.10; 12.77	
[N1111][Arg]	Yellow viscous liquid	2.19	3.18-2.93 (d, 15H, N-CH ₃ e NH- CH ₂ CH ₂ CH ₂ CH-CO ₂), 1.477 (s, 4H, NH-CH ₂ CH ₂ CH ₂ CH-CO ₂)	183.21; 157.47; 55.53; 55.14; 40.94; 31.69; 24.53	
[N4444][Arg]	Yellow solid	3.11	3.316-3.092 (m, 11H, NH- CH ₂ CH ₂ CH ₂ CH-CO ₂ and NCH ₂ CH ₂ CH ₂ CH ₃), 1.75-1.52 (m, 12H, NH-CH ₂ CH ₂ CH ₂ CH-CO ₂ e NCH ₂ CH ₂ CH ₂ CH ₃), 1.367 (h, 8H, NCH ₂ CH ₂ CH ₂ CH ₃), 0.954 (t, 12H, NCH ₂ CH ₂ CH ₂ CH ₃)	183.21; 157.47; 58.09; 55.53; 40.95; 31.69; 24.53; 23.09; 19.10; 12.77	

[N₁₁₁₁][MES]	White solid	3.08	3.766 (t, 4H, O-CH ₂ CH ₂ -N), 3.193 (s, 12H, NCH ₃), 3.140 (m, 2H, N-CH ₂ CH ₂ -SO ₃), 2.832 (m, 2H, N-CH ₂ CH ₂ -SO ₃), 2.607 (t, 4H, O-CH ₂ CH ₂ -N)	66.03; 55.16; 52.50; 52.19; 47.25	
[P₄₄₄₄][MES]	White solid	2.05	3.765 (t, 4H, O-CH ₂ CH ₂ -N), 3.134 (t, 2H, N-CH ₂ CH ₂ -SO ₃), 2.837 (t, 2H, N-CH ₂ CH ₂ -SO ₃), 2.607 (t, 4H, O-CH ₂ CH ₂ -N), 2.270-2.082 (m, 8H, PCH ₂ CH ₂ CH ₂ CH ₃), 1.639-1.400 (m, 16H, PCH ₂ CH ₂ CH ₂ CH ₃), 0.933 (t, 12H, PCH ₂ CH ₂ CH ₂ CH ₃)	66.03; 52.50; 52.24; 47.27; 23.35; 23.14; 22.68; 22.62; 17.92; 17.25; 12.49	
[P₄₄₄₄][Ac]	White solid	2.68	2.270-2.082 (m, 8H, PCH ₂ CH ₂ CH ₂ CH ₃), 1.918 (s, 3H, CH ₃ -CO ₂), 1.639-1.400 (m, 16H, PCH ₂ CH ₂ CH ₂ CH ₃), 0.934 (t, 12H, PCH ₂ CH ₂ CH ₂ CH ₃)	181.32; 23.34; 23.18; 23.14; 22.68; 22.62; 17.89; 17.26; 12.48	

[P4444][Arg]	Yellow solid	2.40	3.297-3.137 (m, 3H, NH-CH ₂ CH ₂ CH ₂ CH-CO ₂), 2.270-2.082 (m, 8H, PCH ₂ CH ₂ CH ₂ CH ₃), 1.882-1.745 (m, 4H, NH-CH ₂ CH ₂ CH ₂ CH-CO ₂), 1.726-1.335 (m, 16H, PCH ₂ CH ₂ CH ₂ CH ₃), 0.932 (t, 12H, PCH ₂ CH ₂ CH ₂ CH ₃)	183.37, 157.32, 55.68, 41.00, 31.63, 25.20, 23.34, 22.74, 17.91, 17.25, 12.736, 12.50	
[C4mim][Ac]	Yellow liquid	1.27	8.731 (s, 1H, N-CH-N), 7.493 (t, 1H, N-CH-CH-N), 7.443 (t, 1H, N-CH-CH-N), 4.210 (t, 2H, CH ₃ CH ₂ CH ₂ CH ₂ -N), 3.903 (s, 3H, N-CH ₃), 1.925 (s, 3H, CH ₃ -CO ₂), 1.863 (quint, 2H, CH ₃ CH ₂ CH ₂ CH ₂ -N), 1.332 (sext, 2H, CH ₃ CH ₂ CH ₂ CH ₂ -N), 0.936 (t, 3H, CH ₃ CH ₂ CH ₂ CH ₂ -N)	181.18; 135.76; 123.39; 122.12; 49.36; 45.49; 31.18; 23.17; 18.65; 12.53	

[C₄mim][MES]	White solid	4.22	7.496 (t, 1H, N-CH-CH-N), 7.435 (t, 1H, N-CH-CH-N), 4.380 - 4.480 (quad, 4H, O-CH ₂ CH ₂ -N), 4.241 (quad, 2H, CH ₃ CH ₂ CH ₂ CH ₂ -N), 3.978 (s, 2H, N-CH ₂ CH ₂ -SO ₃), 3.902 (s, 3H, N-CH ₃), 3.774 (t, 2H, N-CH ₂ CH ₂ -SO ₃), 3.09-3.19 (m, 4H, O-CH ₂ CH ₂ -N), 2.79-2.89 (m, 2H, CH ₃ CH ₂ CH ₂ CH ₂ -N), 2.614 (t, 2H, CH ₃ CH ₂ CH ₂ CH ₂ -N), 1.512-1.405 (m, 3H, CH ₃ CH ₂ CH ₂ CH ₂ -N)	123.32; 121.74; 121.20; 66.01; 52.52; 52.27; 47.26; 45.06; 44.66; 36.41; 35.46; 15.03; 14.38	 <p>The image shows two chemical structures. The top structure is the [C₄mim]⁺ cation, which consists of a five-membered imidazolium ring with a methyl group on one nitrogen and a butyl chain on the other. The bottom structure is the [MES]⁻ anion, which consists of a six-membered morpholine ring with a propyl chain attached to the nitrogen, and a sulfonate group (-SO₃⁻) attached to the end of the propyl chain.</p>
[C₄mim][Arg]	White solid	1.99	7.488 (d, 1H, N-CH-CH-N), 7.427 (d, 1H, N-CH-CH-N), 4.232 (quad, 2H, CH ₃ CH ₂ CH ₂ CH ₂ -N), 3.896 (s, 3H, N-CH ₃), 3.441-3.145 (m, 3H, NH-CH ₂ CH ₂ CH ₂ CH-CO ₂), 1.791-1.569 (m, 2H, CH ₃ CH ₂ CH ₂ CH ₂ -N), 1.505 (t, 3H, CH ₃ CH ₂ CH ₂ CH ₂ -N)	181.19; 180.95; 162.59; 156.69; 67.33; 56.18; 55.52; 55.20; 53.78; 40.77; 30.63; 30.06; 24.24	 <p>The image shows two chemical structures. The top structure is the [C₄mim]⁺ cation, which consists of a five-membered imidazolium ring with a methyl group on one nitrogen and a butyl chain on the other. The bottom structure is the [Arg]⁻ anion, which consists of a side chain starting with a guanidino group (-NH-C(=NH)-NH₂) attached to a propyl chain, which is further attached to a chiral center with an amino group (-NH₂) and a carboxylate group (-COO⁻).</p>

[Ch][MES]	Yellow solid	4.89	4.067 (m, 2H, OH-CH ₂ CH ₂ -N), 3.778 (t, 4H, O-CH ₂ CH ₂ -N), 3.524 (m, 2H, OH-CH ₂ CH ₂ -N), 3.207 (s, 9H, N-CH ₃), 3.152 (m, 2H, N-CH ₂ CH ₂ -SO ₃), 2.870 (m, 2H, N-CH ₂ CH ₂ -SO ₃), 2.651 (t, 4H, O-CH ₂ CH ₂ -N)	67.35; 65.90; 55.55; 53.79; 52.49; 52.18; 47.11;	
[Ch][Arg]	White solid	5.09	4.067 (m, 2H, O-CH ₂ CH ₂ -N), 3.522 (quint, 2H, O-CH ₂ CH ₂ -N), 3.405-3.353 (m, 3H, NH- CH ₂ CH ₂ CH ₂ CH-CO ₂), 3.208 (s, 9H, N-CH ₃), 1.812-1.543 (m, 4H, NH-CH ₂ CH ₂ CH ₂ CH-CO ₂)	181.19; 162.59; 67.33, 56.18; 55.52; 55.20; 53.78; 40.77; 30.64; 24.25	
[Ch][Ac]	Brown liquid	2.38	3.903 (m, 2H, OH-CH ₂ CH ₂ -N), 3.359 (m, 2H, OH-CH ₂ CH ₂ -N), 3.045 (s, 9H, N-CH ₃), 1.825 (s, 3H, CH ₃ -CO ₂)	179.51; 67.38; 55.69; 53.77; 22.32	

3.3.2.2. Phase diagrams of aqueous two-phase systems

After confirming the chemical structures and purity of all ILs, they were further tested for their water miscibility at 25 °C. [N₄₄₄₄][Arg] shown to be insoluble in water and therefore is not able to form an ATPS, while [C_{4mim}][Ac] forms a solid-liquid system in the presence of aqueous solutions of K₂HPO₄/KH₂PO₄ (at 14 wt%). The other synthesized ILs are water-soluble at 25 °C, and were used thereafter to explore their suitability towards the formation of ATPS with K₂HPO₄/KH₂PO₄ at pH 8.2. It was observed that the ILs [N₄₄₄₄][MES], [P₄₄₄₄][MES], [C_{4mim}][MES], [N₄₄₄₄][Ac], [N₁₁₁₁][Ac], [P₄₄₄₄][Ac] and [P₄₄₄₄][Arg] were able to form ATPS with K₂HPO₄/KH₂PO₄ + H₂O (Please see Table 7); the respective phase diagrams were determined and are shown in Figures 33 and 34. The experimental data is shown in both percentage weight fraction and in molality units. The molality units are given since they allow a better understanding of the impact of the ILs nature on the phase diagrams behavior, avoiding differences that could result from different Mws. The detailed experimental data corresponding to the determined ternary phase diagrams are presented in Appendix C. In all the studied ATPS, the top phase corresponds to the IL-rich aqueous phase while the bottom phase is mainly composed of salt and water. The biphasic or two-phase regime is localized above the solubility curve; the larger this region, the higher is the ability of the IL to induce liquid-liquid demixing with K₂HPO₄/KH₂PO₄.

Table 8: Identification of the systems able (✓) and not able (✗) to form aqueous two-phase systems with aqueous solutions of K₂HPO₄/KH₂PO₄ at pH 8.2.

	N ₁₁₁₁			N ₄₄₄₄			P ₄₄₄₄			C _{4mim}			Ch		
	Ac	MES	Arg	Ac	MES	Arg									
K ₂ HPO ₄ / KH ₂ PO ₄	✓	✗	✗	✓	✓	✗	✓	✓	✓	✗	✓	✗	✗	✗	✗

The formation of IL-based ATPS usually occurs due to a salting-out effect exerted by the inorganic salt over the IL in aqueous media. This salting-out effect is mainly explained by the stronger hydration capacity of the salt ions when compared with the IL ions, resulting thus in the exclusion of the IL to a different phase and in the formation of two liquid phases in equilibrium. In this phenomenon, the charge of the anions in the salt mixture (HPO₄²⁻/H₂PO₄⁻) plays a major role (204). Despite the ionic hydration, ionic speciation in aqueous media has been evidenced by Kurnia *et al.* (205) as an important

factor in IL-based ATPS formation, being in some cases responsible for deviation from the Hofmeister series (206).

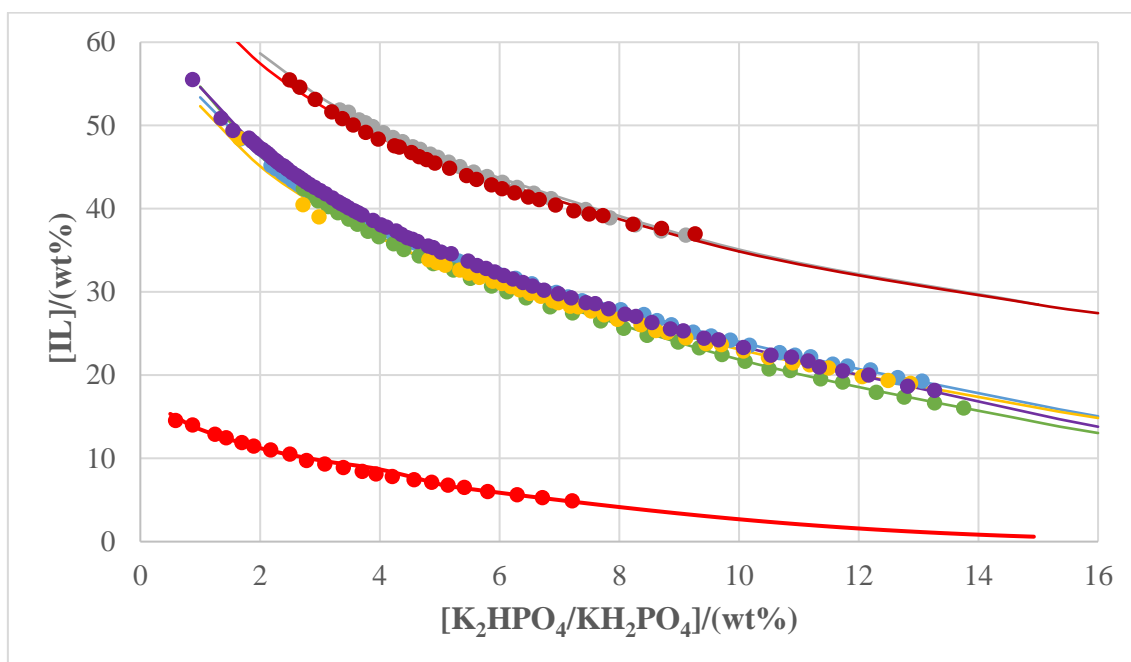


Figure 33: Ternary phase diagrams for systems composed of IL + $\text{K}_2\text{HPO}_4/\text{KH}_2\text{PO}_4$ + H_2O , in wt%. $[\text{N}_{4444}][\text{Ac}]$ (●), $[\text{P}_{4444}][\text{Ac}]$ (●), $[\text{N}_{1111}][\text{Ac}]$ (●), $[\text{N}_{4444}][\text{MES}]$ (●), $[\text{P}_{4444}][\text{MES}]$ (●), $[\text{C}_4\text{mim}][\text{MES}]$ (●), and $[\text{P}_{4444}][\text{Arg}]$ (●), with the corresponding binodal fitting using Equation 2.

The phase-forming ability of each ATPS depends on the competing interactions occurring between the solutes (IL and salt ions) and water or/and between the phase-forming components. Moreover, it is also influenced by the temperature, pH and ionic strength of the aqueous medium (16). According the Figure 34, the ability of the investigated ILs to form ATPS in presence of a fixed amount of $\text{K}_2\text{HPO}_4/\text{KH}_2\text{PO}_4$, e.g. at 0.4 mol.kg^{-1} , increases in the following order: $[\text{N}_{1111}][\text{Ac}] < [\text{C}_4\text{mim}][\text{MES}] < [\text{N}_{4444}][\text{Ac}] \approx [\text{P}_{4444}][\text{Ac}] < [\text{N}_{4444}][\text{MES}] \approx [\text{P}_{4444}][\text{MES}] < [\text{P}_{4444}][\text{Arg}]$.

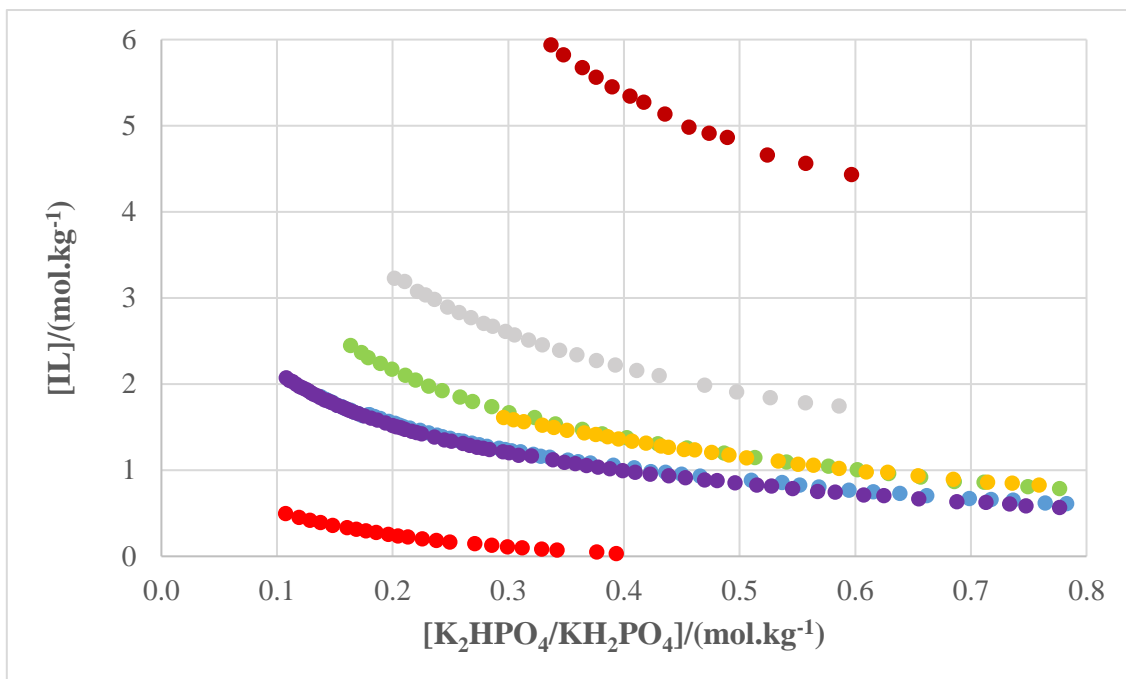


Figure 34: Ternary phase diagrams for ATPS composed of distinct ILs + $\text{K}_2\text{HPO}_4/\text{KH}_2\text{PO}_4 + \text{H}_2\text{O}$, in mol.kg^{-1} . $[\text{N}_{4444}][\text{Ac}]$ (●), $[\text{P}_{4444}][\text{Ac}]$ (●), $[\text{N}_{1111}][\text{Ac}]$ (●), $[\text{N}_{4444}][\text{MES}]$ (●), $[\text{P}_{4444}][\text{MES}]$ (●), $[\text{C}_4\text{mim}][\text{MES}]$ (●) and $[\text{P}_{4444}][\text{Arg}]$ (●).

The first diagram corresponding to the system with $[\text{N}_{1111}][\text{Ac}]$ is located more far from the axis, while the one comprising $[\text{P}_{4444}][\text{Arg}]$ is the closest. The closer to the axis is located the binodal curve, the easier it is to separate the IL from the aqueous solution, meaning that the system formed by $[\text{P}_{4444}][\text{Arg}]$ requires lower amounts of salt or IL to create ATPS in aqueous medium.

For acetate-based ILs, the capability to induce ATPS follows the order: $[\text{N}_{1111}][\text{Ac}] < [\text{N}_{4444}][\text{Ac}] \approx [\text{P}_{4444}][\text{Ac}]$, and for the MES-based ILs the trend is according to: $[\text{C}_4\text{mim}][\text{MES}] < [\text{N}_{4444}][\text{MES}] \approx [\text{P}_{4444}][\text{MES}]$. Tetrabutylammonium and tetrabutylphosphonium cations have more ability to form ATPS with the phosphate buffer used. These ILs present distinct atom cores, $[\text{N}_{4444}]^+$ and $[\text{P}_{4444}]^+$, yet both composed of four alkyl chains of similar size which assign them low affinity for water. Phosphonium-based ILs were described by Neves *et al.* (164) as the most effective ILs in ATPS formation, independently of the salt employed and of the pH of the aqueous media. In this work, the effect of the nitrogen and the phosphorous atoms seems to be negligible. An increase in the alkyl chains, from $[\text{N}_{1111}]^+$ to $[\text{N}_{4444}]^+$, or the use of ILs with an imidazolium leads to a decrease on the ability for the formation of ATPS, as typically described in the literature (164).

Regarding the anion effect, the ability to form ATPS follows the trend: $[\text{Ac}]^- < [\text{MES}]^- < [\text{Arg}]^-$. As described in the literature, the capacity of ILs anions for accepting or receiving protons is connected with the ATPS formation (163, 204), as verified in this work.

For the studied systems, the experimental binodal data were further fitted by the empirical relationship described by Equation 2 (199). The regression parameters were estimated by least-squares regression, and their values and corresponding standard deviations (σ) and correlation coefficients are provided in Table 9. Their representation is shown in Figure 33. The experimental TLs, along with their TLLs, are reported in Table 10, as well as the initial composition of each system.

Table 9: Correlation parameters used to describe the experimental binodal data fitted by Equation 2 and respective standard deviations (σ) and correlation coefficients.

ILs	$A \pm \sigma$	$B \pm \sigma$	$10^{-5} (C \pm \sigma)$	R^2
[N1111][Ac]	86.07 ± 1.41	-0.286 ± 0.009	$1.6 \times 10^{-10} \pm 1.9$	0.9961
[P4444][Ac]	74.75 ± 1.08	-0.357 ± 0.007	4.6 ± 0.8	0.9967
[N4444][Ac]	81.22 ± 0.44	-0.396 ± 0.003	6.0 ± 0.3	0.9998
[N4444][MES]	75.14 ± 0.23	-0.342 ± 0.001	5.8 ± 0.2	0.9997
[P4444][MES]	77.65 ± 0.21	-0.352 ± 0.002	7.8 ± 0.3	0.9997
[C4mim][MES]	88.90 ± 0.58	-0.294 ± 0.003	$4.6 \times 10^{-9} \pm 0.6$	0.9997
[P4444][Arg]	20.96 ± 0.32	-0.441 ± 0.012	90 ± 9.9	0.9993

Some standard deviations for parameter C were found, but in general good correlation coefficients were obtained for the fitting by Equation 2, meaning that these fittings could be used to determine the system composition at given mixtures of interest.

Table 10: Tie-lines (TLs) and tie-line lengths (TLLs). Initial mixture points are represented as IL_M and $Salt_M$; IL_T and $Salt_T$ are the composition of IL and K_2HPO_4/KH_2PO_4 at the IL-rich phase (top phase), and IL_B and $Salt_B$ are the composition of IL and salt at the K_2HPO_4/KH_2PO_4 -phase (bottom phase).

IL	Weight fraction composition/ wt%						TLL
	IL_T	IL_B	IL_M	$Salt_M$	$Salt_B$	$Salt_T$	
[N ₁₁₁₁][Ac]	41.40	10.15	39.92	8.91	55.97	6.56	58.47
[P ₄₄₄₄][Ac]	47.15	0.02	40.08	8.89	49.82	1.67	67.38
[N ₄₄₄₄][Ac]	44.95	40.06	40.04	8.89	63.54	2.23	76.02
[N ₄₄₄₄][MES]	48.08	0.04	40.04	8.89	44.67	1.70	64.46
[P ₄₄₄₄][MES]	48.80	0.03	40.00	8.91	41.50	1.74	62.93
[C _{4mim}][MES]	41.38	10.74	39.95	8.90	51.72	6.77	54.40

3.3.2.3. Purification of interferon alpha-2b using aqueous-two phase systems

The ILs that formed ATPS with K_2HPO_4/KH_2PO_4 and H_2O , described in Table 7, were used aiming at purifying IFN α -2b from the urea-SIB fraction, desalted with HiTrap Desalting as previously described. In general, the initial mixture composition of 40 wt% of IL + 9 wt% of K_2HPO_4/KH_2PO_4 was used, and the composition of each phase is given in the TLs provided in Table 10. The exact composition of the initial mixture of each ATPS is given in Appendix D.

Due to the different phase diagrams and TLs composition, the volume of the phases is different for the diverse ATPS. In the purification assays, and in each ATPS, a concentration between 100-600 μ g/mL of total proteins was used, as determined with the Pierce™ BCA Protein Assay Kit. In general, in the ATPS composed of [N₁₁₁₁][Ac] and [N₄₄₄₄][Ac] a precipitate was formed in the interface, meaning that neither the salt-rich phase or the IL-rich phase are able to solubilize all proteins. The presence of a third (solid) phase in IL-based ATPS was recently described by Alvarez-Guerra et al. (207) as “Ionic-Liquid-Based Three Phase Partitioning” (ILTTP). ILTTP combines the easiness of recovery of a third phase that can contain the target protein together with the advantages associated with IL-based ATPS. It is known that protein concentration is one of the factors that influence their partitioning in ATPS, and that partitioning between the coexisting phases only occurs at relatively low protein concentrations (151).

The top phase, the bottom phase and the precipitate (when it occurred, further solubilized in aqueous solutions of Tris-HCl at 50 mM) were analyzed through SDS-PAGE. Commercial PAGER™ Gold Precast gels (Lonza, Sweden) were used, while the gels used in the first chapters of the thesis were formed *in situ*. Although there are not significant differences in the composition of the gels, it has to be taken into account that each gel may lead to differences on the protein migration according to the pores size. The lab-made gels seem to be more appropriate than the commercial gels used in this section, since it was difficult to detect any protein in the latest. Other possible explanation is the decrease of the proteins content when diluted in ATPS for the purification assays, as well as the salt and IL presence which enhance the viscosity and ionic strength of the sample. The obtained bands in the SDS-PAGE gels are very light, not fully defined and band shifts were also observed in some situations.

The partitioning of proteins in ATPS is a complex process which depends on the phase-forming components nature and content. Some interaction between the protein and the IL and salt may occur, such as hydrogen-bonding, electrostatic interactions, van der Waals forces and hydrophobic interactions, as well as steric effects. Hitherto and to the best of our knowledge, no studies on the IFN- α 2b interactions with ILs are available. Even so, the target protein is negatively charged ($pI = 5.9$ (74)), and thus electrostatic interactions may occur between IFN- α 2b and the IL or salt ions.

In the first results illustrated in Figure 35, a total weight of the ATPS of 0.6 g was used, but few bands corresponding to proteins are visible and few conclusions can be taken. Since proteins were mainly found in the top phases of all the systems, and in the precipitated phase of the [N₁₁₁₁][Ac] and [P₄₄₄₄][Ac] ATPS, it is observed a preferential partitioning of the proteins to the top phase (IL-rich).

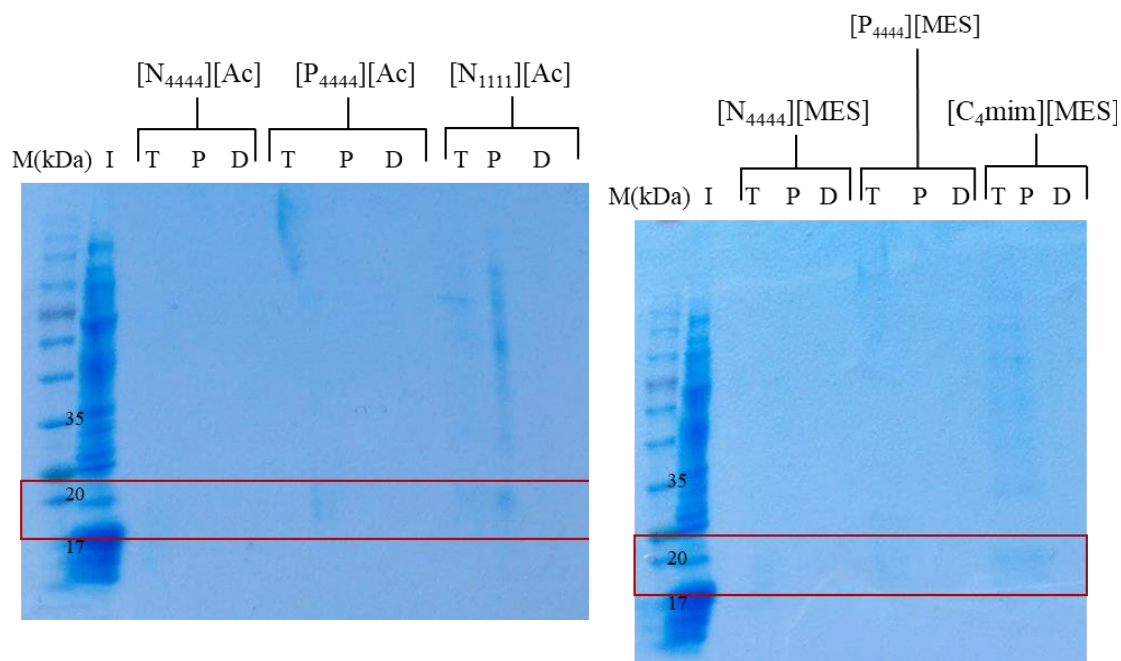


Figure 35: SDS-PAGE results of the IL-based APTS purification assay 1, where the APTS constituted by the ILs $[N_{4444}][Ac]$, $[P_{4444}][Ac]$, $[N_{1111}][Ac]$ (left), $[N_{4444}][MES]$, $[P_{4444}][MES]$, $[C_4mim][MES]$ (right) and + $K_2HPO_4/KH_2PO_4 + H_2O$ with a total mass of 0.6 g were tested for the partition of the IFN α -2b. The initial sample, the top phase, the bottom phase and the precipitate phase are represented as I, T, D and P, respectively. 40 wt% of IL + 9 wt% of K_2HPO_4/KH_2PO_4 .

The next experiments were carried out aiming at optimize the total weight of the APTS in order to ensure a proper phase-separation while minimizing the dilution of the sample. With the attempt of enhance the SDS-protein detection, we decided to increase the system total weight up to 0.8 g, where the respective results are given in Figure 36. In these experiments proteins were mainly found in the precipitate of $[N_{1111}][Ac]$ and $[N_{4444}][Ac]$ APTS, in the bottom phase of the APTS formed by $[C_4mim][MES]$, and in the top phase of the remaining systems. However, the IFN- α 2b is shown to be present in the top phase of the $[C_4mim][MES]$ APTS and in the precipitate formed in the $[N_{1111}][Ac]$ APTS. An interesting result was achieved with the $[N_{1111}][Ac]$ system, where IFN α -2b seems to selectively precipitate at the interphase. Since some selectivity was obtained, further assays must be carried out in order to see if the trend is maintained and if better results of purification can be achieved.

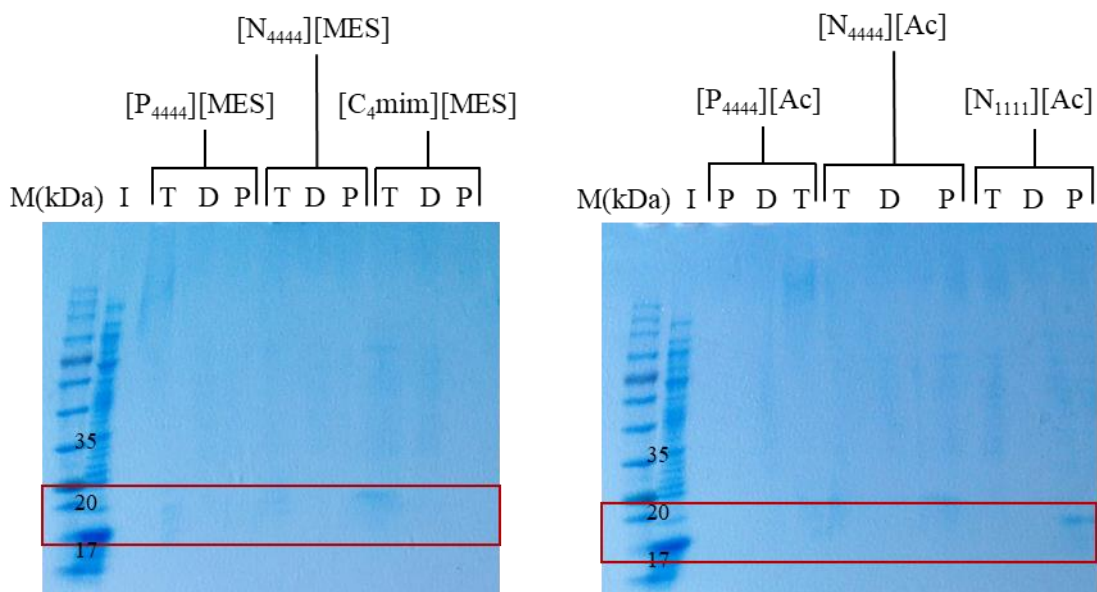


Figure 36: SDS-PAGE results of the IL-based ATPS purification assay 2, where the ATPS constituted by the ILs [P₄₄₄₄][MES], [N₄₄₄₄][MES], [C₄mim][MES] (left) [P₄₄₄₄][Ac], [N₄₄₄₄][Ac] and [N₁₁₁₁][Ac] (right) + K₂HPO₄/KH₂PO₄ + H₂O with a total mass of 0.8 g were tested for the partition of the IFN α -2b. The initial sample, the top phase, the bottom phase and the precipitate phase are represented as I, T, D and P, respectively. The mixture point used in this assay was 40 wt% of IL + 9 wt% of K₂HPO₄/KH₂PO₄.

Aiming at increasing the purity and yield of the target protein, in a further experiment, assay 3, it was used a new mixture composition with the [N₁₁₁₁][Ac] ATPS (40 wt% of IL + 8 wt% of phosphate buffer). The total mass of the [N₁₁₁₁][Ac] ATPS was decreased to 0.6 g, while for the [N₄₄₄₄][Ac] ATPS, 0.8 g of total mass and the previous mixture composition were maintained to evaluate the reproducibility of the previous results. Proteins were found in the top phase of the [N₁₁₁₁][Ac] ATPS and in the precipitate of [N₄₄₄₄][Ac] and [N₁₁₁₁][Ac] systems (Figure 37). IFN α -2b is mainly found in the precipitates, when compared to these systems top phases. In the [N₁₁₁₁][Ac] ATPS, the target protein is mostly present in the precipitate; yet, the change of the mixture point to a lower amount of salt seems to decrease the system selectivity. Regarding the [N₄₄₄₄][Ac] ATPS, few conclusions can be taken since no SDS bands were found in either phase. This trend was previously observed in assay 2 where the proteins in the top phase appeared in very light bands. A possible explanation to these results is that the protein concentration of the top phase can be very low, being untraceable in assay 3. On the other

hand, the increase of the sample introduced in the $[N_{1111}][Ac]$ ATPS can be a possible explanation for the intensification of the SDS bands and consequently, protein concentration. However, with this increase, in the top phase of $[N_{1111}][Ac]$ ATPS, apart from the IFN- α 2b, some high weight contaminants are visible.

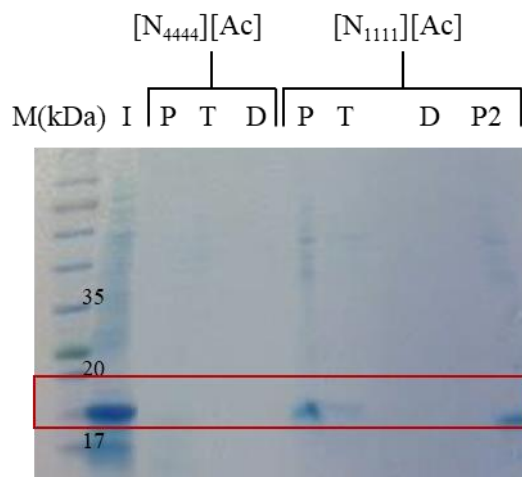


Figure 37: SDS-PAGE results of the IL-based ATPS purification assay 3, where the ATPS constituted by the ILs $[N_{4444}][Ac]$ and $[N_{1111}][Ac]$ + K_2HPO_4/KH_2PO_4 + H_2O with a total mass of 0.8 and 0.6 g, respectively, were tested for the partition of the IFN α -2b. The initial sample, the top phase, the bottom phase and the precipitate phase are represented as I, T, D and P, respectively. The mixture point used for $[N_{4444}][Ac]$ ATPS was 40 wt% of IL + 9 wt% of K_2HPO_4/KH_2PO_4 , while in $[N_{1111}][Ac]$ ATPS the weight fraction of K_2HPO_4/KH_2PO_4 was reduced to 8 wt%.

The purification of IFN- α 2b was attempted using six different IL-based ATPS, in all the systems, similar difficulties were encountered which were related with the SDS-PAGE experiments. The most promising result relies with the $[N_{1111}][Ac]$ ATPS in which the target protein showed, at least to some degree, some selectivity while precipitating in the interface. This IL was showed to be the one with the lowest capacity to form ATPS, and therefore, it is the most hydrophilic IL of the six studied systems. In this case, hydrophilic interactions can occur and can be exploited in the future. However, first these experiments should be repeated to ascertain reproducibility. As future work, an important starting point is the maximization of the IFN- α 2b concentration in the system.

4. Final remarks

4.1. Conclusions and future work

In this work, an optimized protocol for the recombinant biosynthesis and recovery of human IFN α -2b was successfully developed. IFN α -2b was produced from *E. coli* BL21 cells in the insoluble form as inclusion bodies, using the SOB culture medium after 3 h of induction with 0.5 mM IPTG at 37 °C. The optimized primary recovery of IFN α -2b from the inclusion bodies includes two successive washes with Triton-X at 1% and urea at 4 M at pH 8, a solubilization with urea at 8 M at pH 12.5, and a dialysis against decreasing concentrations of urea in presence of the glutathione redox system.

IFN α -2b was also produced in the soluble form using the SOB culture medium after 16 h of induction with IPTG, through the decrease of the temperature down to 16 °C. The soluble expression of IFN should be however further exploited due to its advantage regarding the downstream step.

A two-step chromatographic procedure based on the CIM DEAE monolith for the purification of IFN α -2b was developed. The recovery yields and the purities obtained with this process are similar to those reported by other authors (13, 193). It was verified that the purified IFN displays anti-proliferative activity against tumor breast cells, proving that it is biologically active.

IL-based ATPS were finally investigated as alternative purification platforms for IFN α -2b. However, several obstacles have been found during the optimization of the purification strategy. One of the major limitations found is associated with the quantification of IFN α -2b, particularly due to its low amount which has hampered the use of SE-HPLC for this purpose. In the same line, most of the ILs investigated absorb in the UV region, not allowing the protein quantification by UV spectroscopy. An additional obstacle was found with the heterogeneous protein profile of *E. coli* extracts, reflected in different protein concentrations in the several samples, thus resulting in several failed or inconclusive results by SDS-PAGE analysis. Additional interferences of the IL and salt may also hampered an accurate SDS-PAGE analysis.

Finally, the overall process of bioprocessing described in this work can be further optimized. Aiming at finding alternative platforms for the purification of biopharmaceuticals, further assays should be carried out to confirm the partition behavior of IFN α -2b in the studied ILs-based ATPS. As long as the contaminants or the target protein are selectively precipitated, ILTPP can be used as a cost-effective purification technique. Furthermore, IL-based ATPS can be used if a selective partitioning of IFN α -

2b is found for a given phase. An increase in the protein concentration in the initial SIB fraction may also improve the results of the ATPS-based purification procedures, particularly regarding further decisions on the best systems to investigate and additional optimization steps on the operational conditions. Other ILs and salts, as well as polymers, could be investigated to extract/purify IFN α -2b.

5. References

1. World Health Organization. 2015. World Report on Ageing and Health.
2. Azevedo AM, Aires-Barros MR. 2011. New platforms for the downstream processing of biopharmaceuticals. *1st Portuguese Meeting in Biomedical Engineering, ENBENG 2011*. IEEE.
3. Sekhon BS. 2010. Biopharmaceuticals: An overview. *Thai J Pharm Sci* 34:1–19.
4. Guiochon G, Beaver LA. 2011. Separation science is the key to successful biopharmaceuticals. *J Chromatogr A* 1218:8836–8858.
5. Leader B, Baca QJ, Golan DE. 2008. Protein therapeutics: a summary and pharmacological classification. *Nat Rev Drug Discov* 7:21–39.
6. World Health Organization. 2015. WHO Model Lists of Essential Medicines.
7. Nyman TA, Tölö H, Parkkinen J, Kalkkinen N. 1998. Identification of nine interferon-alpha subtypes produced by Sendai virus-induced human peripheral blood leucocytes. *Biochem J* 329:295–302.
8. El-Baky NA, Redwan EM. 2015. Therapeutic Alpha-Interferons Protein: Structure, Production, and Biosimilar. *Prep Biochem Biotechnol* 45:109–127.
9. Walsh G. 2014. Biopharmaceuticals benchmarks. *Nat Biotechnol* 32:992–1000.
10. Jozala AF, Geraldes D, Tundisi LL, Feitosa V de A, Breyer CA, Mazzola PG, *et al.*. 2016. Biopharmaceuticals from microorganisms: From production to purification. *Brazilian J Microbiol* 170:1–13.
11. Valente CA, Monteiro GA, Cabral JMS, Fevereiro M, Prazeres DMF. 2006. Optimization of the primary recovery of human interferon α 2b from *Escherichia coli* inclusion bodies. *Protein Expr Purif* 45:226–234.
12. Ramanan RN, Tan JS, Mohamed MS, Ling TC, Tey BT, Ariff AB. 2010. Optimization of osmotic shock process variables for enhancement of the release of periplasmic interferon- α 2b from *Escherichia coli* using response surface method. *Process Biochem* 45:196–202.
13. Shi L, Wang D, Chan W, Cheng L. 2007. Efficient expression and purification of human interferon alpha2b in the methylotrophic yeast, *Pichia pastoris*. *Protein Expr Purif* 54:220–226.
14. Lin YK, Ooi CW, Ramanan RN, Ariff A, Ling TC. 2012. Recovery of Human Interferon Alpha-2b from Recombinant *Escherichia coli* by Aqueous Two-Phase System. *Sep Sci Technol* 47:1023–1030.
15. Lin YK, Ooi CW, Tan JS, Show PL, Ariff A, Ling TC. 2013. Recovery of human

- interferon alpha-2b from recombinant *Escherichia coli* using alcohol/salt-based aqueous two-phase systems. *Sep Purif Technol* 120:362–366.
16. Freire MG, Cláudio AFM, Araújo JMM, Coutinho JAP, Marrucho IM, Lopes JNC, Rebelo LPN. 2012. Aqueous biphasic systems: a boost brought about by using ionic liquids. *Chem Soc Rev* 41:4966–4995.
 17. 1982. FDA okays marketing of human insulin. *Chem Eng News*. American Chemical Society.
 18. Lindenmann J, Schleuning W-D. 1999. Interferon: the dawn of recombinant protein drugs. Springer.
 19. Tufts Center for the Study of Drug Development. 2014. How the Tufts Center for the Study of Drug Development Pegged the Cost of a New Drug at \$2.6 Billion.
 20. Azevedo AM, Rosa PAJ, Ferreira IF, Aires-Barros MR. 2009. Chromatography-free recovery of biopharmaceuticals through aqueous two-phase processing. *Trends Biotechnol* 27:240–247.
 21. Przybycien TM, Pujar NS, Steele LM. 2004. Alternative bioseparation operations: Life beyond packed-bed chromatography. *Curr Opin Biotechnol* 15:469–478.
 22. Das RC. 2003. Progress and prospects of protein therapeutics (application note). *Am Biotechnol Lab* 8–12.
 23. Research and Markets. Global Interferon Market & Pipeline Analysis 2015. [Online]. Available: <http://www.researchandmarkets.com/reports/3161900/global-interferon-market-and-pipeline-analysis>. [Accessed: 20-Dec-2016].
 24. Foster GR, Finter NB. 1998. Are all Type I human interferons equivalent? *J Viral Hepat* 5:143–152.
 25. Pestka S, Baron S. 1981. Definition and Classification of the Interferons, p. 3–14. *In Methods in Enzymology*.
 26. Pestka S, Langer JA, Zoon KC, Samuel CE. 1986. Interferon from 1981 to 1986. *Annu Rev Biochem* 119:3–23.
 27. Pestka S, Langer J, Zoon K, Samuel C. 1987. Interferons and their actions. *Annu Rev Biochem* 56:727–777.
 28. Allen G, Diaz MO. 1994. Nomenclature of the human interferon proteins. *J Interferon Res* 14:223–226.
 29. Nagata S, Taira H, Hall A, Johnsrud L, Streuli M, Ecsödi J *et al.*. 1980. Synthesis in *E. coli* of a polypeptide with human leukocyte interferon activity. *Nature*

- 284:316–320.
30. Pfeffer LM, Dinarello CA, Herberman RB, Williams BR, Borden EC, Bordens R *et al.*. 1998. Biological properties of recombinant alpha-interferons: 40th anniversary of the discovery of interferons. *Cancer Res* 58:2489–2499.
 31. Emanuel SL, Pestka S. 1993. Human interferon-alpha A, -alpha 2, and -alpha 2(Arg) genes in genomic DNA. *J Biol Chem* 268:12565–12569.
 32. Wheelock EF. 1965. Interferon-Like Virus-Inhibitor Induced in Human Leukocytes by Phytohemagglutinin. *Science (80-)* 149:310–311.
 33. Ank N, West H, Paludan SR. 2006. IFN- λ : Novel Antiviral Cytokines. *J Interf Cytokine Res* 26:373–379.
 34. Isaacs A, Lindenmann J. 1957. Virus interference. I. The interferon. *Proc R Soc Lond. Ser B, Biol Sci* 147:258–267.
 35. Friedman RM. 2008. Clinical uses of interferons. *Br J Clin Pharmacol* 65:158–162.
 36. Cavalieri RL, Havell EA, Vilcek J, Pestka S. 1977. Synthesis of human interferon by *Xenopus laevis* oocytes: two structural genes for interferons in human cells. *Proc Natl Acad Sci U S A* 74:3287–3291.
 37. Borden EC. 1979. Interferons: rationale for clinical trials in neoplastic disease. *Ann Intern Med* 91:472–479.
 38. Scherer P. 1987. New drugs. *Am J Nurs* 87:448-454.
 39. George PM, Badiger R, Alazawi W, Foster GR, Mitchell JA. 2012. Pharmacology and therapeutic potential of interferons. *Pharmacol Ther* 135:44–53.
 40. Kieseier BC. 2011. The Mechanism of Action of Interferon- β in Relapsing Multiple Sclerosis. *CNS Drugs* 25:491–502.
 41. Buster EHCJ, Flink HJ, Cakaloglu Y, Simon K, Trojan J, Tabak F *et al.*. 2008. Sustained HBeAg and HBsAg Loss After Long-term Follow-up of HBeAg-Positive Patients Treated With Peginterferon α -2b. *Gastroenterology* 135:459–467.
 42. Hoofnagle JH, Seeff LB. 2006. Peginterferon and ribavirin for chronic hepatitis C. *N Engl J Med* 355:2444–2451.
 43. Petersen CS, Bjerring P, Larsen J, Blaakaer J, Hagdrup H, From E. 1991. Systemic interferon alpha-2b increases the cure rate in laser treated patients with multiple persistent genital warts: a placebo-controlled study. *Genitourin Med* 67:99–102.
 44. Krown SE, Li P, Von Roenn JH, Paredes J, Huang J, Testa MA. 2002. Efficacy of

- Low-Dose Interferon with Antiretroviral Therapy in Kaposi's Sarcoma: A Randomized Phase II AIDS Clinical Trials Group Study. *J Interf Cytokine Res* 22:295–303.
45. Cameron DA, Cornbleet MC, Mackie RM, Hunter JA, Gore M, Hancock B *et al.*. 2001. Adjuvant interferon alpha 2b in high risk melanoma - the Scottish study. *Br J Cancer* 84:1146–1149.
 46. Foon KA, Sherwin SA, Abrams PG, Longo DL, Fer MF, Stevenson HC *et al.*. 1984. Treatment of advanced non-Hodgkin's lymphoma with recombinant leukocyte A interferon. *N Engl J Med* 311:1148–1152.
 47. Michallet M, Maloisel F, Delain M, Hellmann A, Rosas A, Silver RT. 2004. Pegylated recombinant interferon alpha-2b vs recombinant interferon alpha-2b for the initial treatment of chronic-phase chronic myelogenous leukemia: a phase III study. *Leukemia* 18:309–315.
 48. Braide J; Hasselbalch H; Hippe E, Lisse I, Rockert L, Swolin Zador BGIW. 1991. Demonstrated benefit of continuous interferon-alpha-2b therapy in hairy cell leukemia. A two-year follow-up. *Leuk Lymphoma* 5:23–31.
 49. Lyrdal D, Stierner U, Lundstam S. 2009. Metastatic renal cell carcinoma treated with Peg-interferon alfa-2b. *Acta Oncol* 48:901–8.
 50. Foster GR. 2004. Review article: pegylated interferons: chemical and clinical differences. *Aliment Pharmacol Ther* 20:825–830.
 51. Jansen PLM, De Bruijne J. 2012. Controlled-release interferon alpha 2b, a new member of the interferon family for the treatment of chronic hepatitis C. *Expert Opin Investig Drugs* 21:111–118.
 52. Wang Y Sen, Youngster S, Grace M, Bausch J, Bordens R, Wyss DF. 2002. Structural and biological characterization of pegylated recombinant interferon alpha-2b and its therapeutic implications. *Adv Drug Deliv Rev* 54:547–570.
 53. Foser S, Schacher A, Weyer KA, Brugger D, Dietel E, Marti S. 2003. Isolation, structural characterization, and antiviral activity of positional isomers of monopegylated interferon α -2a. *Protein Expr Purif* 30:78–87.
 54. Helsper CW, Hellinga HL, van Essen GA, de Wit GA, Bonten MJM, van Erpecum KJ *et al.*. 2012. Real-life costs of hepatitis C treatment. *Neth J Med* 70:145–153.
 55. Marciano BE, Wesley R, De Carlo ES, Anderson VL, Barnhart LA, Darnell D *et al.*. 2004. Long-term interferon-gamma therapy for patients with chronic granulomatous disease. *Clin Infect Dis* 39:692–699.

56. Key LL, Rodriguiz RM, Willi SM, Wright NM, Hatcher HC, Eyre DR *et al.*. 1995. Long-term treatment of osteopetrosis with recombinant human interferon gamma. *N Engl J Med* 332:1594–1599.
57. Hermant P, Michiels T. 2014. Interferon- λ in the context of viral infections: Production, response and therapeutic implications. *J Innate Immun* 6:563–574.
58. Hoffmann-La Roche. 2002. Pegasys® (peginterferon alfa-2a, recombinant) Product information.
59. Schering Corporation. 2001. PEG-Intron® (peginterferon alfa-2b, recombinant) Product information.
60. Hoffmann-La Roche. 2008. Roferon-A® (Interferon alfa-2a, recombinant) Product information.
61. Schering Corporation. 2011. Intron-A® (Interferon alfa-2b, recombinant) Product information.
62. De Leede LGJ, Humphries JE, Bechet AC, Van Hoogdalem EJ, Verrijk R, Spencer DG. 2008. Novel controlled-release Lemna-derived IFN-alpha2b (Locteron): pharmacokinetics, pharmacodynamics, and tolerability in a phase I clinical trial. *J Interferon Cytokine Res* 28:113–122.
63. Biogen. 2003. Avonex® (Interferon beta-1a, recombinant) Product information.
64. EMD Serono I. 2012. Rebif® (interferon beta-1a, recombinant) Product information.
65. Berlex Laboratories. 1903. Betaseron® (interferon beta-1b, recombinant) Product information.
66. Novartis Pharmaceuticals Corporation. 2009. Extavia® (Interferon beta-1b, recombinant) Product information.
67. InterMune I. 2007. Actimmune® (interferon gamma-1b, recombinant) Product information.
68. Fried MW. 2002. Side effects of therapy of hepatitis C and their management. *Hepatology* 36:237–243.
69. Garib JR, Garcia GF, Teixeira R, das Chagas Lima e Silva F. 2011. Dyspnoea in patients with chronic hepatitis C treated with pegylated interferon and ribavirin. *Scand J Infect Dis* 43:625–631.
70. Hézode C, Forestier, Dusheiko GM, Ferenci, Pol S, Goeser T, Bronowicki J-P, Bourlière M, Gharakhanian, Bengtsson, McNair, George, Kieffer TL, Kwong AD, Kauffman RS, Alam J, Pawlotsky J-M, Zeuzem S. 2009. Telaprevir and

- peginterferon with or without ribavirin for chronic HCV infection. *N Engl J Med* 360:1839–1850.
71. Feld JJ, Lutchman GA, Heller T, Hara K, Pfeiffer JK, Leff RD *et al.*. 2010. Ribavirin Improves Early Responses to Peginterferon Through Improved Interferon Signaling. *Gastroenterology* 139:154–162.
 72. Fruehauf S, Steiger S, Topaly J, Ho AD. 2001. Pulmonary artery hypertension during interferon- α therapy for chronic myelogenous leukemia. *Ann Hematol* 80:308–310.
 73. Dhillon S, Kaker A, Dosanjh A, Japra D, Vanthiel DH. 2010. Irreversible pulmonary hypertension associated with the use of interferon α for chronic hepatitis C. *Dig Dis Sci* 55:1785–1790.
 74. Srivastava P, Bhattacharaya P, Pandey G, Mukherjee KJ. 2005. Overexpression and purification of recombinant human interferon α 2b in *Escherichia coli*. *Protein Expr Purif* 41:313–322.
 75. Sen GC, Lengyel P. 1992. Interferon System. A Bird's Eye View of its Biochemistry. *J Biol Chem* 267:5017–5020.
 76. Nyman TA, Kalkkinen N, Tölö H, Helin J. 1998. Structural characterisation of N-linked and O-linked oligosaccharides derived from interferon- α 2b and interferon- α 14c produced by Sendai-virus-induced human peripheral blood leukocytes. *Eur J Biochem* 253:485–493.
 77. Wetzel R. 1981. Assignment of the disulphide bonds of leukocyte interferon. *Nature* 289:606–607.
 78. Radhakrishnan R, Walter LJ, Hruza A, Reichert P, Trotta PP, Nagabhushan TL. 1996. Zinc mediated dimer of human interferon- α 2b revealed by X-ray crystallography. *Structure* 4:1453–1463.
 79. Asmana Ningrum R, Asmana Ningrum R, Ningrum A, Ratih. 2014. Human interferon α -2b: a therapeutic protein for cancer treatment. *Scientifica* 2014:1–8.
 80. Liu YH, Wylie D, Zhao J, Cure R, Cutler C, Cannon-Carlson S *et al.*. 2011. Mass spectrometric characterization of the isoforms in *Escherichia coli* recombinant DNA-derived interferon α -2b. *Anal Biochem* 408:105–117.
 81. Gitlin G, Tsarbopoulos A, Patel ST, Sydor W, Pramanik BN, Jacobs S *et al.*. 1996. Isolation and characterization of a monomethioninesulfoxide variant of interferon α -2b. *Pharm Res* 13:762–769.

82. Díaz M, Pomykala HM, Bohlander SK, Maltepe E, Malik K, Brownstein B. 1994. Structure of the Human Type-I Interferon Gene Cluster Determined from a YAC Clone Contig. *Genomics* 22:540–552.
83. Ghosh D, Ghosh D, Parida P. 2016. Physiological Proteins in Therapeutics: A Current Review on Interferons. *Mini Rev Med Chem* 16:947–952.
84. Génin P, Lin R, Hiscott J, Civas A. 2009. Differential regulation of human interferon A gene expression by interferon regulatory factors 3 and 7. *Mol Cell Biol* 29:3435–3450.
85. Lehmann C, Lafferty M, Garzino-Demo A, Jung N, Hartmann P, Fätkenheuer G *et al.*. 2010. Plasmacytoid dendritic cells accumulate and secrete interferon alpha in lymph nodes of HIV-1 patients. *Plos one* 5:e11110.
86. Keating SE, Baran M, Bowie AG. 2011. Cytosolic DNA sensors regulating type I interferon induction. *Trends Immunol* 32:574–581.
87. Ankel H, Westra DF, Welling-Wester S, Lebon P. 1998. Induction of interferon-alpha by glycoprotein D of herpes simplex virus: a possible role of chemokine receptors. *Virology* 251:317–326.
88. Botos I, Segal DM, Davies DR. 2011. The structural biology of Toll-like receptors. *Structure* 19:447–459.
89. Akira S, Takeda K. 2004. Toll-like receptor signalling. *Nat Rev Immunol* 4:499–511.
90. Erlandsson L, Blumenthal R, Eloranta M-L, Engel H, Alm G, Weiss S. 1998. Interferon- β is required for interferon- α production in mouse fibroblasts. *Curr Biol* 8:223–226.
91. Hertzog P, Forster S, Samarajiwa S. 2011. Systems biology of interferon responses. *J Interferon Cytokine Res* 31:5–11.
92. Gibbert K, Schlaak JF, Yang D, Dittmer U. 2013. IFN- α subtypes: Distinct biological activities in anti-viral therapy. *Br J Pharmacol* 168:1048–1058.
93. Jaks E, Gavutis M, Uzé G, Martal J, Piehler J. 2007. Differential Receptor Subunit Affinities of Type I Interferons Govern Differential Signal Activation. *J Mol Biol* 366:525–539.
94. Lavoie TB, Kalie E, Crisafulli-Cabatu S, Abramovich R, DiGioia G, Moolchan K *et al.*. 2011. Binding and activity of all human alpha interferon subtypes. *Cytokine* 56:282–289.
95. Kalie E, Jaitin DA, Podoplelova Y, Piehler J, Schreiber G. 2008. The stability of

- the ternary interferon-receptor complex rather than the affinity to the individual subunits dictates differential biological activities. *J Biol Chem* 283:32925–32936.
96. Jonasch E, Haluska FG. 2001. Interferon in oncological practice: review of interferon biology, clinical applications, and toxicities. *Oncologist* 6:34–55.
 97. Antonelli G. 2008. Biological basis for a proper clinical application of alpha interferons. *New Microbiol* 31:305–318.
 98. Samuel CE. 2001. Antiviral actions of interferons. *Clin Microbiol Rev* 14:778–809.
 99. Kimchi-Sarfaty C, Schiller T, Hamasaki-Katagiri N, Khan MA, Yanover C, Sauna ZE. 2013. Building better drugs: Developing and regulating engineered therapeutic proteins. *Trends Pharmacol Sci* 34:534–548.
 100. Demain AL, Vaishnav P. 2009. Production of recombinant proteins by microbes and higher organisms. *Biotechnol Adv* 27:297–306.
 101. Jia B, Jeon CO. 2016. High-throughput recombinant protein expression in *Escherichia coli*: current status and future perspectives. *Open Biol* 6:1–17.
 102. Francis DM, Page R. 2010. Strategies to optimize protein expression in *E. coli*. *Curr Protoc Protein Sci* 5.24:1-29.
 103. Gräslund S, Nordlund P, Weigelt J, Bray J. 2008. Protein production and purification. *Nat Methods* 5:135–146.
 104. Cheong DE, Ko KC, Han Y, Jeon HG, Sung BH, Kim GJ *et al.*. 2015. Enhancing functional expression of heterologous proteins through random substitution of genetic codes in the 5' coding region. *Biotechnol Bioeng* 112:822–826.
 105. Mutalik VK, Guimaraes JC, Cambray G, Lam C, Christoffersen MJ, Mai Q-A *et al.*. 2013. Precise and reliable gene expression via standard transcription and translation initiation elements. *Nat Methods* 10:354–360.
 106. Marsischky G, LaBaer J. 2004. Many paths to many clones: A comparative look at high-throughput cloning methods. *Genome Res* 14:2020–2028.
 107. Festa F, Steel J, Bian X, Labaer J. 2013. High-throughput cloning and expression library creation for functional proteomics. *Proteomics* 13:1381–1399.
 108. Schmidt FR. 2004. Recombinant expression systems in the pharmaceutical industry. *Appl Microbiol Biotechnol* 65:363–372.
 109. Berlec A, Štrukelj B. 2013. Current state and recent advances in biopharmaceutical production in *Escherichia coli*, yeasts and mammalian cells. *J Ind Microbiol Biotechnol* 40:257–274.

110. Gonçalves AM, Pedro AQ, Maia C, Sousa F, Queiroz JA, Passarinha LA. 2013. *Pichia pastoris*: A recombinant microfactory for antibodies and human membrane proteins. *J Microbiol Biotechnol* 23:587–601.
111. Karg SR, Kallio PT. 2009. The production of biopharmaceuticals in plant systems. *Biotechnol Adv* 27:879–894.
112. Park KY, Wi SJ. 2016. Potential of plants to produce recombinant protein products. *J Plant Biol* 59:559–568.
113. Vallin C, Pimienta E, Ramos A, Rodriguez C, Van L, Anné J. 2005. *Streptomyces* as a host for the secretion of heterologous proteins for the production of biopharmaceuticals. *J Bus Chem* 2:107–111.
114. Sørensen HP, Mortensen KK. 2005. Advanced genetic strategies for recombinant protein expression in *Escherichia coli*. *J Biotechnol* 115:113–128.
115. Hitzeman RA, Hagie FE, Levine HL, Goeddel DV, Ammerer G. 1981. Expression of human gene for interferon in yeast. *Nature* 293:717–722.
116. Neves FO, Ho PL, Raw I, Pereira CA, Moreira C. 2004. Overexpression of a synthetic gene encoding human alpha interferon in *Escherichia coli*. *Protein Expr Purif* 35:353–359.
117. Ayed A, Rabhi I, Dellagi K, Kallel H. 2008. High level production and purification of human interferon α 2b in high cell density culture of *Pichia pastoris*. *Enzyme Microb Technol* 42:173–180.
118. Zhang Q, Zhong J, Liang X, Liu W, Huan L. 2010. Improvement of human interferon alpha secretion by *Lactococcus lactis*. *Biotechnol Lett* 32:1271–1277.
119. Landowski CP, Mustalahti E, Wahl R, Croute L, Sivasiddharthan D, Westerholm-Parvinen A *et al.* 2016. Enabling low cost biopharmaceuticals: high level interferon alpha-2b production in *Trichoderma reesei*. *Microb Cell Fact* 15:1–15.
120. Arlen PA, Falconer R, Cherukumilli S, Cole A, Cole AM, Oishi KK. 2007. Field production and functional evaluation of chloroplast-derived interferon- α 2b. *Plant Biotechnol J* 5:511–525.
121. Luchakivskaya Y, Kishchenko O, Gerasymenko I, Olevinskaya Z, Simonenko Y, Spivak M. 2011. High-level expression of human interferon alpha-2b in transgenic carrot (*Daucus carota* L.) plants. *Plant Cell Rep* 30:407–415.
122. Gasmi N, Fudalej F, Kallel H, Nicaud J-M. 2011. A molecular approach to optimize hIFN α 2b expression and secretion in *Yarrowia lipolytica*. *Appl Microbiol Biotechnol* 89:109–119.

123. Rossmann C, Sharp N, Allen G, Gewert D. 1996. Expression and purification of recombinant, glycosylated human interferon alpha 2b in murine myeloma NSo cells. *Protein Expr Purif* 7:335–342.
124. Addgene | Search results. [Online]. Available: https://www.addgene.org/search/advanced/?q=IFNa2b&depositor=&article=&gene=&vector=&tags=&advanced_query=&results_per_page=20&page=1. [Accessed: 19-Dec-2016].
125. DNASU | Search results. [Online]. Available: <https://dnasu.org/DNASU/SearchTemplate.do?searchString=interferon+alpha>. [Accessed: 19-Dec-2016].
126. ATCC | Search results. [Online]. Available: https://www.lgcstandards-atcc.org/Search_Results.aspx?dsNav=Ntk:PrimarySearch%7CINTERFERON+ALPHA%7C3%7C,Ny:True,N:1000552-1000575&searchTerms=INTERFERON+ALPHA&redir=1. [Accessed: 19-Dec-2016].
127. Streuli M, Nagata S, Weissmann C. 1980. At least three human type a interferons: structure of a2. *Science (80-)* 209:1343–1347.
128. Koehn J, Hunt I. 2009. High Throughput Protein Expression and Purification: Methods and Protocols, p. 1–18. In Methods in molecular biology.
129. Fischer B, Sumner I, Goodenough P. 1993. Isolation, renaturation, and formation of disulfide bonds of eukaryotic proteins expressed in Escherichia coli as inclusion bodies. *Biotechnol Bioeng* 41:3–13.
130. Vu TTT, Jeong B, Krupa M, Kwon U, Song JA, Do BH, *et al.*. 2016. Soluble Prokaryotic Expression and Purification of Human Interferon Alpha-2b Using a Maltose-Binding Protein Tag. *J Mol Microbiol Biotechnol* 26:359–368.
131. Prasad S, Khadatare PB, Roy I. 2011. Effect of chemical chaperones in improving the solubility of recombinant proteins in Escherichia coli. *Appl Environ Microbiol* 77:4603–4609.
132. Yamaguchi H, Miyazaki M. 2014. Refolding techniques for recovering biologically active recombinant proteins from inclusion bodies. *Biomolecules* 4:235–251.
133. Batas B, Chaudhuri JB. 1996. Protein refolding at high concentration using size-exclusion chromatography. *Biotechnol Bioeng* 50:16–23.
134. Dashbolaghi A, Khatami S, Sardari S, Cohan RA, Norouzian D. 2015. Improved

- refolding efficacy of recombinant human interferon α -2b via pH modulation. *Trop J Pharm Res* 14:385–390.
135. Poole CF, Poole CF. 2003. General Concepts in Column Chromatography, p. 1–78. In *The Essence of Chromatography*.
 136. Rosa PAJ, Ferreira IF, Azevedo AM, Aires-Barros MR. 2010. Aqueous two-phase systems: A viable platform in the manufacturing of biopharmaceuticals. *J Chromatogr A* 1217:2296–2305.
 137. Sarfert FT, Etzel MR. 1997. Mass transfer limitations in protein separations using ion-exchange membranes. *J Chromatogr A* 764:3–20.
 138. Beijerinck MW. 1896. Über eine Eigentümlichkeit der löslichen Stärke. *Centr-Bl f Bakter u Parasitenk* 2:698–699.
 139. Albertsson P-Å. 1958. Particle fractionation in liquid two-phase systems. The composition of some phase systems and the behaviour of some model particles in them application to the isolation of cell walls from microorganisms. *Biochim Biophys Acta* 27:378–395.
 140. Iqbal M, Tao Y, Xie S, Zhu Y, Chen D, Wang X. 2016. Aqueous two-phase system (ATPS): an overview and advances in its applications. *Biol Proced Online* 18:1–18.
 141. Raja S, Murty VR, Thivaharan V, Rajasekar V, Ramesh V. 2012. Aqueous Two Phase Systems for the Recovery of Biomolecules – A Review. *Sci Technol* 1:7–16.
 142. Raghavarao KSMS, Rastogi NK, Gowthaman MK, Karanth NG. 1995. Aqueous Two-Phase Extraction for Downstream Processing of Enzymes/Proteins. *Adv Appl Microbiol* 41:97–171.
 143. Bensch M, Selbach B, Hubbuch J. 2007. High throughput screening techniques in downstream processing: Preparation, characterization and optimization of aqueous two-phase systems. *Chem Eng Sci* 62:2011–2021.
 144. Aguilar O, Albiter V, Serrano-Carreón L, Rito-Palomares M. 2006. Direct comparison between ion-exchange chromatography and aqueous two-phase processes for the partial purification of penicillin acylase produced by *E. coli*. *J Chromatogr B Anal Technol Biomed Life Sci* 835:77–83.
 145. Bolar S, Belur PD, Iyyaswami R. 2013. Partitioning studies of glutaminase in polyethylene glycol and salt-based aqueous two-phase systems. *Chem Eng Technol* 36:1378–1386.

146. Nitsawang S, Hatti-Kaul R, Kanasawud P. 2006. Purification of papain from *Carica papaya* latex: Aqueous two-phase extraction versus two-step salt precipitation. *Enzyme Microb Technol* 39:1103–1107.
147. Madhusudhan MC, Raghavarao KSMS, Nene S. 2008. Integrated process for extraction and purification of alcohol dehydrogenase from Baker's yeast involving precipitation and aqueous two phase extraction. *Biochem Eng J* 38:414–420.
148. Schwienheer C, Prinz A, Zeiner T, Merz J. 2015. Separation of active laccases from *Pleurotus sapidus* culture supernatant using aqueous two-phase systems in centrifugal partition chromatography. *J Chromatogr B Anal Technol Biomed Life Sci* 1002:1–7.
149. Cabezas H. 1996. Theory of phase formation in aqueous two-phase systems. *J Chromatogr B Biomed Appl* 680:3–30.
150. Zhi W, Song J, Bi J, Ouyang F. 2004. Partial purification of α -amylase from culture supernatant of *Bacillus subtilis* in aqueous two-phase systems. *Bioprocess Biosyst Eng* 27:3–7.
151. Asenjo JA, Andrews BA. 2011. Aqueous two-phase systems for protein separation: A perspective. *J Chromatogr A* 1218:8826–8835.
152. Hachem F, Andrews BA, Asenjo JA. 1996. Hydrophobic partitioning of proteins in aqueous two-phase systems. *Enzyme Microb Technol* 19:507–517.
153. Du Z, Yu Y-L, Wang J-H. 2007. Extraction of Proteins from Biological Fluids by Use of an Ionic Liquid/Aqueous Two-Phase System. *Chem - A Eur J* 13:2130–2137.
154. Zafarani-Moattar MT, Hamzehzadeh S, Nasiri S. 2012. A new aqueous biphasic system containing polypropylene glycol and a water-miscible ionic liquid. *Biotechnol Prog* 28:146–156.
155. Cleland JL, Hedgepeth C, Wang DIC. 1992. Polyethylene glycol enhanced refolding of bovine carbonic anhydrase B: Reaction stoichiometry and refolding model. *J Biol Chem* 267:13327–13334.
156. Berthod A, Ruiz-Ángel MJ, Carda-Broch S. 2008. Ionic liquids in separation techniques. *J Chromatogr A* 1184:6–18.
157. Walden P. 1914. Molecular weights and electrical conductivity of several fused salts. *Bull l'Academie Imp des Sci (St Petersburg)* 1800:405–422.
158. Plechkova N V, Seddon KR. 2008. Applications of ionic liquids in the chemical industry. *Chem Soc Rev* 37:123–150.

159. Zhao D, Liao Y, Zhang ZD. 2007. Toxicity of ionic liquids. *Clean - Soil, Air, Water* 35:42–48.
160. Ventura SPM, Gonçalves AMM, Sintra T, Pereira JL, Gonçalves F, Coutinho JAP. 2013. Designing ionic liquids: The chemical structure role in the toxicity. *Ecotoxicology* 22:1–12.
161. Pereira JFB, Vicente F, Santos-Ebinuma VC, Araújo JM, Pessoa A, Freire MG *et al.*. 2013. Extraction of tetracycline from fermentation broth using aqueous two-phase systems composed of polyethylene glycol and cholinium-based salts. *Process Biochem* 48:716–722.
162. Gutowski KE, Broker GA, Willauer HD, Huddleston JG, Swatoski RP, Holbrey JD *et al.*. 2003. Controlling the aqueous miscibility of ionic liquids: Aqueous biphasic systems of water-miscible ionic liquids and water-structuring salts for recycle, metathesis, and separations. *J Am Chem Soc* 125:6632–6633.
163. Ventura SPM, Neves CMSS, Freire MG, Marrucho IM, Oliveira J, Coutinho JAP. 2009. Evaluation of Anion Influence on the Formation and Extraction Capacity of Ionic-Liquid-Based Aqueous Biphasic Systems. *J Phys Chem B* 113:9304–9310.
164. Neves CMSS, Ventura SPM, Freire MG, Marrucho IM, Coutinho JAP. 2009. Evaluation of Cation Influence on the Formation and Extraction Capability of Ionic-Liquid-Based Aqueous Biphasic Systems. *J Phys Chem B* 113:5194–5199.
165. Li Z, Pei Y, Wang H, Fan J, Wang J. 2010. Ionic liquid-based aqueous two-phase systems and their applications in green separation processes. *Trends Anal Chem* 29:1336–1346.
166. Pereira JFB, Lima ÁS, Freire MG, Coutinho JAP. 2010. Ionic liquids as adjuvants for the tailored extraction of biomolecules in aqueous biphasic systems. *Green Chem* 12:1661–1669.
167. Pereira JFB, Rebelo LPN, Rogers RD, Coutinho JAP, Freire MG. 2013. Combining ionic liquids and polyethylene glycols to boost the hydrophobic-hydrophilic range of aqueous biphasic systems. *Phys Chem Chem Phys* 15:19580–19583.
168. Souza RL, Ventura SPM, Soares CMF, Coutinho JAP, Lima ÁS. 2015. Lipase purification using ionic liquids as adjuvants in aqueous two-phase systems. *Green Chem* 17:3026–3034.
169. Almeida MR, Passos H, Pereira MM, Lima ÁS, Coutinho JAP, Freire MG. 2014. Ionic liquids as additives to enhance the extraction of antioxidants in aqueous two-

- phase systems. *Sep Purif Technol* 128:1–10.
170. de Souza RL, Campos VC, Ventura SPM, Soares CMF, Coutinho JAP, Lima ÁS. 2014. Effect of ionic liquids as adjuvants on PEG-based ABS formation and the extraction of two probe dyes. *Fluid Phase Equilib* 375:30–36.
 171. Capela E. 2016. “Production and purification of antibodies using aqueous biphasic systems composed of ionic liquids as adjuvants”. University of Aveiro.
 172. Vahidnia M, Pazuki G, Abdolrahimi S. 2016. Impact of polyethylene glycol as additive on the formation and extraction behavior of ionic-liquid based aqueous two-phase system. *AIChE J* 62:264–274.
 173. Ruiz-Angel MJ, Pino V, Carda-Broch S, Berthod A. 2007. Solvent systems for countercurrent chromatography: An aqueous two phase liquid system based on a room temperature ionic liquid. *J Chromatogr A* 1151:65–73.
 174. Cláudio AFM, Marques CFC, Boal-Palheiros I, Freire MG, Coutinho JAP. 2014. Development of back-extraction and recyclability routes for ionic-liquid-based aqueous two-phase systems. *Green Chem* 16:259–268.
 175. Freire MG, Pereira JFB, Francisco M, Rodríguez H, Rebelo LPN, Rogers RD *et al.*. 2012. Insight into the interactions that control the phase behaviour of new aqueous biphasic systems composed of polyethylene glycol polymers and ionic liquids. *Chem - A Eur J* 18:1831–1839.
 176. Cláudio AF, Pereira JFB, McCrary PD, Freire MG, Coutinho JAP, Rogers RD. 2016. A critical assessment of the mechanisms governing the formation of aqueous biphasic systems composed of protic ionic liquids and polyethylene glycol. *Phys Chem Chem Phys* 18:30009–30019.
 177. Pereira JFB, Kurnia KA, Freire MG, Coutinho JAP, Rogers RD. 2015. Controlling the Formation of Ionic-Liquid-based Aqueous Biphasic Systems by Changing the Hydrogen-Bonding Ability of Polyethylene Glycol End Groups. *ChemPhysChem* 16:2219–2225.
 178. Tomé LIN, Pereira JFB, Rogers RD, Freire MG, Gomes JRB, Coutinho JAP. 2014. “Washing-out” ionic liquids from polyethylene glycol to form aqueous biphasic systems. *Phys Chem Chem Phys* 16:2271–2274.
 179. Pereira JFB, Rebelo LPN, Rogers RD, Coutinho JAP, Freire MG. 2013. Combining ionic liquids and polyethylene glycols to boost the hydrophobic-hydrophilic range of aqueous biphasic systems. *Phys Chem Chem Phys* 15:19580–3.

180. Du Z, Yu YL, Wang JH. 2007. Extraction of proteins from biological fluids by use of an ionic liquid/aqueous two-phase system. *Chem - A Eur J* 13:2130–2137.
181. Dreyer S, Kragl U. 2008. Ionic liquids for aqueous two-phase extraction and stabilization of enzymes. *Biotechnol Bioeng* 99:1416–1424.
182. Quental MV, Caban M, Pereira MM, Stepnowski P, Coutinho JAP, Freire MG. 2015. Enhanced extraction of proteins using cholinium-based ionic liquids as phase-forming components of aqueous biphasic systems. *Biotechnol J* 10:1457–1466.
183. Li Z, Liu X, Pei Y, Wang J, He M. 2012. Design of environmentally friendly ionic liquid aqueous two-phase systems for the efficient and high activity extraction of proteins. *Green Chem* 14:2941–2950.
184. Taha M, Almeida MR, e Silva FA, Domingues P, Ventura SPM, Coutinho JAP *et al.*. 2015. Novel Biocompatible and Self-buffering Ionic Liquids for Biopharmaceutical Applications. *Chem - A Eur J* 21:4781–4788.
185. Desai RK, Streefland M, Wijffels RH, Eppink HMM. 2014. Extraction and stability of selected proteins in ionic liquid based aqueous two phase systems. *Green Chem* 16:2670.
186. Zeng Q, Wang Y, Li N, Huang X, Ding X, Lin X *et al.*. 2013. Extraction of proteins with ionic liquid aqueous two-phase system based on guanidine ionic liquid. *Talanta* 116:409–416.
187. Ventura SPM, de Barros RLF, de Pinho Barbosa JM, Soares CMF, Lima AS, Coutinho JAP. 2012. Production and purification of an extracellular lipolytic enzyme using ionic liquid-based aqueous two-phase systems. *Green Chem* 14:734.
188. Good NE, Winget GD, Winter W, Connolly TN, Izawa S, Sing RMM. 1966. Hydrogen ion buffers for biological research. *Biochemistry* 5:467–477.
189. Taha M, e Silva FA, Quental MV, Ventura SPM, Freire MG, Coutinho JAP. 2014. Good's buffers as a basis for developing self-buffering and biocompatible ionic liquids for biological research. *Green Chem* 16:3149–3159.
190. Lee SY, Vicente FA, e Silva FA, Sintra TE, Taha M, Khoiroh I *et al.*. 2015. Evaluating Self-buffering Ionic Liquids for Biotechnological Applications. *ACS Sustain Chem Eng* 3:3420–3428.
191. Mondal D, Sharma M, Quental MV, Tavares APM, Prasad K, Freire MG. 2016. Suitability of bio-based ionic liquids for the extraction and purification of IgG antibodies. *Green Chem* 18:6071–6081.

192. Taha M, Quental MV, Correia I, Freire MG, Coutinho JAP. 2015. Extraction and stability of bovine serum albumin (BSA) using cholinium-based Good's buffers ionic liquids. *Process Biochem* 50:1158–1166.
193. Xu Z, Cen P. 2002. Primary Purification of Co-expressed Soluble and Insoluble Alpha-interferon 2b from Recombinant E.coli. *Chinese J Chem Eng* 10:686–689.
194. Beldarraín A, Cruz Y, Cruz O, Navarro M, Gil M. 2001. Purification and conformational properties of a human interferon alpha2b produced in Escherichia coli. *Biotechnol Appl Biochem* 33:173–182.
195. Cao Y, Bai G, Chen J, Tian W, Wang S, Yang W. 2006. Preparation and characterization of magnetic microspheres for the purification of interferon alpha-2b. *J Chromatogr B Analyt Technol Biomed Life Sci* 833:236–244.
196. Ningrum RA, Wisnuwardhani PH, Santoso A, Herawati N. 2015. Antiproliferative activity of recombinant human interferon alpha2b on estrogen positive human breast cancer MCF-7 cell line. *Indones J Pharm* 26:86.
197. Wang C, Guo L, Li H, Wang Y, Weng J, Wu L. 2006. Preparation of simple ammonium ionic liquids and their application in the cracking of dialkoxypropanes. *Green Chem* 8:603–607.
198. Ohno H, Fukumoto K. 2007. Amino acid ionic liquids. *Acc Chem Res* 40:1122–1129.
199. Merchuk JC, Andrews BA, Asenjo JA. 1998. Aqueous two-phase systems for protein separation: Studies on phase inversion. *J Chromatogr B Biomed Sci Appl* 711:285–293.
200. Johnston MJW, Nembr K, Hefford MA. 2010. Influence of bovine serum albumin on the secondary structure of interferon alpha 2b as determined by far UV circular dichroism spectropolarimetry. *Biologicals* 38:314–320.
201. Pedro AQ, Pereira P, Bonifácio MJ, Queiroz JA, Passarinha LA. 2015. Purification of Membrane-Bound Catechol-O-Methyltransferase by Arginine-Affinity Chromatography. *Chromatographia* 78:1339–1348.
202. Pereira P, Sousa Â, Queiroz J, Correia I, Figueiras A, Sousa F. 2014. Purification of pre-miR-29 by arginine-affinity chromatography. *J Chromatogr B Anal Technol Biomed Life Sci* 951–952:16–23.
203. Francis A. Carey. On-Line Learning Center for “Organic Chemistry”. [Online]. Available: <http://www.mhhe.com/physsci/chemistry/carey5e/Ch27/ch27-1-4-2.html> [Accessed: 04-Set-2016].

204. Mourão T, Cláudio AFM, Boal-Palheiros I, Freire MG, Coutinho JAP. 2012. Evaluation of the impact of phosphate salts on the formation of ionic-liquid-based aqueous biphasic systems. *J Chem Thermodyn* 54:398–405.
205. Kurnia KA, Freire MG, Coutinho JAP. 2014. Effect of polyvalent ions in the formation of ionic-liquid-based aqueous biphasic systems. *J Phys Chem B* 118:297–308.
206. Pegram LM, Record MT. 2007. Hofmeister salt effects on surface tension arise from partitioning of anions and cations between bulk water and the air-water interface. *J Phys Chem B* 111:5411–5417.
207. Alvarez-Guerra E, Irabien A. 2014. Ionic Liquid-Based Three Phase Partitioning (ILTTP) for Lactoferrin Recovery. *Sep Sci Technol* 49:957–965.

6. List of communications

- Covilhã**
May, 2017
Oral communication at the II International Health Science and Research Congress: Antunes, J; Pedro, AQ; Pereira, P; Sousa, F; Passarinha, L; Coutinho, JAP; Freire, MG; “*Novel alternatives for interferon alpha-2b purification: chromatography vs ionic liquid aqueous biphasic systems*”
- Aveiro**
March, 2017
Best poster award at the III National Meeting of Biotechnology Students: Antunes, J; Pedro, AQ; Pereira, P; Sousa, F; Passarinha, L; Coutinho, JAP; Freire, MG; “*Production and purification of biopharmaceuticals: are ionic liquids relevant in bioprocessing?*”
- Coimbra**
February, 2017
Oral communication at the 5th IEEE Portuguese BioEngineering Meeting: Antunes, J; Pedro, AQ; Pereira, P; Sousa, F; Passarinha, L; Coutinho, JAP; Freire, MG “*Purification of interferon alpha-2b using biocompatible ionic liquids*”

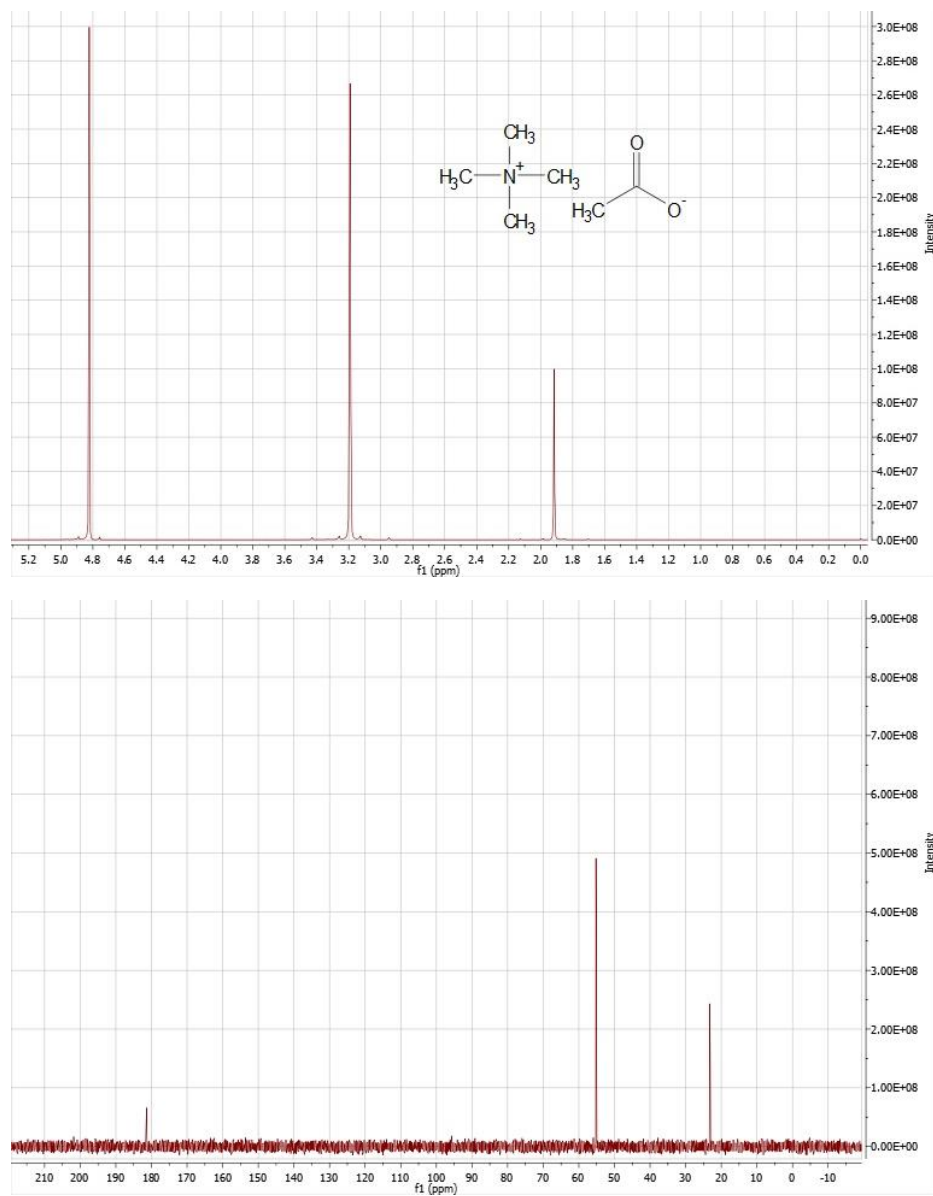
Appendix A

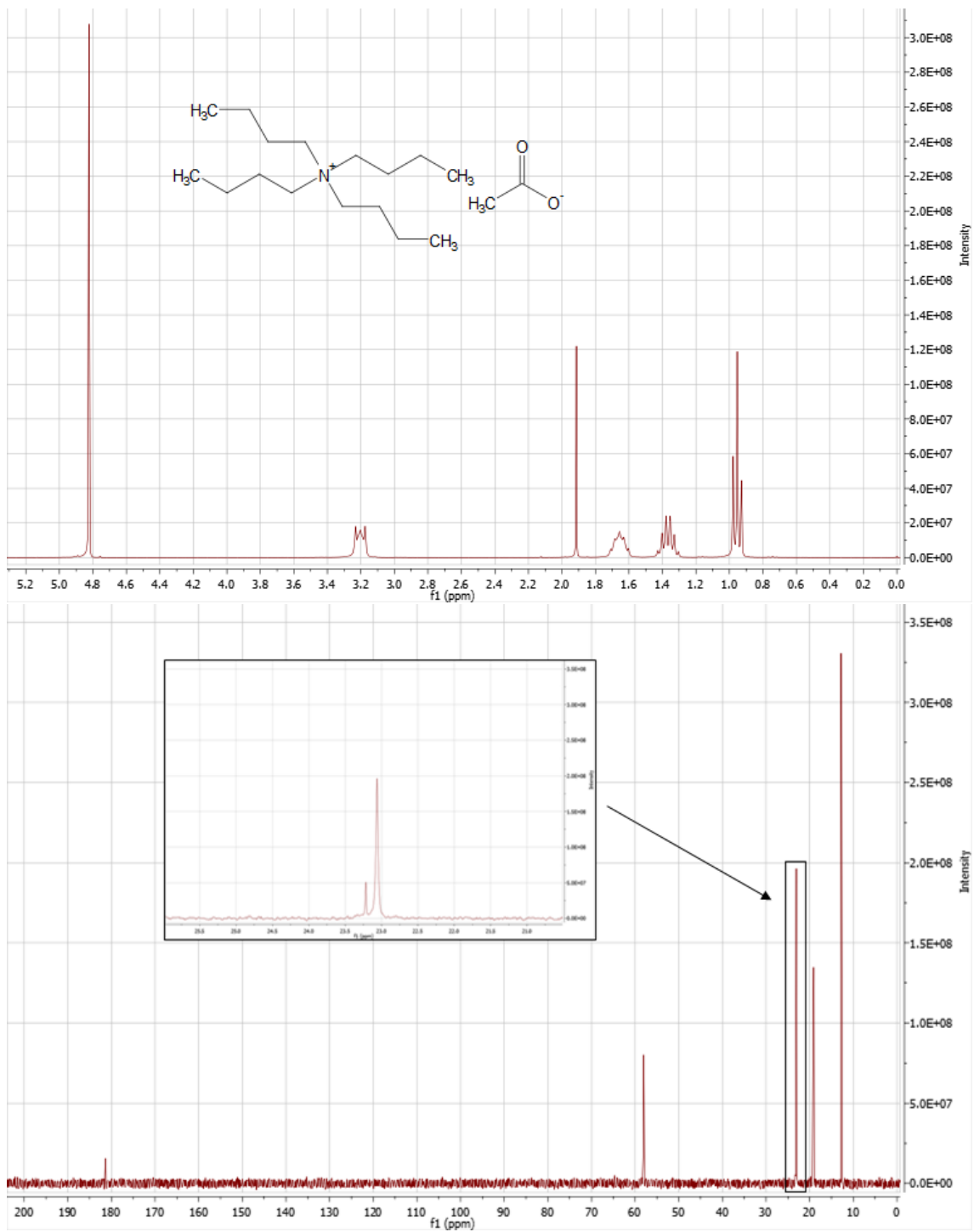
Experimental data of the growth profile of *E. coli*, in the LB, SOC and SOB media.

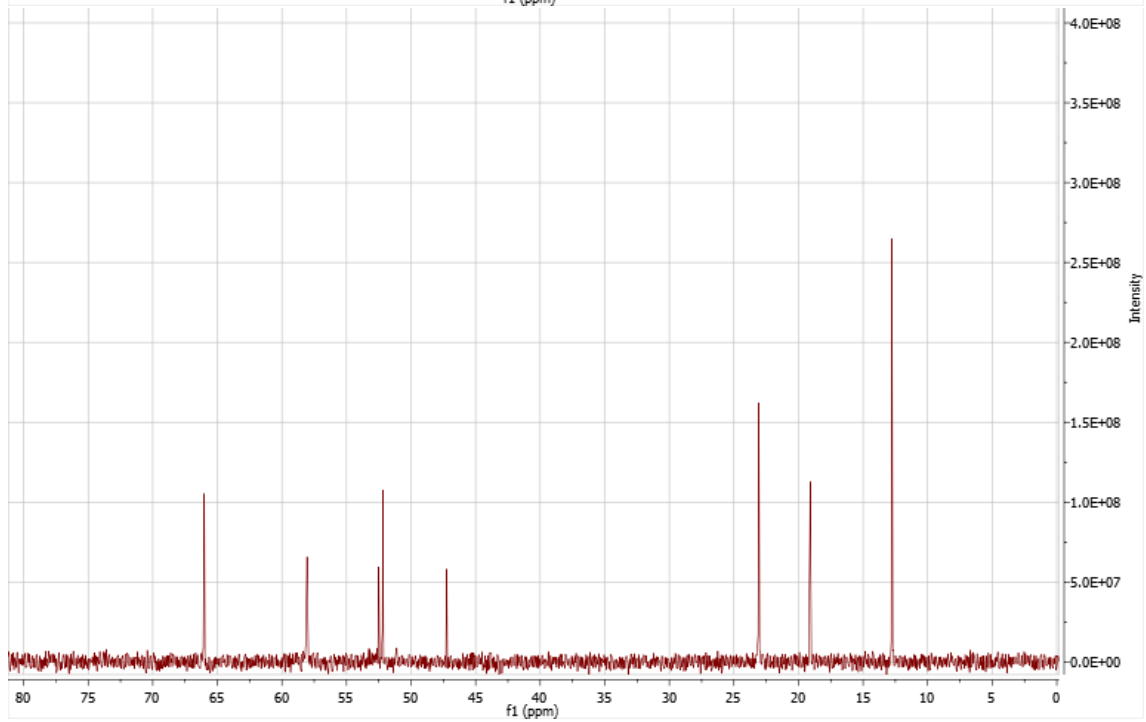
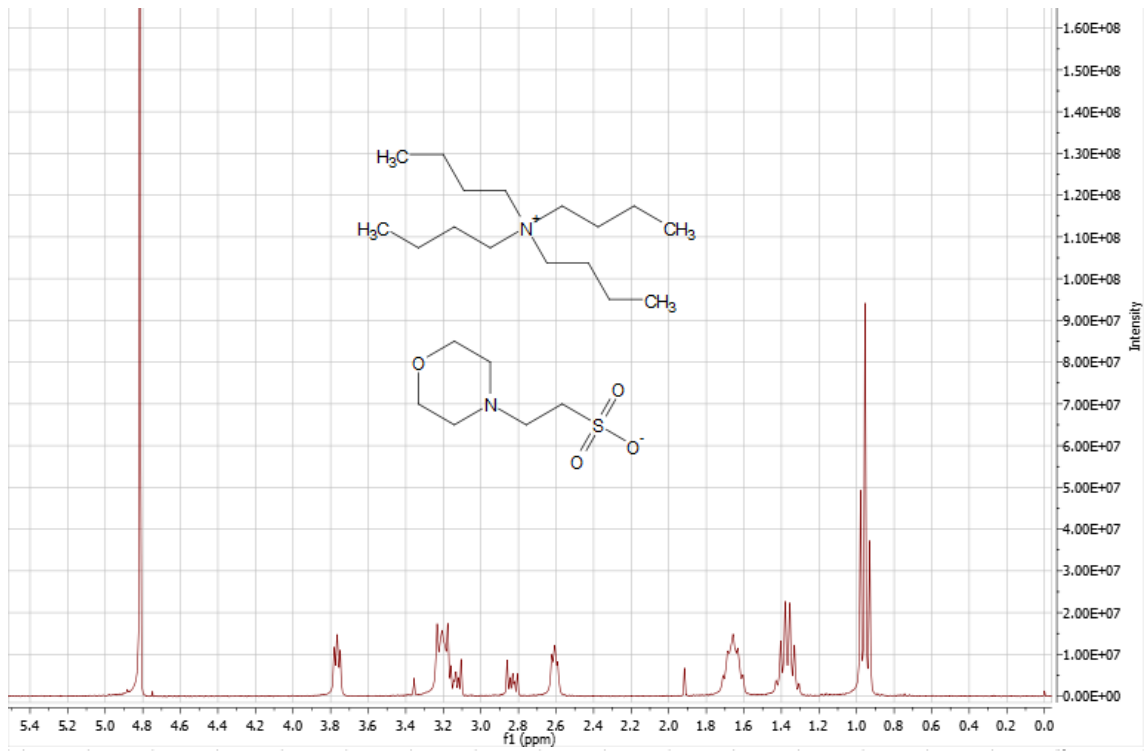
Time (h)	OD ₆₀₀ LB medium	OD ₆₀₀ SOC medium	OD ₆₀₀ SOB medium
0	0.21	0.23	0.23
1	0.53	0.58	0.69
2	0.99	1.48	1.40
3	1.20	1.76	1.78
4	1.34	2.10	2.00
5	1.48	2.49	2.21
6	1.66	2.94	2.32
7	1.80	3.52	2.52
8	-	3.82	2.70
9	-	4.13	2.84

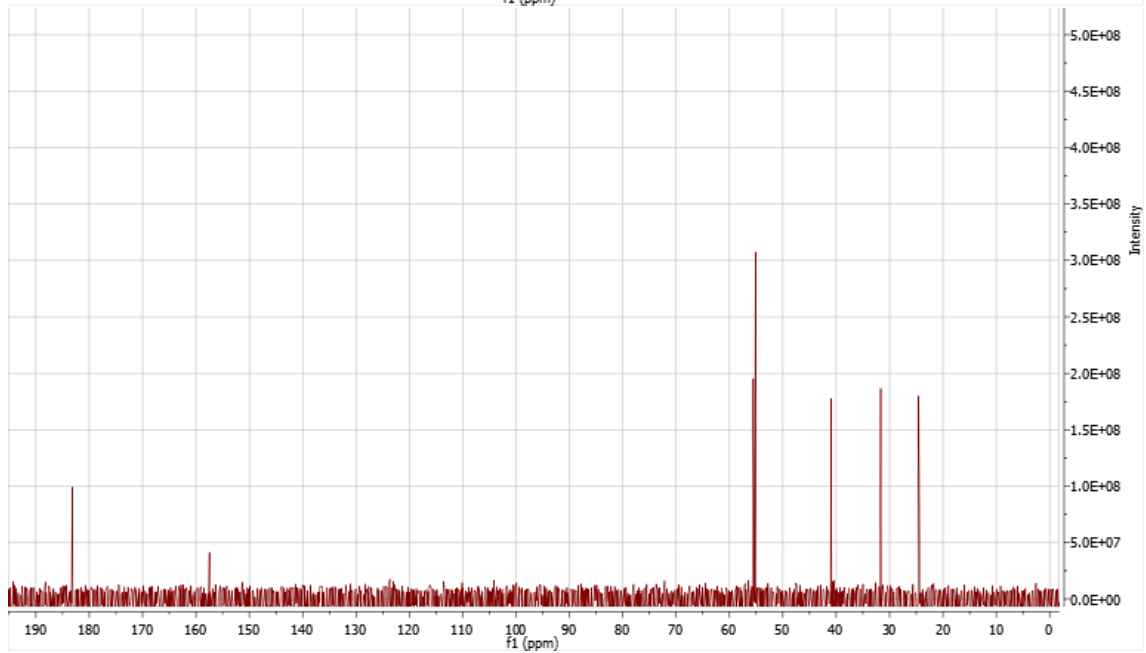
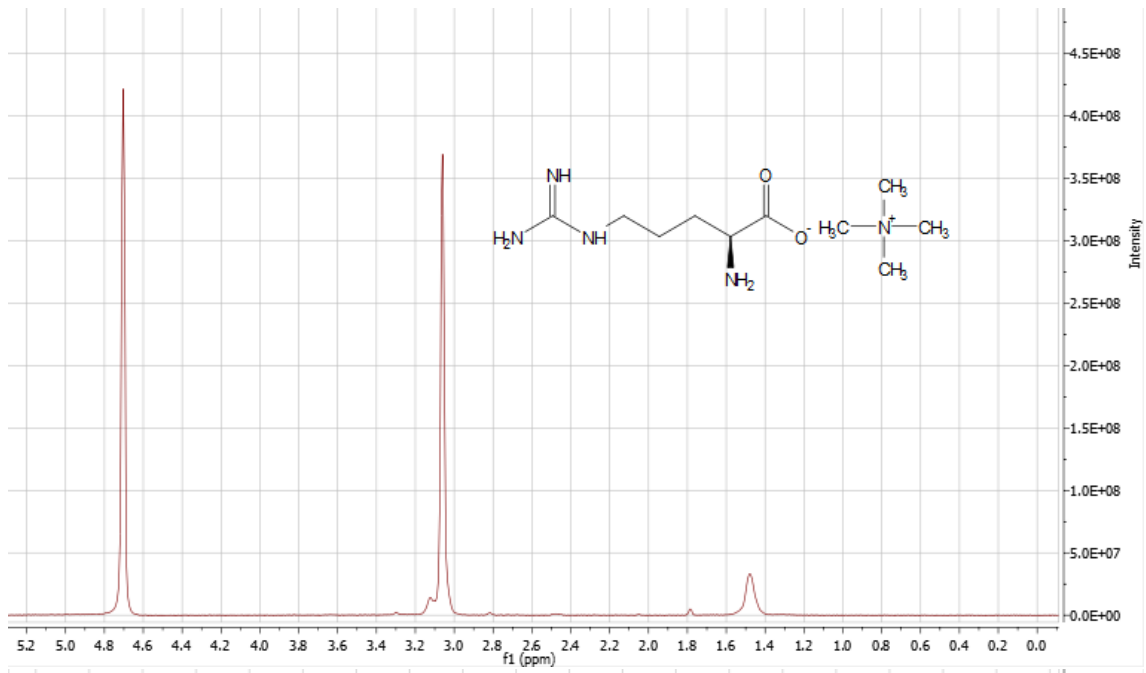
Appendix B

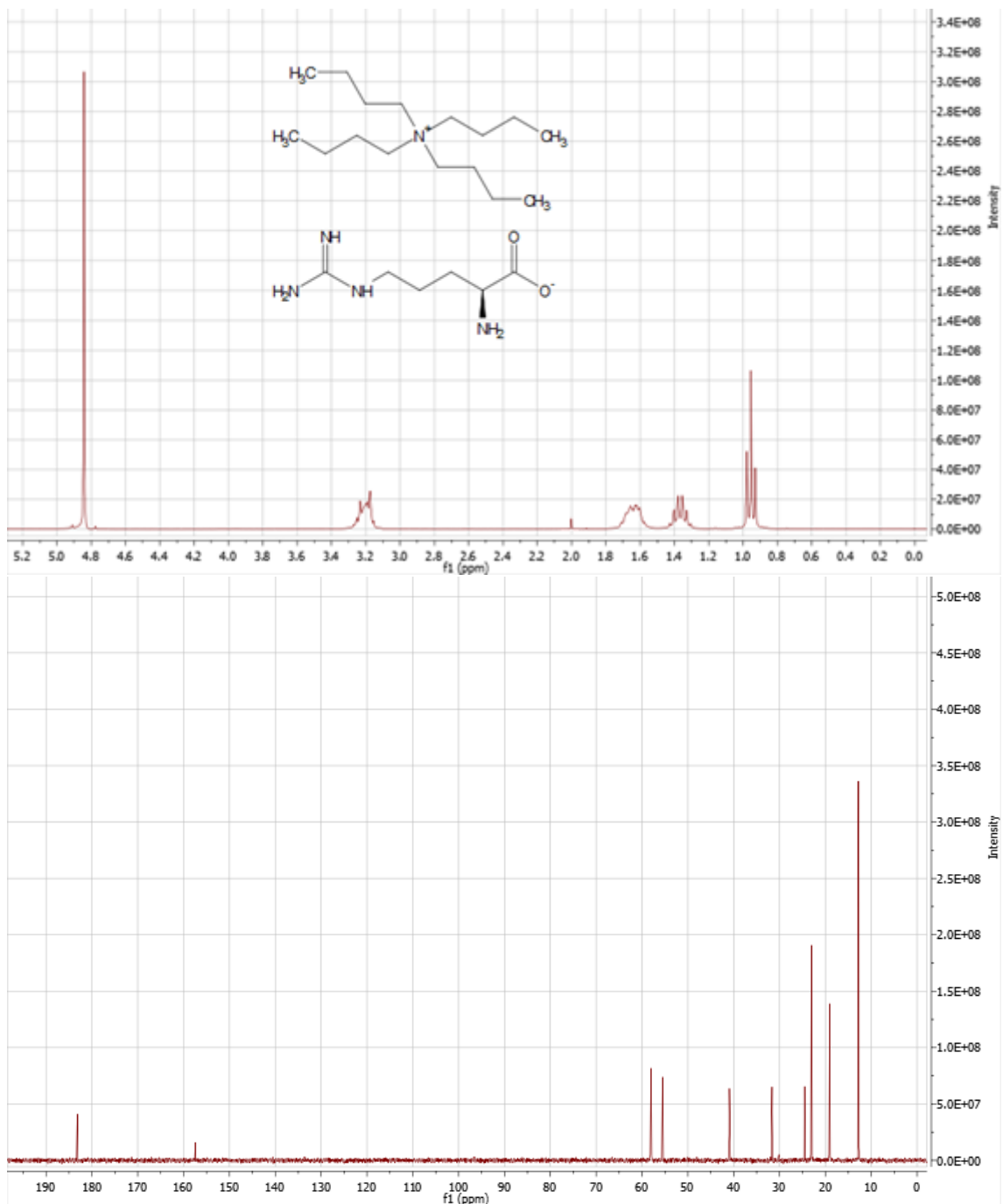
^1H and ^{13}C RMN spectra of the synthesized ILs

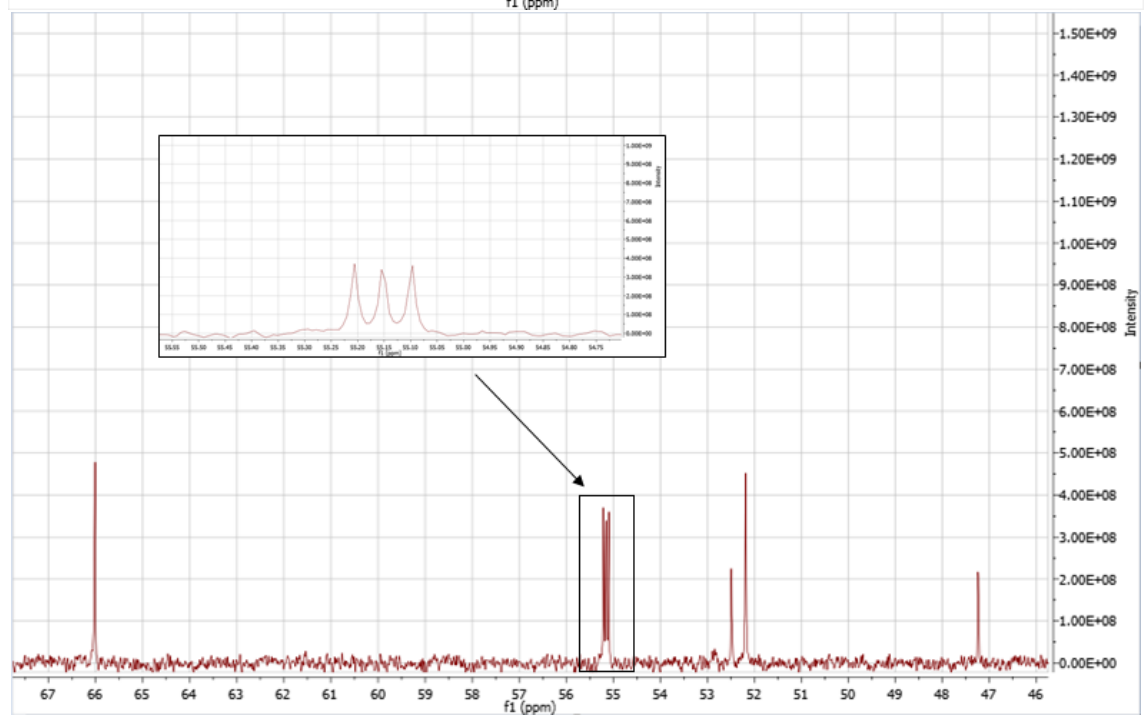
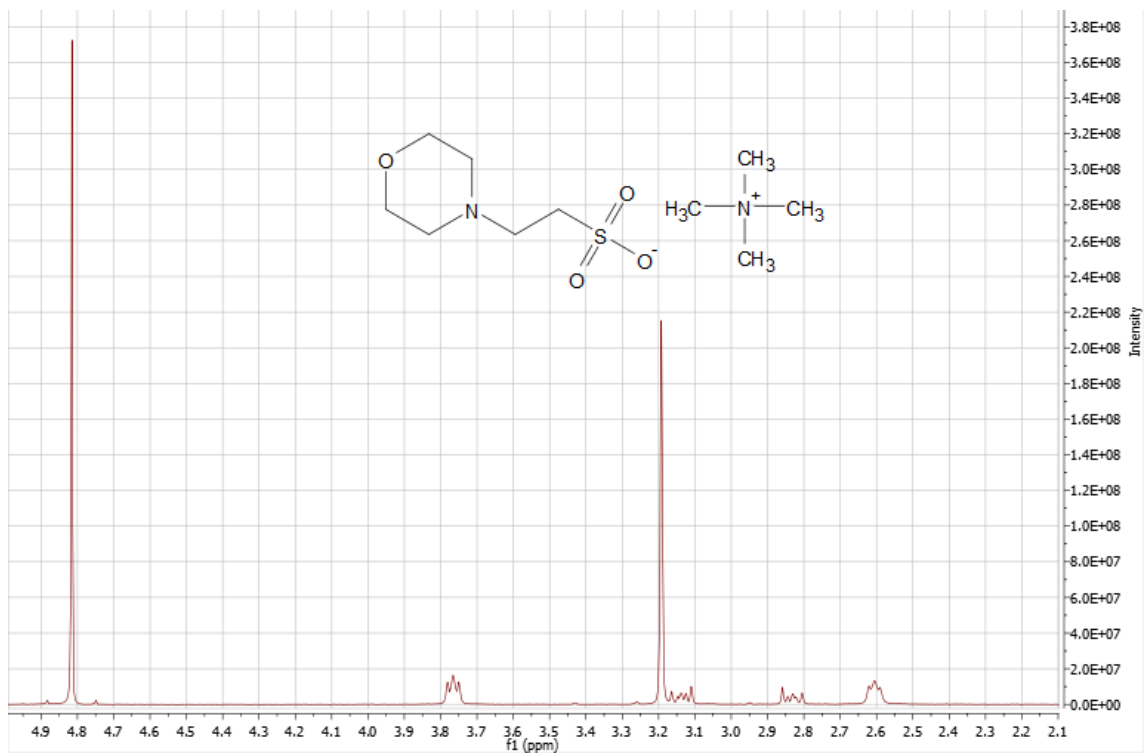


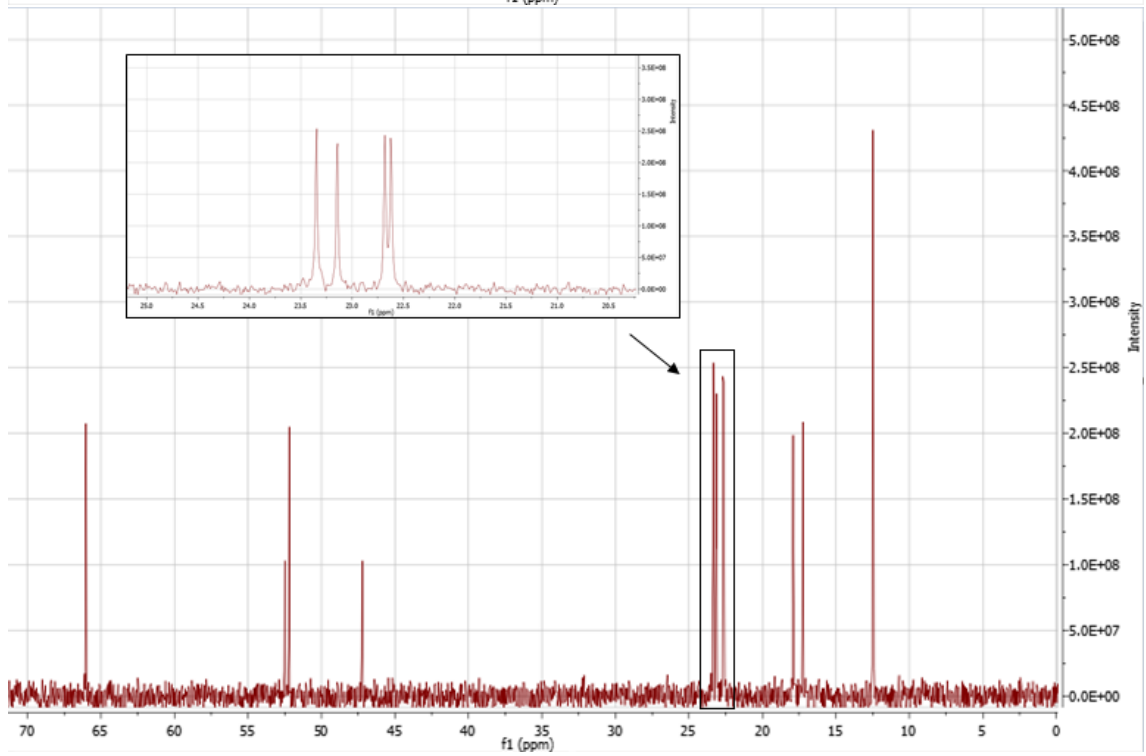
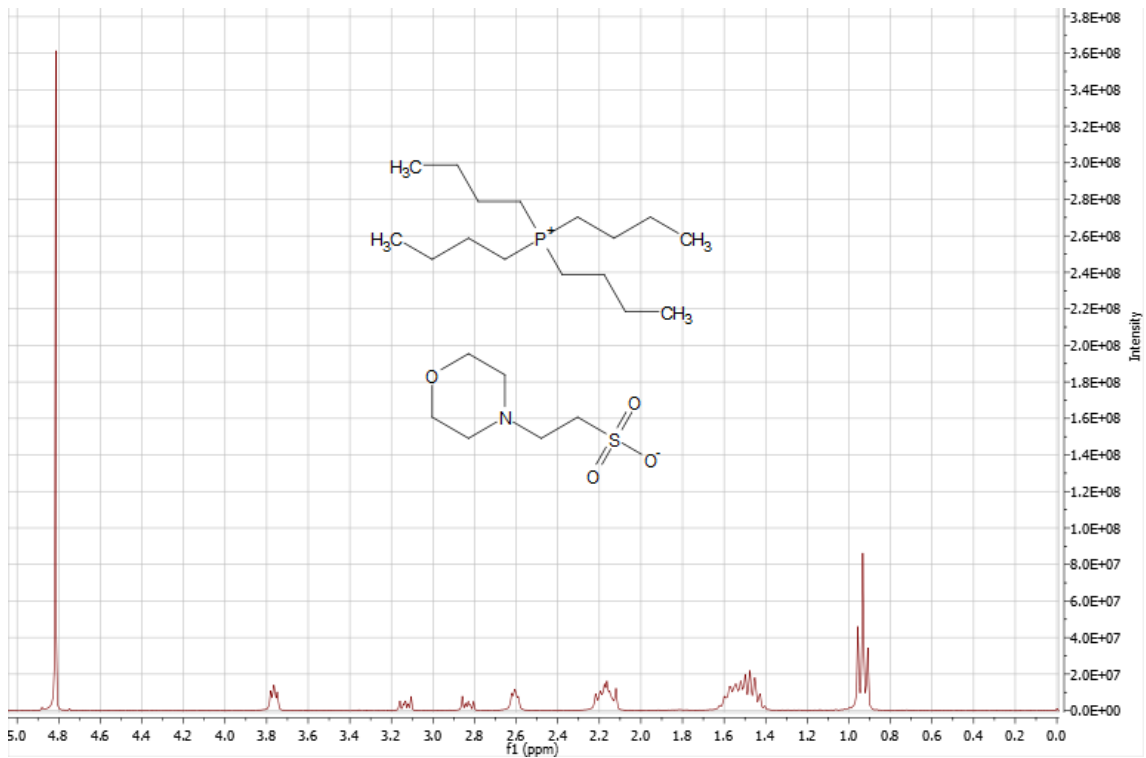


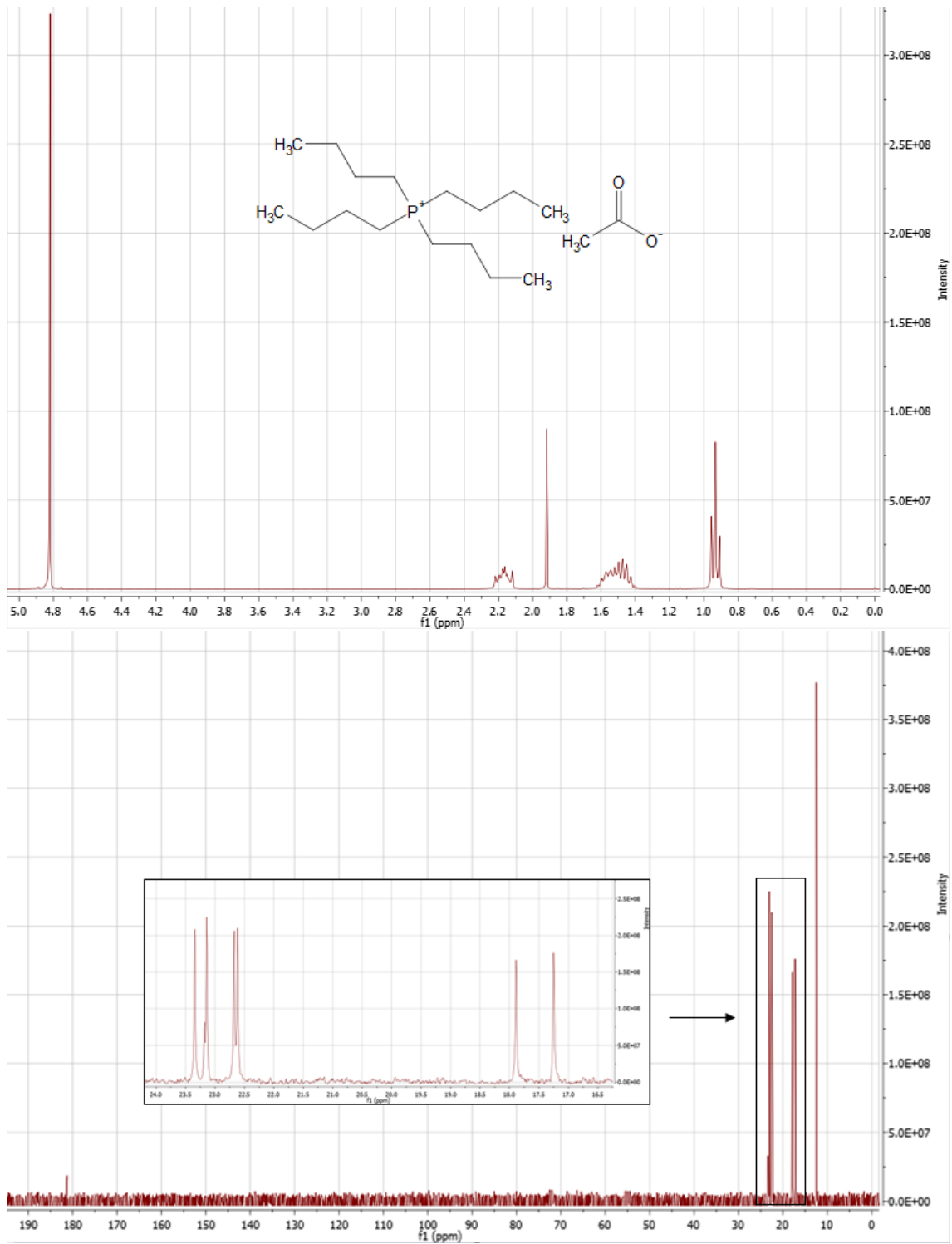


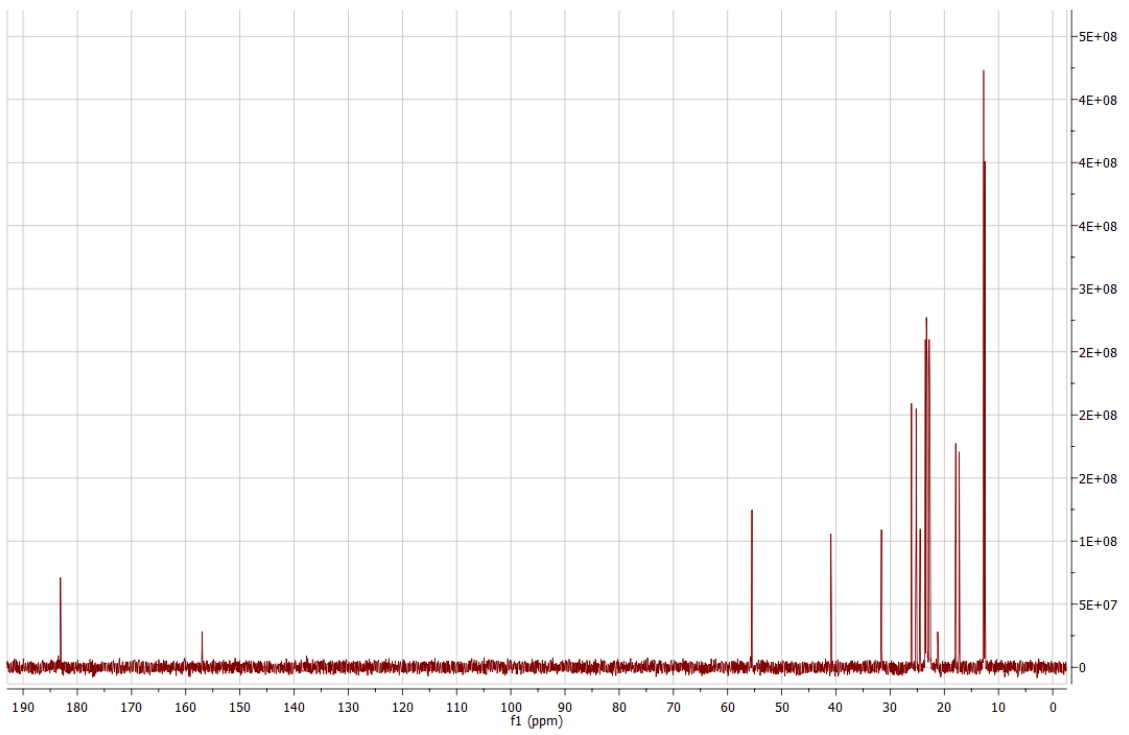
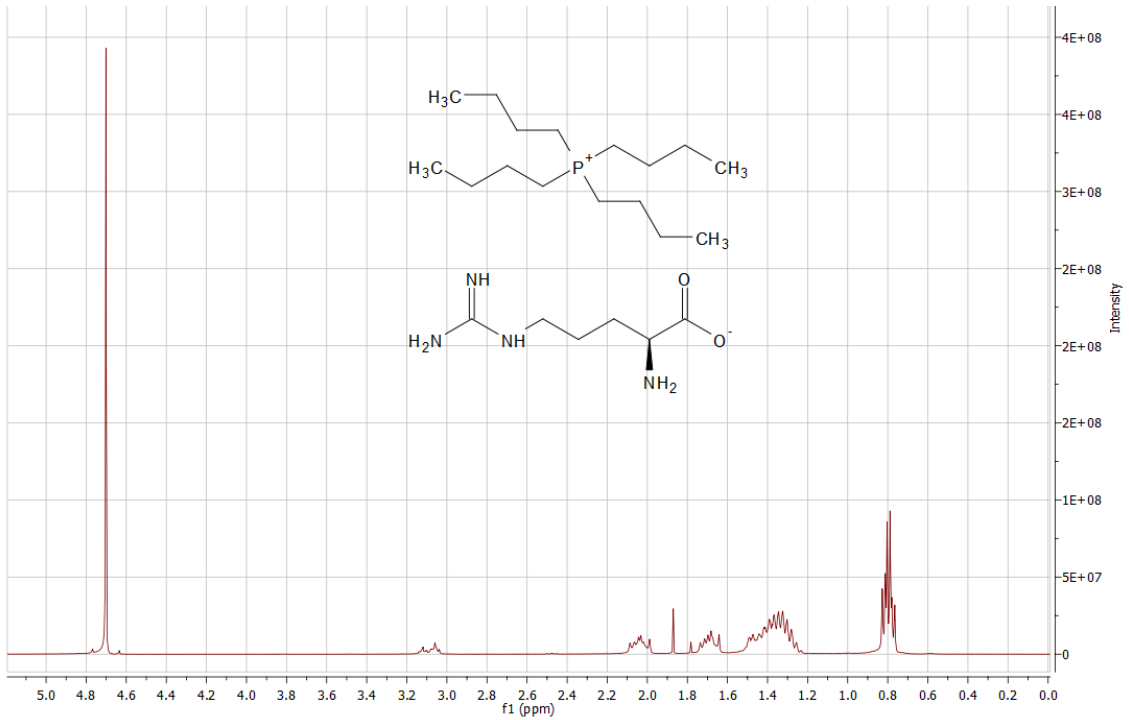


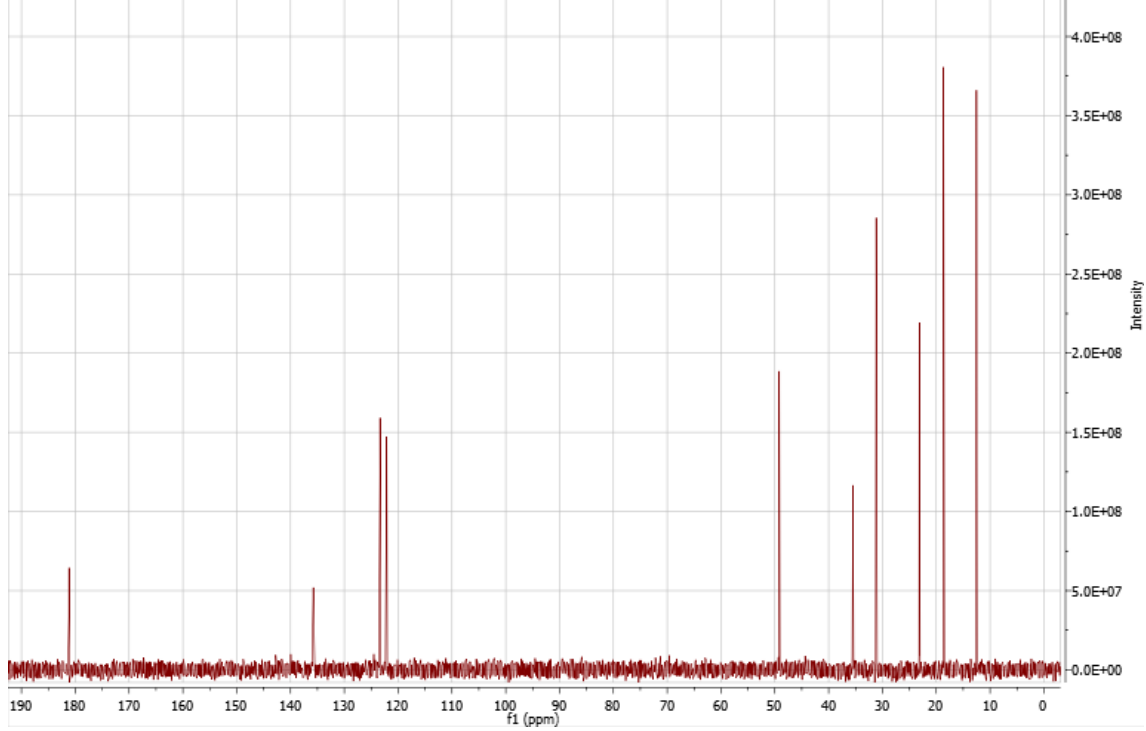
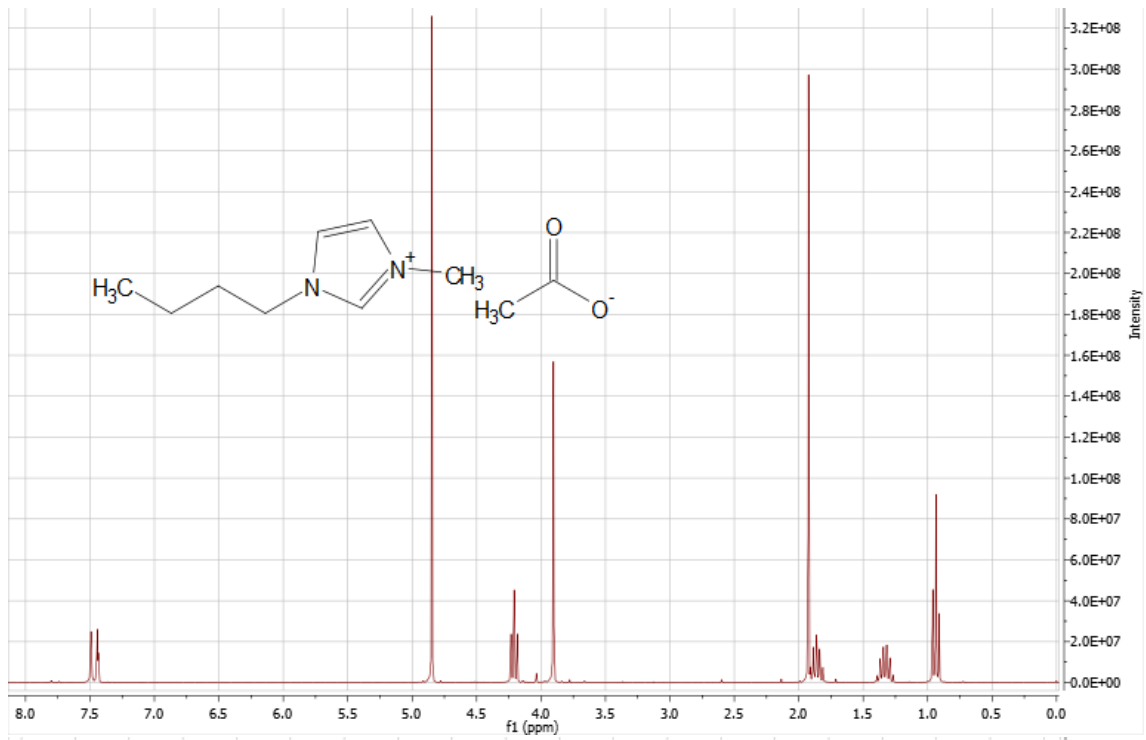


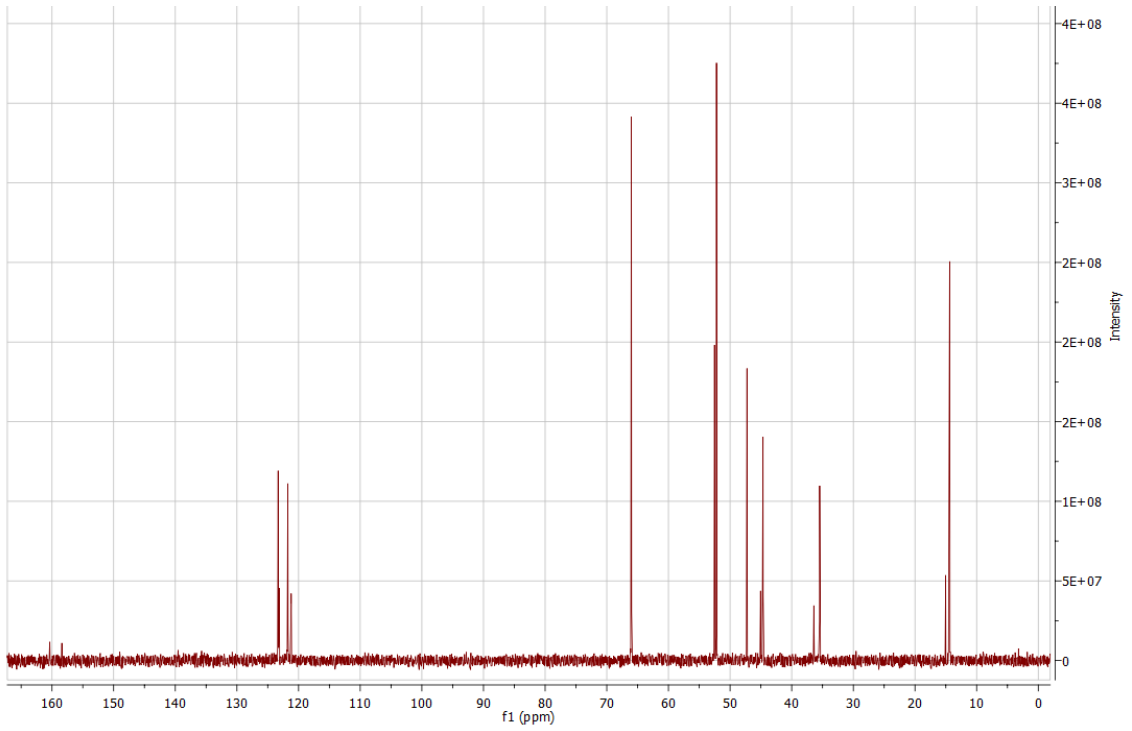
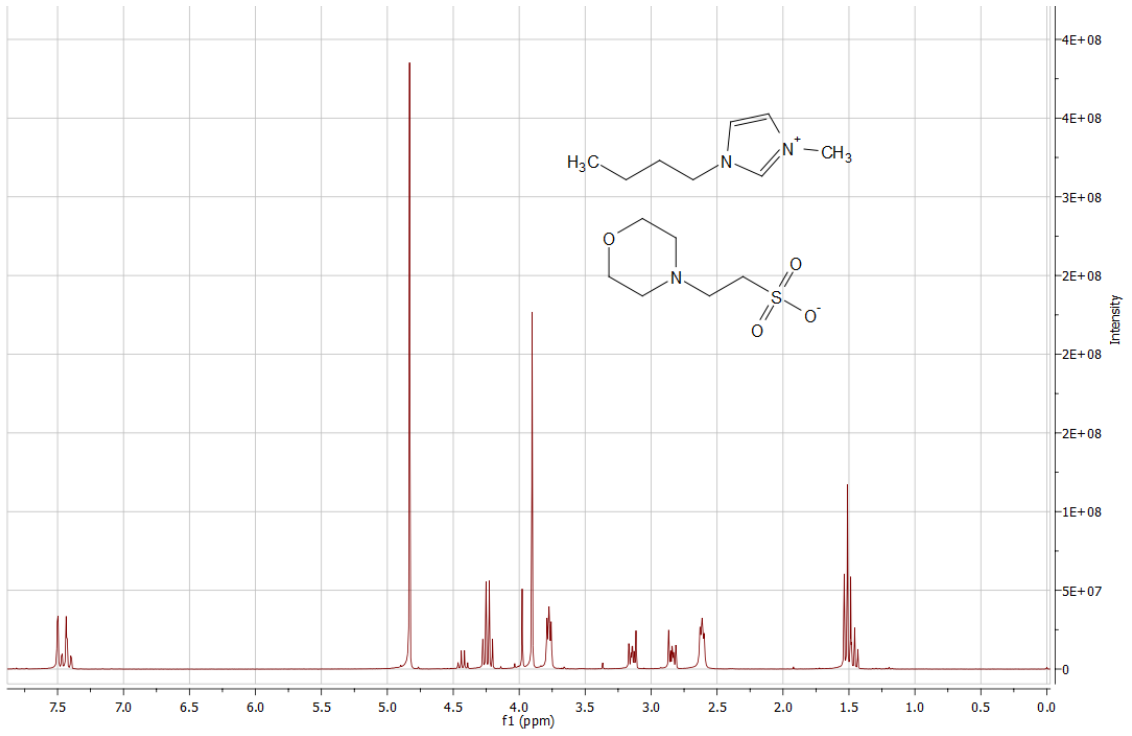


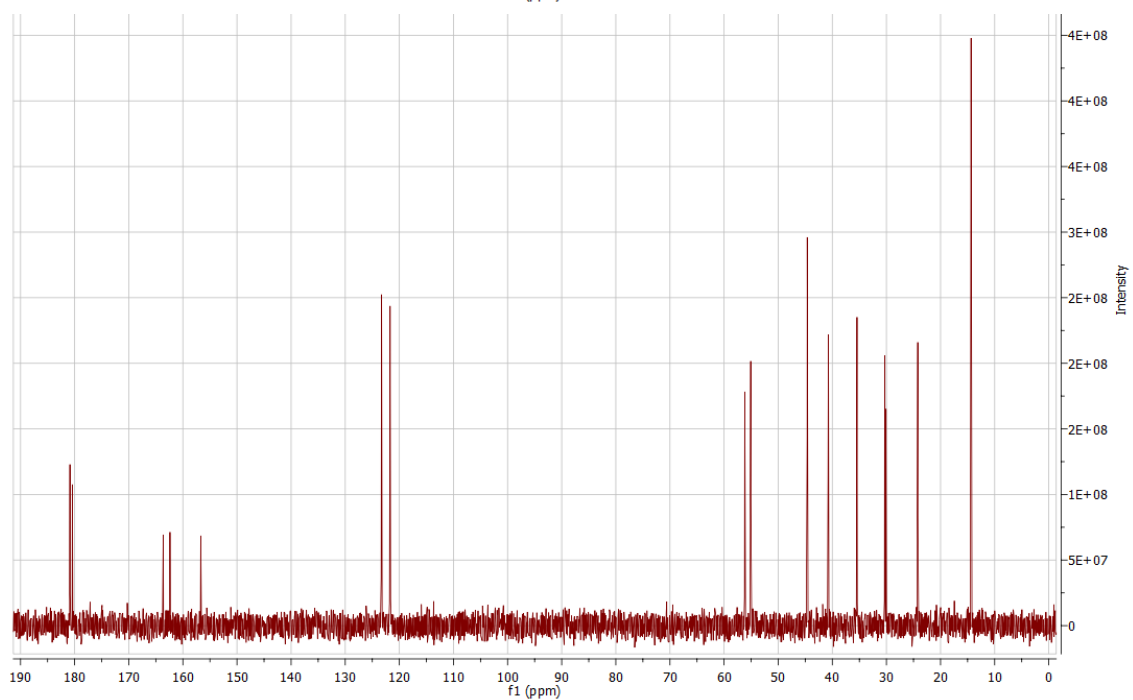
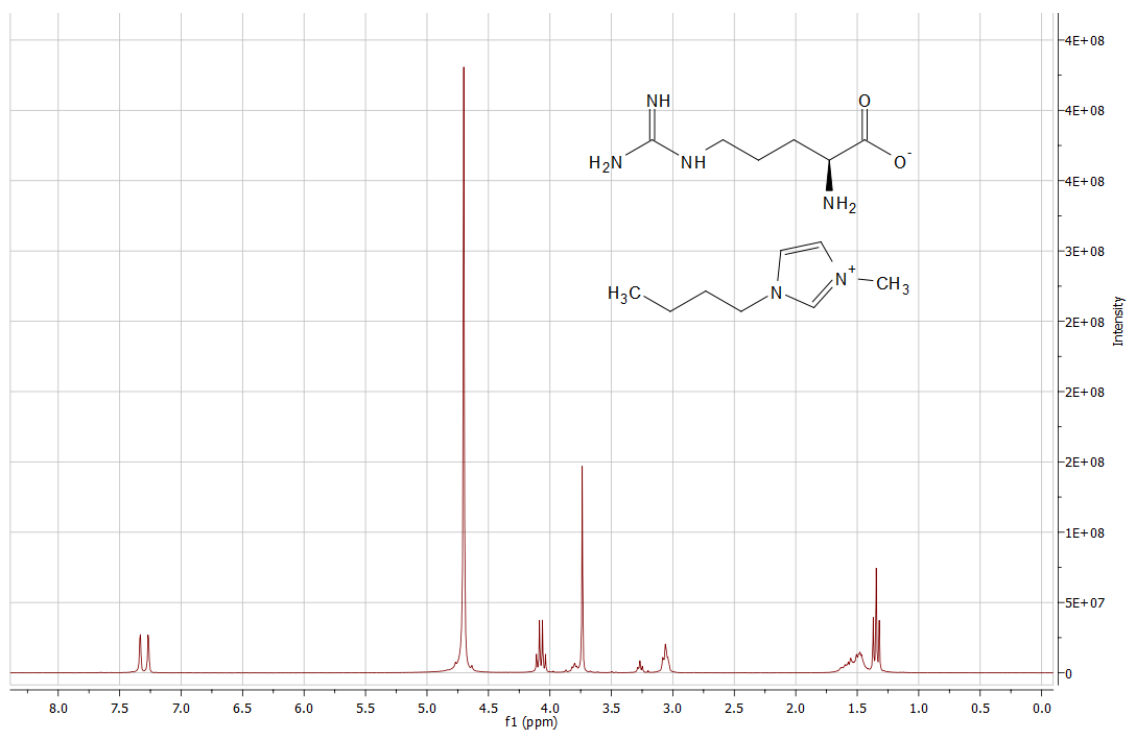


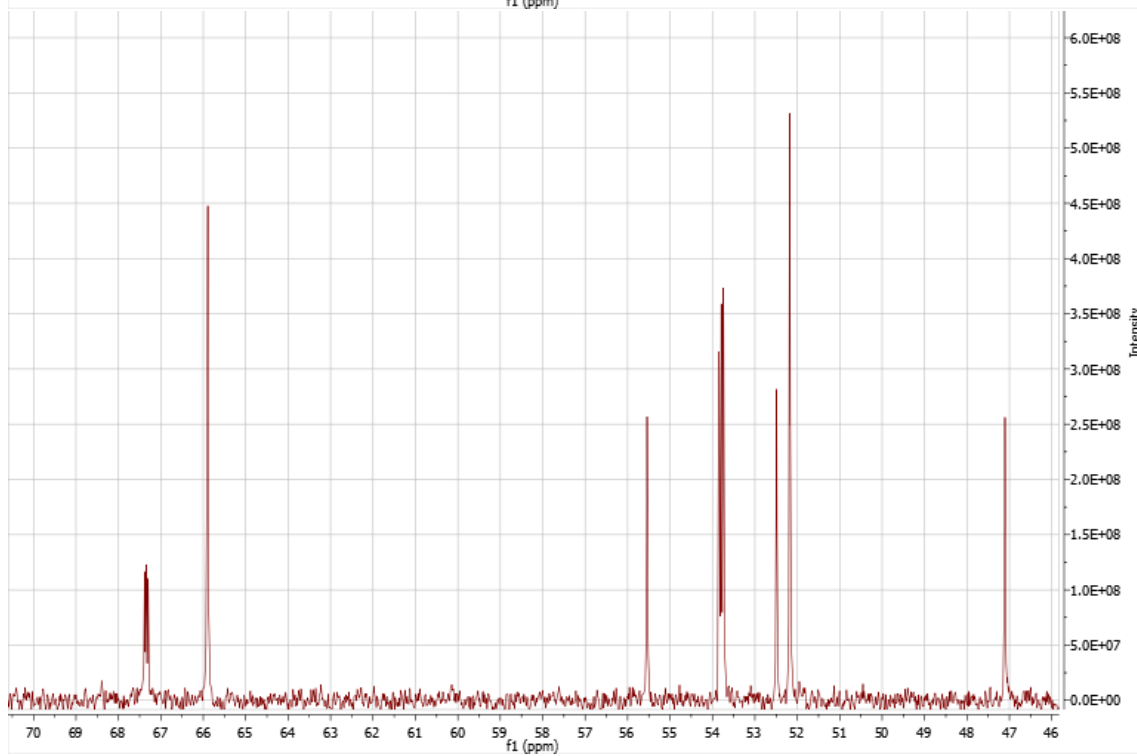
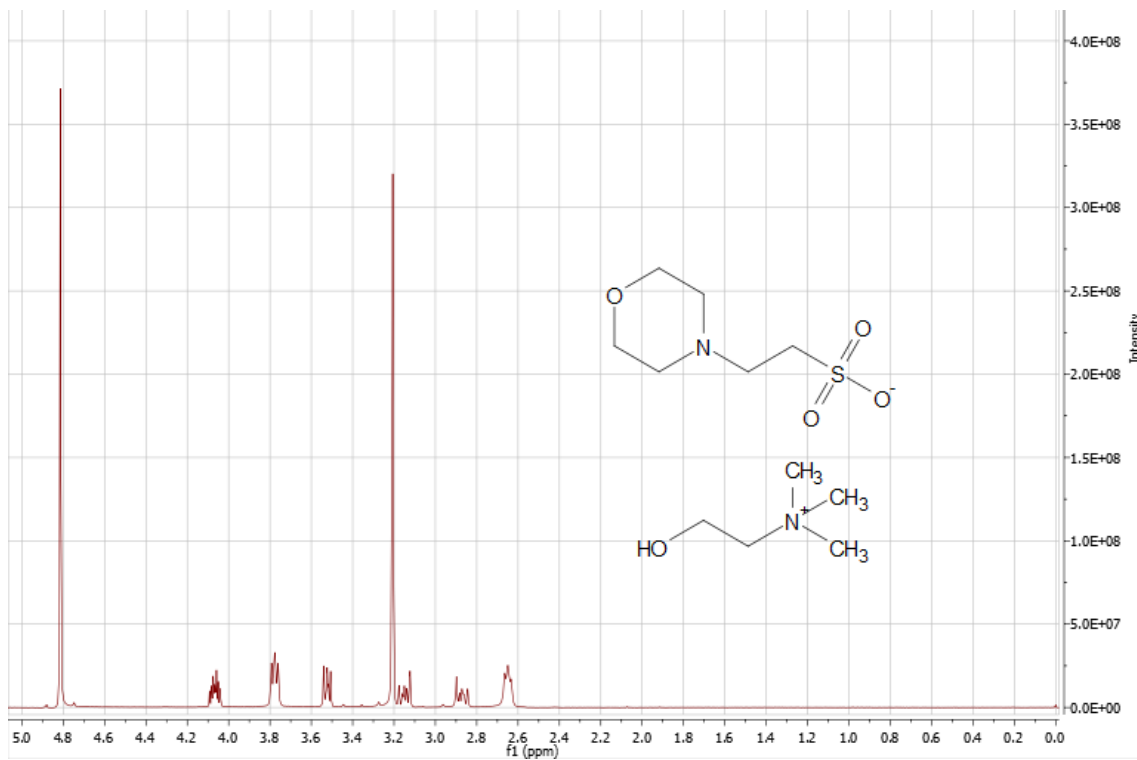


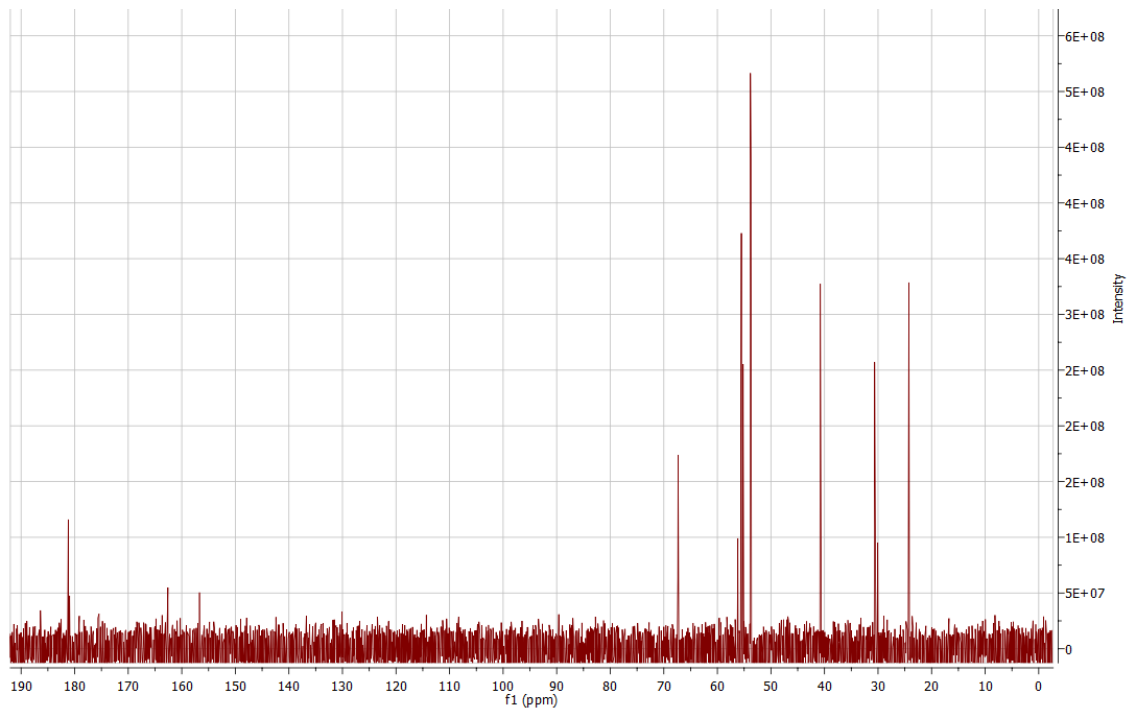
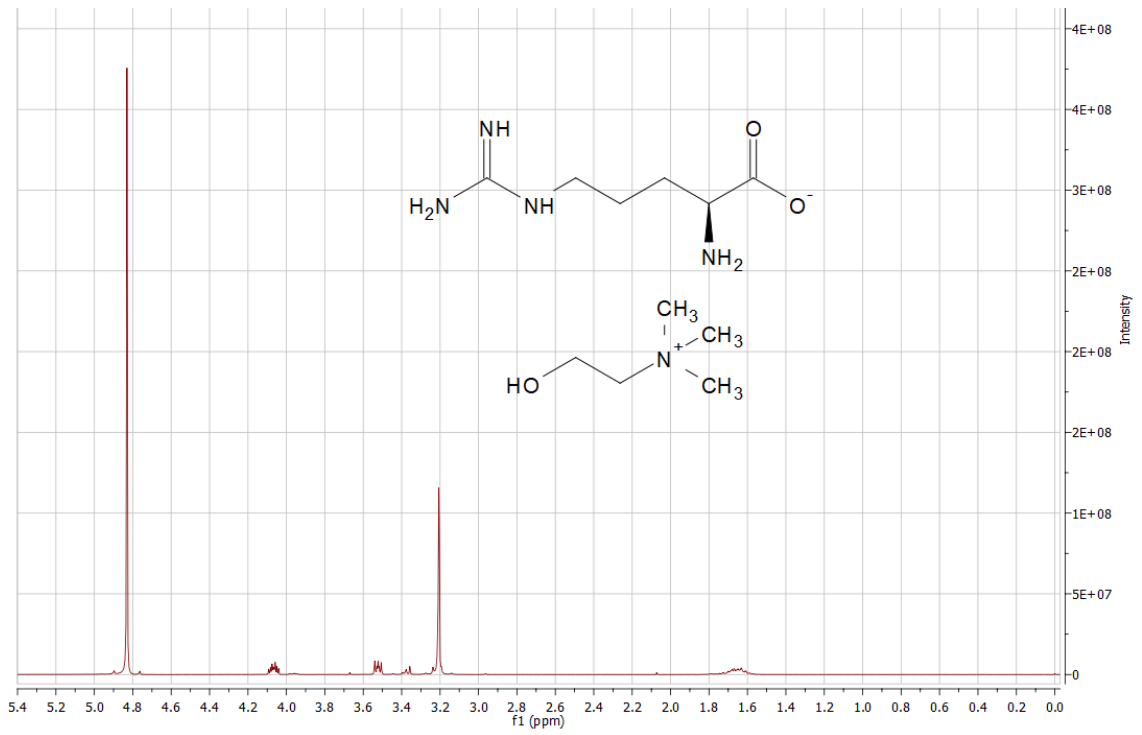


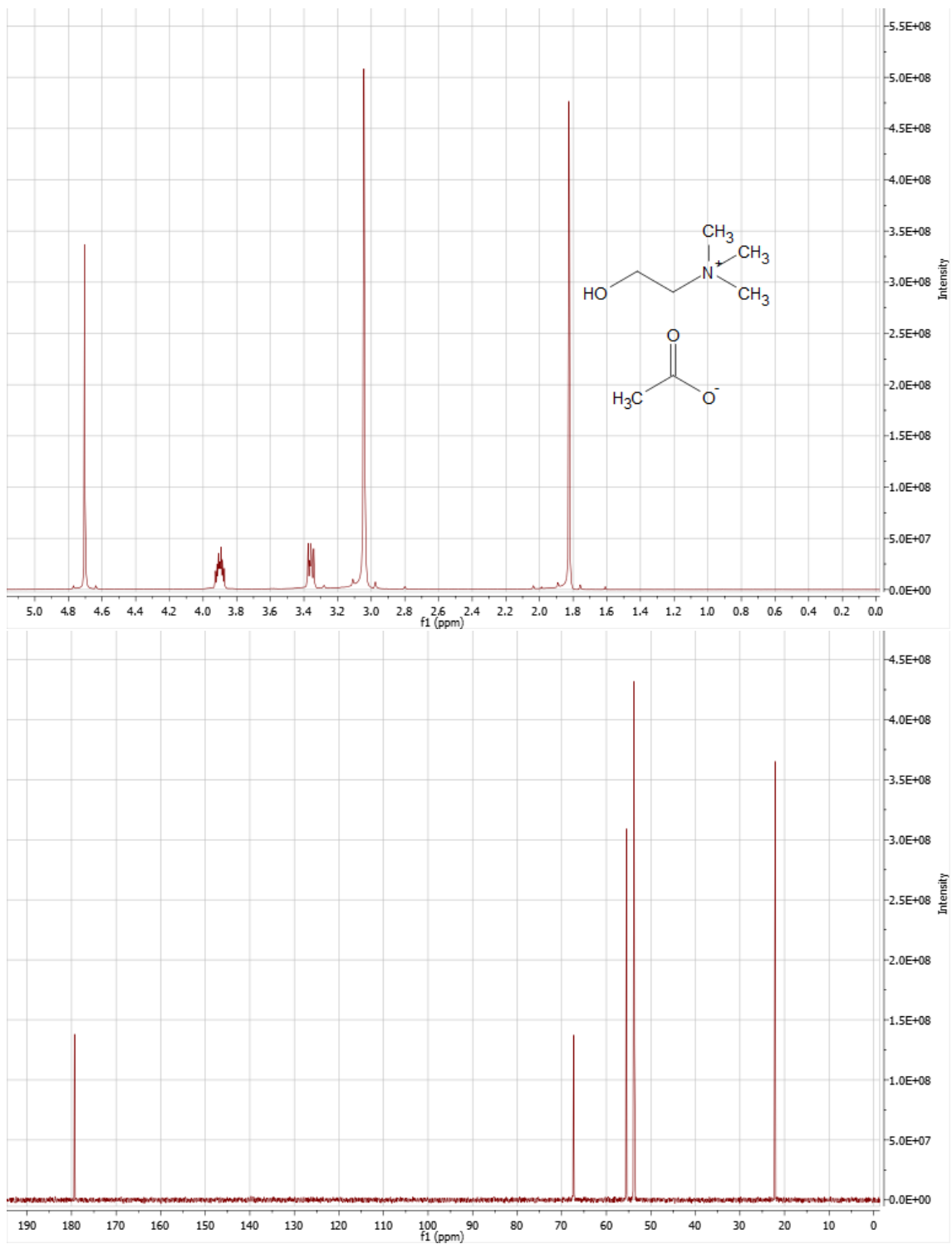












Appendix C

Experimental weight fraction data of the ternary phase diagrams of ATPS of composed of ILs + K₂HPO₄/KH₂PO₄ + H₂O, at pH 8.2.

[N1111][Ac] <i>M_w</i> = 132.2 g.mol ⁻¹		[N4444][Ac] <i>M_w</i> = 300.6 g.mol ⁻¹		[P4444][Ac] <i>M_w</i> = 317.5 g.mol ⁻¹		[N4444][MES] <i>M_w</i> = 436.7 g.mol ⁻¹		[P4444][MES] <i>M_w</i> = 453.7 g.mol ⁻¹		[C4mim][MES] <i>M_w</i> = 333.4 g.mol ⁻¹		[P4444][Arg] <i>M_w</i> = 432.7 g.mol ⁻¹	
100w _{Salt}	100w _{IL}	100w _{Salt}	100w _{IL}	100w _{Salt}	100w _{IL}	100w _{Salt}	100w _{IL}	100w _{Salt}	100w _{IL}	100w _{Salt}	100w _{IL}	100w _{Salt}	100w _{IL}
9.27	36.96	13.75	16.03	12.87	19.01	13.06	19.27	13.27	18.17	9.12	36.81	0.59	14.55
8.71	37.63	13.27	16.65	12.50	19.35	12.66	19.72	12.82	18.66	8.70	37.31	0.87	14.01
8.23	38.14	12.76	17.37	12.06	19.82	12.20	20.63	12.17	20.03	8.27	38.07	1.25	12.90
7.73	39.15	12.30	17.94	11.50	20.86	11.82	21.10	11.74	20.49	7.85	38.89	1.44	12.46
7.50	39.37	11.74	19.17	11.19	21.25	11.57	21.33	11.35	20.98	7.44	39.89	1.70	11.89
7.24	39.73	11.37	19.55	10.90	21.47	11.20	22.21	11.16	21.70	6.86	41.20	1.90	11.46
6.94	40.44	10.86	20.55	10.49	22.13	10.94	22.39	10.88	22.16	6.57	41.87	2.18	11.00
6.66	41.08	10.51	20.75	10.08	22.90	10.68	22.71	10.53	22.39	6.30	42.56	2.50	10.49
6.49	41.40	10.11	21.67	9.71	23.66	10.18	23.59	10.08	23.31	6.05	43.15	2.78	9.74
6.25	41.89	9.72	22.47	9.45	23.77	9.86	24.20	9.66	24.23	5.80	43.84	3.08	9.33
6.05	42.39	9.34	23.27	9.12	24.48	9.53	24.70	9.42	24.45	5.57	44.39	3.39	8.89
5.87	42.87	8.99	23.96	8.80	25.14	9.24	25.17	9.07	25.30	5.34	45.04	3.71	8.45
5.62	43.50	8.47	24.78	8.61	25.35	8.87	26.05	8.86	25.54	5.15	45.58	3.94	8.13
5.45	43.98	8.08	25.64	8.37	26.04	8.64	26.57	8.55	26.33	4.97	46.18	4.21	7.82
5.17	44.87	7.69	26.51	7.97	26.69	8.41	27.28	8.28	27.06	4.85	46.55	4.57	7.44

4.92	45.48	7.22	27.47	7.75	27.24	8.03	27.85	8.10	27.31	4.67	47.13	4.87	7.11
4.78	45.89	6.85	28.22	7.53	27.69	7.38	28.93	7.83	27.96	4.55	47.44	5.14	6.80
4.66	46.26	6.45	29.30	7.32	28.19	7.15	29.41	7.60	28.58	4.38	48.04	5.42	6.50
4.53	46.75	6.13	29.99	7.18	28.28	6.95	29.94	7.44	28.71	4.22	48.57	5.81	6.02
4.33	47.40	5.87	30.72	6.98	28.71	6.76	30.11	7.20	29.30	4.06	49.13	6.30	5.61
4.25	47.54	5.51	31.63	6.89	28.93	6.54	30.98	6.99	29.79	3.88	49.87	6.72	5.26
3.98	48.35	5.23	32.64	6.69	29.45	6.27	31.62	6.75	30.21	3.76	50.31	7.22	4.90
3.77	49.17	4.89	33.39	6.51	29.80	5.97	32.16	6.55	30.71	3.65	50.65	7.86	4.44
3.56	50.05	4.66	34.31	6.34	30.23	5.81	32.48	6.39	31.11	3.48	51.57		
3.37	50.81	4.40	35.08	6.20	30.62	5.68	32.81	6.23	31.56	3.33	51.85		
3.20	51.64	4.23	35.76	6.04	30.99	5.44	33.49	6.07	31.98	9.12	36.81		
2.92	53.13	3.99	36.64	5.89	31.29	5.32	33.71	5.92	32.40	8.70	37.31		
2.67	54.57	3.81	37.30	5.66	31.72	5.22	34.09	5.78	32.82	8.27	38.07		
2.50	55.49	3.63	38.11	5.49	32.23	5.05	34.67	5.63	33.15	7.85	38.89		
		3.48	38.74	5.34	32.63	4.93	34.88	5.48	33.71	7.44	39.89		
		3.30	39.52	5.09	33.21	4.84	35.14	5.19	34.58	6.86	41.20		
		3.14	40.25	4.96	33.51	4.76	35.44	5.03	34.78	6.57	41.87		
		2.97	40.95	4.82	33.85	4.60	35.85	4.90	35.31	6.30	42.56		
		2.88	41.57	2.99	39.03	4.49	36.19	4.81	35.51	6.05	43.15		
		2.73	42.39	2.72	40.49	4.39	36.47	4.63	36.04	5.80	43.84		
				1.66	48.42	4.28	36.87	4.55	36.32	5.57	44.39		

						4.21	37.04	4.46	36.50	5.34	45.04		
						4.10	37.45	4.37	36.90	5.15	45.58		
						3.99	37.79	4.27	37.31	4.97	46.18		
						3.92	38.07	4.12	37.78	4.85	46.55		
						3.81	38.53	4.02	38.06	4.67	47.13		
						3.69	38.98	3.89	38.58	4.55	47.44		
						3.55	39.43	3.71	39.25	4.38	48.04		
						3.46	39.75	3.64	39.50	4.22	48.57		
						3.41	39.94	3.58	39.76	4.06	49.13		
						3.34	40.28	3.48	40.09	3.88	49.87		
						3.25	40.64	3.42	40.37	3.76	50.31		
						3.14	41.14	3.36	40.58	3.65	50.65		
						3.06	41.48	3.31	40.82	3.48	51.57		
						2.99	41.81	3.21	41.27	3.33	51.85		
						2.96	41.77	3.10	41.78				
						2.89	41.68	3.01	42.15				
						2.83	41.98	2.92	42.55				
						2.77	42.29	2.83	42.90				
						2.73	42.57	2.77	43.19				
						2.65	42.86	2.71	43.49				
						2.60	43.15	2.66	43.74				

						2.54	43.38	2.61	43.98				
						2.47	43.82	2.54	44.33				
						2.43	44.03	2.47	44.71				
						2.39	44.26	2.44	44.90				
						2.36	44.41	2.40	45.11				
						2.31	44.73	2.36	45.19				
						2.27	44.82	2.30	45.54				
						2.23	45.03	2.27	45.77				
						2.18	45.21	2.21	46.06				
						1.67	48.41	2.17	46.30				
								2.14	46.58				
								2.09	46.80				
								2.04	47.07				
								2.00	47.25				
								1.95	47.55				
								1.90	47.91				
								1.86	48.14				
								1.82	48.47				
								1.55	49.39				
								1.35	50.85				
								0.87	55.49				

Appendix D

Composition of each ATPS used to purify the IFN α -2b, at pH 8.2.

Assay	IL	IL _M		K ₂ HPO ₄ /KH ₂ PO _{4M}		Extract _M	
		(g)	(wt%)	(g)	(wt%)	(g)	(wt%)
1	[N ₄₄₄₄][Ac]	0.2404	39.29	0.3205	9.00	0.0510	8.33
	[P ₄₄₄₄][Ac]	0.2400	39.89	0.3123	8.92	0.0494	8.21
	[N ₁₁₁₁][Ac]	0.3214	39.97	0.4164	8.90	0.0663	8.24
	[N ₄₄₄₄][MES]	0.2404	39.77	0.3145	8.94	0.0496	8.20
	[P ₄₄₄₄][MES]	0.2406	39.86	0.3138	8.94	0.0492	8.15
	[C ₄ mim][MES]	0.2402	40.05	0.3102	8.89	0.0493	8.22
2	[N ₄₄₄₄][Ac]	0.3203	39.93	0.4161	8.92	0.0657	8.19
	[P ₄₄₄₄][Ac]	0.3209	40.08	0.4143	8.89	0.0655	8.18
	[N ₁₁₁₁][Ac]	0.3205	39.89	0.4174	8.93	0.0656	8.16
	[N ₄₄₄₄][MES]	0.3207	39.77	0.4199	8.95	0.0657	8.15
	[P ₄₄₄₄][MES]	0.3207	40.00	0.4155	8.91	0.0655	8.17
	[C ₄ mim][MES]	0.3202	39.95	0.4152	8.90	0.0661	8.25
3	[N ₄₄₄₄][Ac]	0.3600	44.47	0.3815	8.10	0.0681	8.41
	[N ₁₁₁₁][Ac]	0.2400	39.92	0.3115	8.91	0.0497	8.27